Flow and thermal regimes in river networks: effects of hydropower regulation and climate extremes

Inaugural-Dissertation
to obtain the academic degree
Doctor of Philosophy (Ph.D.) in River Science

submitted to the Department of Biology, Chemistry and Pharmacy
of Freie Universität Berlin

by

MEILI FENG

from Trento - Italy

2016

This thesis work was conducted during the period 1st November 2013 - 20th December 2016, under the supervision of Prof. Guido Zolezzi (University of Trento, Italy), Prof. Klement Tockner (Freie Universität Berlin), Prof. Martin T. Pusch (Leibniz Institute of Freshwater Ecology and Inland Fisheries Berlin), and Dr. Markus Venohr (Leibniz Institute of Freshwater Ecology and Inland Fisheries Berlin), at University of Trento, Italy, Freie Universität Berlin, and Leibniz Institute of Freshwater Ecology and Inland Fisheries Berlin.

Supervisors:

Prof. Dr. Klement Tockner (Freie Universität Berlin)

Prof. Dr. Guido Zolezzi (University of Trento, Italy)

Prof. Dr. Martin T. Pusch (Leibniz Institute of Freshwater Ecology and Inland Fisheries Berlin)

Dr. Markus Venohr (Leibniz Institute of Freshwater Ecology and Inland Fisheries Berlin)

1st Reviewer: Prof. Dr. Paolo Perona (University of Edinburgh)

2nd Reviewer: Prof. Dr. Donatella Termini (University of Palermo)

3rd Reviewer: Prof. Dr. Walter Bertoldi (University of Trento)

Date of defence: 20th December 2016

UNIVERSITY OF TRENTO - Italy
Department of Civil, Environmental and Mechanical Engineering

Freie Universität Berlin

IGB
Leibniz-Institute of Freshwater Ecology and Inland Fisheries

Erasmus Mundus Joint Doctorate School in Science for MAnagement of Rivers and their Tidal System

---

Meili Feng

Flow and thermal regimes in river networks: effects of hydropower regulation and climate extremes

Erasmus Mundus

Autumn, 2016

Doctoral thesis in "Science for Management of Rivers and their Tidal System"

Cycle (III)

Primary Institution: Department of Civil, Environmental and Mechanical Engineering, University of Trento, Italy

Secondary Institution: Department of Biology, Chemistry and Pharmacy, Freie Universität Berlin, Germany

Associate partner: Department of Ecohydrology, Leibniz-Institute of Freshwater Ecology and Inland Fisheries, IGB Berlin, Germany

Supervisors:

Prof. Guido Zolezzi, Department of Civil, Environmental and Mechanical Engineering, University of Trento

Prof. Martin Pusch, Department of Ecosystem Research, Leibniz-Institute of Freshwater Ecology and Inland Fisheries, IGB Berlin

Dr. Markus Venohr, Department of Ecohydrology, Leibniz-Institute of Freshwater Ecology and Inland Fisheries, IGB Berlin

Academic year **2016/2017**

Meili Feng

Trento, Italy

November 2016

The SMART Joint Doctorate Programme

Research for this thesis was conducted with the support of the Erasmus Mundus Programme[1] , within the framework of the Erasmus Mundus Joint Doctorate (EMJD) SMART (Science for MAnagement of Rivers and their Tidal systems). EMJDs aim to foster cooperation between higher education institutions and academic staff in Europe and third countries with a view to creating centers of excellence and providing a highly skilled 21st century workforce enabled to lead social, cultural and economic developments. All EMJDs involve mandatory mobility between the universities in the consortia and lead to the award of recognised joint, double or multiple degrees. The SMART programme represents collaboration among the University of Trento, Queen Mary University of London, and Freie Universität Berlin. Each doctoral candidate within the SMART programme has conformed to the following during their 3 years of study:

i. Supervision by a minimum of two supervisors in two institutions (their primary and secondary institutions).

ii. Study for a minimum period of 6 months at their secondary institution.

iii. Successful completion of a minimum of 30 ECTS of taught courses.

iv. Collaboration with an associate partner to develop a particular component / application of their research that is of mutual interest.

v. Submission of a thesis within 3 years of commencing the programme.

[1]This project has been funded with support from the European Commission. This publication reflects the views only of the author, and the Commission cannot be held responsible for any use, which may be made of the information contained therein.

Acknowledgements

The author thanks the funding opportunity of this thesis within the SMART Joint Doctorate programme “Science for the MAnagement of Rivers and their Tidal systems” funded by the Erasmus Mundus programme of the European Union.

I would also like to thank everybody who directly or indirectly contributed to the successfully completion of this thesis. My special thanks go to:

My supervisor Prof. Guido Zolezzi for the patient guidance, encouragement, efforts and great visions of the topics provided for me during the three years.

My supervisor Prof. Martin Pusch for introducing me the chance to join the excellent SMART programme, and for his continuous support and advice throughout the three years’ Ph.D. journey.

My supervisor Dr. Markus Venohr for accepting me in his working group, and for the constructive discussions and supports during my stay at IGB Berlin.

All the colleagues in Adlershof and IGB, Berlin for their invaluable accompany and discussion, and all the bureaucratic assistance.

Miss Judith Mahnkopf and Mrs Annet Wetzig in Dr. Markus Venohr's group for helping me with the hydrological data collection and the GIS dataset pre-processing for the analysis in the 2nd Chapter.

Dr. Mauro Carolli and Dr. Davide Vanzo in Prof. Zolezzi’s group in Trento, Italy who helped me with the peaking indicators application and modeling debug in the 4th Chapter.

My dear friends in Trento, Berlin, China, and the rest of the world, together with the other SMART PhD students for the not only scientific chats and nice time we shared.

My dear families for constantly encouraging me and for being always there for me.

Abstract

Interactive impacts of climate change and human activities (e.g. hydropower production) have posed urgency in examining the patterns of hydrological and thermal response in riverine ecosystems, and the potential ecological implications manifested. Hydro-geomorphic conditions are the major factors in shaping water qualities in river networks, especially under the extreme climatic events. However, when the power of nature is encountered with human regulations, represented by hydropower production, it would be well worth discussing how the pictures of riverine hydro- and thermal regimes would change over the certain range of time and space. Moreover, the possible utility of hydropower regulation as mitigation of extreme climate changes is still open question to be verified.

Above-mentioned questions are answered in three aspects specifically:

- Governing factors and the spatial distribution model for water residence time in river networks of Germany. Based on the machine learning technique of boosted regression trees (BRT), spatial distribution of water residence time is estimated for the long-term annual average hydrological conditions and extreme cases of flood and drought.
- Impacts of hydropower over temporal and spatial range are investigated by analyzing the mechanisms of hydropeaking propagation. Hydrologic and geomorphic contribution framework is proposed and applied for the upper Rhone River basin in Switzerland, a typical hydropower exploited river basin in the mountainous area.
- River water temperature response as an indication for ecological status is investigated for the alpine rivers across Switzerland, excellent representatives of sensitivity and vulnerability to climate

change while under highly exploitation of hydropower activities. Extreme climate change case of heatwaves in 2003 and 2006 are selected and analysed especially.

Results of the three research components in correspondents to the listed research questions showed that river hydrological regimes have more direct influence on the variation of water residence time in comparison with the geomorphologic settings. Nevertheless, geomorphologic and topologic conditions (e.g. river width, slope, and roughness coefficient) that largely control the hydraulic waves diffusion processes in a hydropower-dominated river basin determine the spatial range of hydropeaking impacts. A hierarchy framework of geophysical obstructions, hydrology, and hydraulic waves diffusion process is proposed for analyzing the spatial range of hydropeaking propagation. When the effects of hydropeaking and thermopeaking are dominated in the river reach, hydropower regulation offers as great potential to mitigate extreme climate events (i.e. heatwaves).

By looking into specific perspectives of riverine hydro- and thermal regimes, hydropower regulation, and climate extremes via different temporal-spatial scales, we investigated the interactive effects between riverine ecosystem and human-climatic impacts. We expanded the approach of water residence time estimation into the field of machine learning with spatial predictions. Impacts of hydropower regulation are first elaborated with a framework of hydropeaking propagation mechanisms. Hydropower regulation has been identified to have great potential to mitigate extreme heatwaves through altering thermal regimes in rivers. Results of the study not only contribute to river hydrology and ecology studies, but also to the river management and climate change mitigation practices.

List of Contents

List of Figures

List of Tables

Chapter 1

General introduction

River discharge and water temperature, together with the light availability are traditionally considered as the ‘master’ variables controlling the structures and functions of freshwater ecosystems (e.g. Richter et al., 1996, Ward, 1985, Westlake et al., 1965). They overall control a complex array of physical, chemical, biological processes and related mutual interactions on which the stream and riparian biota has been adapting at different life stages.

For a variety of reasons, the level of scientific consideration given to the three above master variables as fundamental ecological drivers is highly different and biased towards discharge, with a huge number of studies addressing the linkages of flow regimes with river ecology, especially in consideration of the increasing levels of flow regime alterations by human effects worldwide (e.g. Nilsson et al., 2005; Zarfl et al., 2015). River thermal regimes have received comparatively much less attention, at least until approximately the last decade (Webb et al., 2007). Finally, light availability in rivers has been much less studied even compared with the rivers’ thermal regimes, with quantitative analysis being developed only in recent years (e.g., Julian et al., 2008).

The research developed in the present thesis is framed in such broad paradigm and focuses on the analysis of selected aspects of the hydrological and thermal regime of rivers that are of recognized ecological significance. The developed research mainly focuses on its physical dimension, without explicitly analyzing its ecological implications, though attempting to discuss them at various stages. The selected topics investigate ecologically relevant flow and thermal regimes characteristics at different spatial and temporal

scales, focusing on controls that are of hydro-geomorphic, anthropic and climatic origin.

The hydrology of river ecosystems as the ‘pulse’ of the river dynamics is characterized by variations both of flow and of water temperature, and often shows distinct seasonal flood pulses (Junk et al. 1989, Webb and Nobbis, 2007). The hydrological and thermal regimes of rivers have fundamental implications for the structure and functioning of river ecosystems (Pringle, 2003), as river connectivity (Amoros and Bornette, 2002), ecological selection on the catchment-scale distribution of benthic invertebrates (Ceola et al., 2013; Ceola et al., 2014), biodiversity functions (Bunn and Arthington, 2002), and ecosystem integrity (Olden and Naiman, 2010).

The documented decline of biodiversity worldwide is mostly accelerated in freshwater compared to terrestrial ecosystems (Dudgeon et al., 2006; Rodríguez et al., 2012) with one of the major causes being river fragmentation, caused by impoundments and human water abstractions (e.g. Nilsson et al., 2005; Poff and Schmidt, 2016). Hydropower is among the main causes of river fragmentation and related flow and thermal regimes alteration, and is projected to witness rapid increase worldwide (Lehner et al., 2011; Zarfl et al., 2015). While some of its downstream impacts on aquatic ecology are already well known and documented, still the associated spatial scales and time scales, particularly in relation to the projected climatic changes, are still poorly understood and quantified.

The flow and the thermal regimes of rivers also have strong consequences on the physical – chemical water quality, especially by acting on the spiraling of nutrients in river systems (e.g. Ensign and Doyle, 2006). Despite the increasing availability of physically based hydrological models for flow regime simulations at the river reach and catchment levels, linkages between river hydrology and water quality studies in terms of nutrient retention processes are limited to input parameters as part of process-based models, or

empirical function of the mean annual change in river water residence time (Vörösmarty et al., 2003). Moreover, these applications are subject to the difficulties of varying river geomorphologic conditions and the availability of experimental data.

However, nutrient pollution has effects at spatial scales that go beyond regional or local impacts on water qualities and it also affects the functioning of stream ecosystems especially at the scale of entire river catchments (Woodward et al., 2012). The concept of residence time represents a key parameter both in hydrology, where it is especially used to predict the move of flood waves, and for the modelling of water quality in rivers (Shamsaei et al., 2013). In this case, water residence time appears alternatively as a useful proxy to develop quantitative predictions of ecological and water quality status through variation of flow regimes under anthropic and climatic effects.

This introductory chapter presents a summary of the state-of-art for the three elements of the study, sets out the main scientific questions behind them, and introduces the general outline of the thesis.

1.1 Hydrological residence time in river networks and linkages to water quality

The time that a certain amount of water travels through a river reach controls the greatest potential of time during which nutrient spiraling processes take place. Nutrient transportation in streams involves both physical dynamics and biological uptake processes along the longitudinal and vertical direction in rivers (Kronvang et al., 1999; Runkel, 2007). The retention of biologically labile dissolved substances largely depends on the travel time through a river system during which processes contributing to nutrient spiraling processes may take place (Ensign and Doyle, 2006). The nutrient cycle, in conjunction with the downstream transport, is described as spiraling processes (Figure 1.1)

(Newbold et al., 1981).

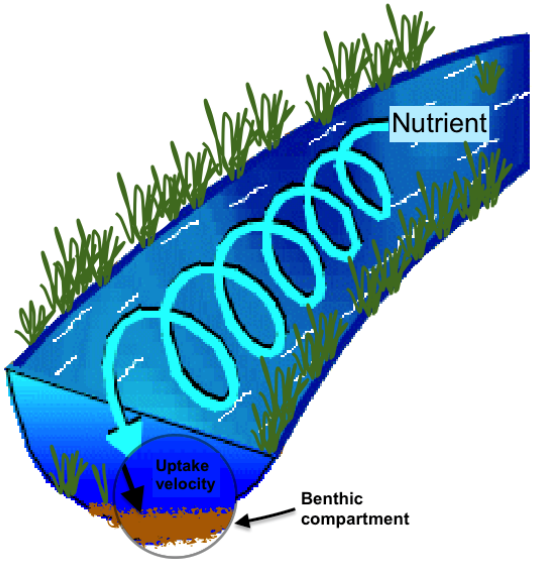

Figure 1.1 The nutrient cycle, in conjunction with downstream transport, described as spiraling. (Modified from: Hebert, P.D.N, ed. Canada's Aquatic Environments [Internet]. CyberNatural Software, University of Guelph.)

The travel time of nutrient flux has been investigated through experimental techniques, labors and thus resource-limited (Drummond et al., 2016; Nieuwenhuyse, 2005; Soulsby et al., 2006). However, insights into the processes of nutrient spiraling process by experiments are biased and condition dependent due to the fact that nutrient addition often brings much higher concentration than the background level, which results with overestimated nutrient uptake length (Mulholland et al., 2002). Modelling studies on nutrient export are mostly based on steady state hydrologic conditions assuming variations in pressure from pollution sources (Ingestad and Ågren, 1988; Powers et al., 2009; Runkel, 2007; Runkel and Bencala, 1995). This assumes that the hydraulic gradients that drive the transports are maintained the whole time the stream water remains in the water body, which is unrealistic (McCallum and Shanafield, 2016).

The biogeochemical functioning of a river ecosystem is largely dependent

on the transportation processes of water and dissolved substances within the geomorphic context of river networks (Withers and Jarvie, 2008; Benettin et al., 2015). The transport mechanisms are mainly shaped by hydromorphological parameters such as river discharge, water depth and velocity, and by other related physical ones as water temperature. Nutrient dynamics are controlled by the interaction of several key parameters, i.e. river discharge, channel geometry and vertical exchanges of water (Maazouzi et al., 2013). River hydromorphological shapes those processes and plays a major role in structuring the hydrological, ecological and biogeochemical dynamics in streams and rivers that are essential to ecosystem functioning (Doyle et al., 2003). Therefore, an improved understanding of the functions of nutrient retention time and transportation processes needs to tackle the challenge from the perspective of water residence time by quantifying its interactions hydromorphological parameters in space and time (Ambrosetti et al., 2003; Bouwman et al., 2013; Tong and Chen, 2002).

It should be noted that there exist differences between the flow velocities in the system (that set the velocity of conservative solutes) and the celerity (or speed with which hydraulic perturbations are conveyed, which control the hydrograph), are to be the velocity of conservative solutes, expected since they are controlled by different mechanisms. The nutrient transportation velocity in streams is always slower than the kinematic flow celerity of gravity-driven hydraulic waves. Studies on the differentiation and translation of these two velocities under varying flow conditions have been thoroughly discussed by McDonnell and Beven (2014). The water residence time discussed in this paper is coherently referred to flow velocity.

1.2 The time and space dimensions of peaking flows from hydropower regulation

Human impacts (i.e. through hydropower operation, land use changes,

river restoration) have greatly changed the natural flow regimes and the ecological connectivity of rivers (Crook et al., 2015; Daufresne et al., 2015; Lamouroux and Olivier, 2015). Variability of stream flow represents a major determinant for the ecological status of rivers, especially in mountainous river systems with highly exploitation of hydropower production (Geris et a., 2015). Many studies have documented a set of downstream ecological effects of hydropower operations (e.g. Bruno et al., 2013; Gorla et al., 2015). Disturbance of the flow regimes of riverine ecosystems generate ecological feedbacks between biological and physical processes (Lytle and Poff, 2004). Dams greatly transform natural patterns of rivers by distorting flow and thermal regimes and habitats downstream (Bruno et al., 2010; Poff and Schmidt, 2016). A more sustainable operation of hydropower plants would require, at least adopting standards for environmental flows, which therefore have been widely studied (Acreman and Dunbar, 2004; Alfieri et al., 2006; Baron et al., 2002; Geris et al., 2015; Richter et al., 1997; Rossel et al., 2015).

Among the different effects associated with hydropower operations, a specific set of processes is that associated with intermittent flow releases downstream of hydropower plants, which is often termed “hydropeaking” (e.g. Moog et al., 1993; see Figure 1.2 and Figure 1.3 for an illustration). Hydropeaking is resulted from the typical production of storage hydropower plants and it consists of artificially imposed flow oscillations caused by the typical intermittent functioning of hydropower plants, which aim at producing hydroelectricity during peak demand hours when the energy price is higher. Hydropower is privileged among the renewable energy sources because the typical functioning of the plants allows nearly real-time operations, with the possibility to start energy production within few minutes needed to start the turbines.

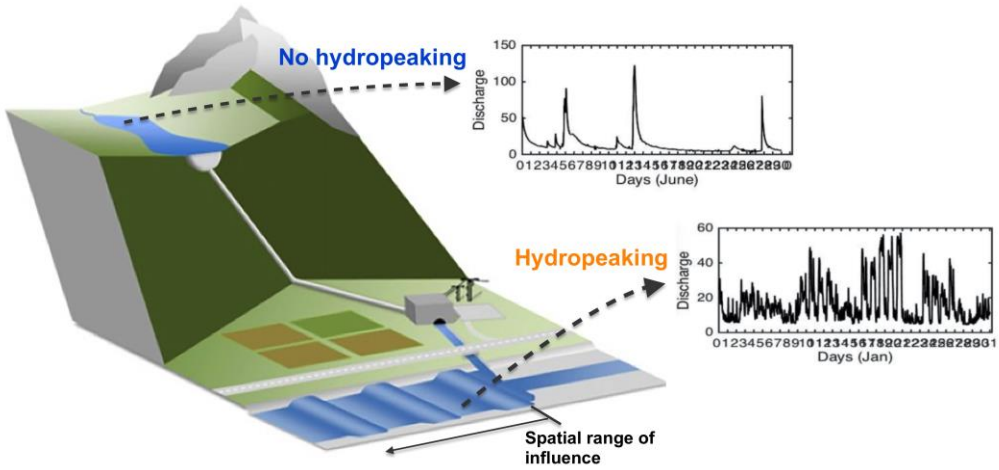

Figure 1.2 Illustration of the hydropeaking phenomenon in mountainous rivers where hydropower plants are connected with a penstock. Representative flow hydrograph characterized by no hydropeaking (station: Reckingen) and by hydropeaking (station: Brig) on the Rhone River in Switzerland. (Modified from: Bruder et al., 2016.)

Richard Feynman quotes - I don't know anything, but I do know that everything is interesting if you go into it deeply enough

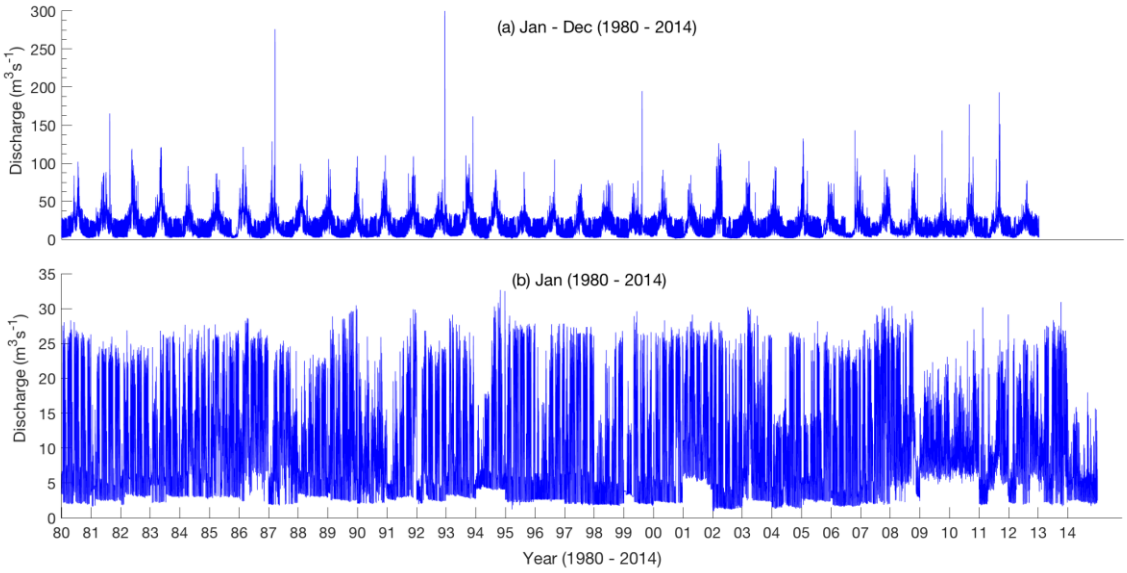

Figure 1.3 Illustration of the hydropeaking effect below hydropower plant. Example of the hydrograph is taken from the gauging station Visp at the Rhone river basin, Switzerland. (a) Discharge value of 10-min resolution from 1980 to 2014; (b) Same resolution but discharge only in January of 1980-2014.

The hydrographs of recipient water bodies downstream of hydropower plant releases often take the peculiar shape depicted in Figure 1.3, which shows the markedly fast rate of changes in streamflow in the gauging station of Reckingen and Brig on the Rhone River in Switzerland. Temporally varied hydropower production, which aims to meet the varying requests for electricity demand by consumers, creates artificial peaks of flows released to the downstream river sections. This feature is referred to as hydropeaking, which results in sub-daily fluctuations of flows (Zolezzi et al., 2009) that vary according to the demand of the energy market. These sub-daily fluctuations of river flows are accompanied by parallel variation of water temperature, as the water is released on most cases from the hypolimnetic zone of large reservoirs. In Alpine regions, such hypolimnetic water is usually colder than river water during summer, and warmer during winter (XXX). Hence, especially temporal variation of the release of hypolimnetic water profoundly disrupts the natural daily pattern of water temperature in rivers. These artificial fluctuations of river water temperature are referred to as thermopeaking (Carolli et al., 2008; Zolezzi et al., 2011; Bakken et al., 2016). Approaches to characterize the variations generated by hydropeaking (Carolli et al., 2015; Alonso et al., 2017) and thermopeaking (Davide et al., 2015) have been studied for some cases (Céréghino et al., 2002; Leitner et al., 2017; Kelly et al., 2016; Valentin et al., 1996).

While hydropeaking and, most recently thermopeaking have been extensively studied in terms of their ecological effects and of their physical characteristics, still most information on such alteration of the flow regime concentrate on specific time scales and are based on data collected at-a-station, i.e., rigorously applying to the river cross section where hydrological and thermal data have been collected. Very few studies examine on a quantitative basis the actual spatial scale of river reaches affected by hydropeaking propagation and the temporal evolution of hydropeaking over a

time scale of decades. We make a step forward in this direction by addressing such general question in Chapter 3 by referring to the phenomenon of hydropeaking in several Alpine rivers that are heavily used for hydropower production (see Chapter 3).

1.3 Impacts of extreme climatic events on riverine ecosystem

Besides human factors, like those associated with hydropower regulation, the discharge and temperature of running waters can be affected in several ways by climatic changes. Climate change does not only involve an increase of average temperatures, but also an increased frequency of extreme climatic and hydrologic events. Managing the risks of extreme events and disasters to advance climate change adaptation represents a major challenge for freshwater management (IPCC, 2012; Leigh et al., 2015).

Extreme climatic events such as heatwaves and cold spells may represent severe thermal stress situations also for aquatic ecosystems, as temperature represents one of the most direct drivers of ecological impacts in the aquatic ecosystems. Heatwaves are spikes of abnormally hot weather, and although relatively few studies have explicitly investigated their effects in rivers, experimentally increasing the frequency, intensity and duration of warming can alter the rates of emergence of aquatic insects and community composition. For instance, the 2003 European heatwaves caused high mortality among riverine benthic invertebrates (Mouthon and Daufresne, 2015).

Similarly, extreme hydrological events as exceptional floods and droughts may represent most critical impacts on riverine ecosystems, which differ in their effects significantly from the effects of usual annual flow dynamics (Ledger and Milner, 2015; Leigh et al., 2015; Reid and Ogden, 2006; Webb, 1996; Woodward et al., 2016), also in respect to their ecological impacts on

aquatic organisms (Death et al., 2015; George et al., 2015).

Chapter 4 presents an analysis of the potential linkages between climatic extreme events associated with heatwaves and the dynamics of river water temperature, by separately examining the response of Alpine rivers with hydropeaking –regulated flow regimes and of Alpine rivers that are not subject to intermittent flow releases. Some potential ecological effects of such dynamics are analysed and discussed as well. Previous studies that investigate the impacts of hydropower regulation on riverine ecosystems have not considered the impacts of extreme climatic events at the same time, which represents an important issue of water management especially in the vulnerable Alpine river systems. Thus, Chapter 4 addresses such gap in respect to the available knowledge on combined effects of hydropower regulations and extreme climatic events on the river hydrological and thermal regimes.

1.4 Research gaps

So far, few studies have aimed to improve the understanding of water residence time considering hydromorphological impacts on river channels as both driving force and the carrier. The estimation of the hydrological regimes in complex river systems is investigated by both detailed process-based models on one side, and over simplified empirical methods on the other side. This gap appears to be even larger when it comes to the application of large-scale river basins. Given this consideration, we explored in Chapter 2 the application of a nonlinear statistical approach of a spatial distribution model that integrates the factors of water residence time and different interactions between roughness features (river bed and bank roughness), river bed morphology, transient zone storage in hierarchical river systems.

The research gap addressed in Chapter 3 relates (i) to the typical spatial of hydropeaking in regulated rivers and on its main hydro-morphological

controls, and (ii) to the temporal evolution of hydropeaking on seasonal and multi-decadal time scales. Particularly, little is known about how hydrological effects associated with lateral tributaries and hydrodynamic effects associated with the propagation of sub-daily hydraulic waves induced by hydropeaking interact with each other to control the space scale of actual hydropeaking wave attenuation in Alpine rivers. Despite the existence of qualitative maps indicating the location and length of river reaches subject to high, moderate or low hydropeaking pressure, a systematic approach that could capture the mechanisms of spatial propagation of hydropeaking waves has not been developed so far.

Furthermore, as the use of hydropower and accompanying hydropower-induced effects are spread worldwide, ecological status of a river system is widely affected. The fragile river systems may become increasingly vulnerable in presence of extreme climate changes. In Alpine rivers it has been suggested (Hari et al., 2013) that hydropeaking-affected river reaches may be paradoxically ‘protected’ against heatwaves by thermal regulation associated with hydropeaking, as the release of hypolimnetic water from large reservoirs may dampen the effects of heatwaves on downstream river water temperature with their unique aquatic habitats. This hypothesis is analysed in chapter 4.

1.5 Aims and structure of the thesis

Hence, this thesis broadly aims to identify the role of some hydromorphological features of rivers on their hydrological and thermal regimes, especially if these rivers are affected by the use of hydropower and by extreme climatic events. The residence time of river water and water temperature have been selected as an indicators for the hydrological and thermal regimes, respectively; hydropeaking and thermopeaking are characterized as effects of hydropower regulation on rivers; finally, extreme events are analysed as representatives climatic extremes.

The second chapter investigates the governing factors and spatial distribution model for water residence time in river networks in Germany. The spatial distribution of water residence time is estimated for the long-term average hydrological conditions, and also for extreme cases of flood and drought by applying the spatial distribution model of Boost Regression Trees.

The third chapter evaluates the spatial and temporal properties of hydropeaking in rivers through a combined analysis of the propagation of hydropeaking waves over different temporal and spatial ranges by analyzing the effects of hydrologic and geomorphic features. These analyses are conducted on the example of the upper Rhone river system in Switzerland, a typical Alpine river exploited by hydropower.

The fourth chapter investigates the response of river water temperature response as an indication for ecological status in the Alpine rivers across Switzerland to the extreme heatwaves in 2003 and 2006. River reaches, which are subjected to hydropeaking and thermopeaking, are compared to other river reaches without hydropower regulation. Related potential ecological effects are presented and discussed.

Chapter 2

Estimating water residence time distribution in river networks by boosted regression trees (BRT) model

Abstract

In-stream water residence time (WRT) in river networks is a crucial driver for key biogeochemical processes that contribute to the functioning of river ecosystems. Dynamics of the WRT is critical for forecasting the nutrient retention time in the surface runoff, especially the over-saturated overland flow during flood events. This study illustrates the potential utility of integrating spatial landscape analysis with machine learning statistics to understand the hydrologic and geomorphic functioning of river networks on WRT especially at large scales. We applied the Boosted Regression Trees (BRT) model for the estimation of water residence time, a promising multi-regression spatial distribution model with consistent cross-validation procedure, and identified the crucial factors of influence. Reach-average WRTs were estimated for the annual mean hydrologic conditions as well as the flood and drought month, respectively. Results showed that the three most contributing factors in shaping the WRT distribution are river discharge (57%), longitudinal slope (21%), and the drainage area (15%). This study enables the identification of key controlling factors of the reach-average WRT and estimation of WRT under predictive hydrological conditions with more readily application. Resulting distribution model of WRT at national level may serve to improved water quality modelling and water management practices that aim to estimate or maximize nutrient retention in river systems.

Keywords: Water residence time; river networks; spatial distribution model;

Boosted Regression Trees (BRT).

2.1 Introduction

Water residence time (WRT) (also known as in-stream water residence time, Worral et al., 2014) refers to the average time that a certain amount of water travels through the defined river reach. Reach-average WRT represents one of the most important determinants for in-stream biogeochemistry recycling processes (Catalán et al., 2016; Drummond et al., 2016; Ensign and Doyle, 2006; Gibson, 2000; Hrachowitz et al., 2016; Stanley and Doyle, 2002). Residence time studies especially for extreme hydrologic regimes (i.e. flood and drought events) are of particular importance for water management practice. Hence, understanding the controlling factors and spatial distribution of reach-average WRT would greatly facilitate the modelling of water quality in river networks. It should be noted that the velocity of conservative solutes, which indicates the nutrient transportation velocity in streams, is always slower than the kinematic flow celerity of pure water itself. Studies on the differentiation and translation of these two measurements in different flow conditions have been well discussed by McDonnell and Beven (2014). The water residence time discussed in this paper is coherently referred to flow velocity in a given river reach.

Despite of its importance for water management, WRT may only be modeled either by sophisticated and time-consuming hydraulic models, or by over-simplified input-output estimation at large scales. We are not aware of an existing model to estimate the spatial distribution of WRT within river networks which does not require the availability and processing of detailed information on channel morphology. This chapter aims at evaluating the reach-average WRT across the wide range of hydro-geomorphologic settings by applying the spatial distribution model of Boosted Regression Trees (BRT).

Studies on WRT are often based on process-based deterministic models

for hydrological cycles including groundwater, precipitation and surface runoff in the river basin (such as SWAT (Grizzetti et al., 2003), SPARROW (Preston et Seitzinger al., 2011), NEWS2 (Mayorga et al., 2010) etc.). However, these deterministic models are time consuming and data demanding while applying to networks of large river systems. Besides that, WRT is estimated based on the travel time of dissolved solute tracers that are experimentally added to the river, which may also be used to analyse their retention efficiency especially if the dissolved matter may be retained by biological processes (Drummond et al., 2016; Nieuwenhuyse, 2005; Soulsby et al., 2006). Further improvements of the process-based models will likely require addressing spatial heterogeneities within basins (Mayorga et al., 2010) and a better understanding of river network retention and the factors controlled by runoff within watershed (Dumont et al., 2005).

In the meantime, computational and empirical methods (i.e. MONERIS, Venohr et al., 2011) offer more diversified options in combining statistical and process-based models at different scales (Gottschalk et al., 2006; Nieuwenhuyse, 2005; Soulsby et al., 2006). The 1-D hydraulic modelling based on the Manning-Strickler formula, which calculates flow velocity according to channel slope and cross-section variations, has been widely used in estimating flow velocity and thus water residence time (Verzano et al., 2012; Worrall et al., 2014). Water residence time in rivers networks differs due to the variability of inflow rates, river topology and geomorphology parameters (e.g. slope) (Doyle et al., 2005; Wang et al., 2015). Governing factors and the reach-average WRT estimation remains in difficulty due to distinguished geomorphological conditions. Understanding the WRT distribution in river networks, especially at large scales, still showed needs for improvements of more readily feasible approach between the time-consuming hydrology/ hydraulic models and the over-simplified input-output estimations.

The response of river flow to precipitation is highly nonlinear, and so are

the in-stream processes of water retention (Heidbüchel et al., 2012). To determine how differences in geomorphologic settings influence spatial heterogeneity in transport and retention of nutrient, research has suggested that a network perspective is needed to understand how connectivity, residence times, and reactivity interact to influence dissolved nutrient processing in hierarchical river systems (Stewart et al., 2011). Beyond the traditional insights of nonlinear processes using 1-D, 2-D or 3-D hydrodynamics equations, other nonlinear statistical approach such as the Boosted Regression Trees (BRT) is becoming to play a part in hydrodynamic studies (Ouedraogo and Vanclooster, 2016; Toprak and Cigizoglu, 2008; Toprak et al., 2014). The BRT model, which combines the advantages of regression trees and boosted adaptive method, has been widely applied in studies on ecological traits and species distributions (Zimmermann et al., 2010). Due to its powerful functionality and feasibility, BRT modelling has being increasingly applied recently in other environmental issues, too (Roe et al., 2005). Related topics such as natural flow regimes, groundwater and hydraulic conductivity (Jorda et al., 2015; Naghibi et al., 2016; Snelder et al., 2009), soil science (Martin et al., 2009; Jalabert et al., 2009), air pollution (Carslaw et al., 2009), energy (Kusiak et al., 2010), or climate change (Shabani et al., 2016) etc. has been applied with the BRT modelling.

With consistent cross-validation procedure and the feature of easy application, the BRT model suggests a highly potential for applying large-scale WRT analysis while considering multiple hydro-geomorphological parameters. In this study, we employed the BRT model to map the spatial distribution of water residence time of 82 river networks across gradients of climate, human impacts, and landscape characteristics in Germany. Distribution of WRT under long-term average discharge situation and hydrologic extremes of flood and drought are analysed especially. In order to juxtapose the new perspective of the spatial distribution modelling approach with the established methods, we

compared results of the BRT model with that of the empirical fitted equation by sampled datasets.

2.2 Materials and Methods

2.2.1 Study area and dataset

We collected the discharge data, which are recorded with a temporal resolution of 15 minutes, for the years 2008-2014 from 132 gauging stations in Germany. Among these stations, 82 river reaches were identified which are delimited at both the upstream and downstream ends by gauging stations (Figure 2.1). These reaches are geographically widely distributed and thus well represent the hydromorphological conditions (Table 2.1) of 13 stream types in Germany that differ in their biogeochemical conditions, too (Table 2.2). Substrate classes of the soil type for each river reach are represented in percentage (up to 100% all classes in sum) according to their length that falls into each class. All the geographic analyses and calculations were performed in ArcGIS Desktop (Version 10.0, ESRI, 2010).

To be noted, discontinuities in the river system, such as lakes and impoundments (produced by weirs or dams) are not considered in this paper, as water residence time in these conditions is usually much longer (decades to hundred years), and is controlled by different mechanisms (Heidbüchel et al., 2012; Ji, 2008; Rueda et al., 2006).

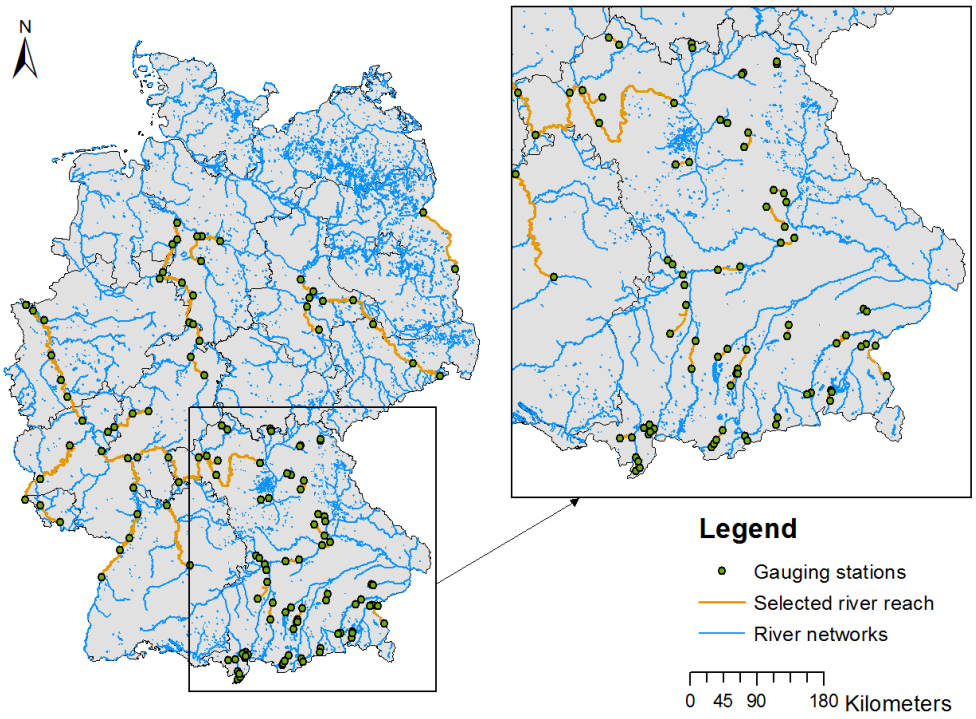

Figure 2.1 Map of river networks in Germany, with selected river reaches (orange) and the corresponding upstream-downstream gauging stations (circles).

Table 2.1 Hydrologic and geographic variables of studied river reaches. (Please see Table A.1 in supplementary materials for detailed information of attributes for all river reaches).

Categorical variables				
	Stream type	See Table 2.2		
	Substrate class [a]	Sand (S), Clay (C), Silt (U), Loam (L), Peat bog (HM), Fen (NM)		
Continuous variables		**Mean**	**Range**	**Std dev**
	Length (km)	30.8	1.01 - 145.4	30.34
	Slope (m/m)	0.00379	0.00005, 0.04104	0.00776
	Width (m)	88.40	1.73 - 408.42	105.91
	Drainage area (km^2)	25115.28	11.15 - 159427.5	41625.53
	Mean discharge (m^3/s)	327.86	0.253 - 2259.32	610.45

a The substrate classes are based on the German soil classification system (Working Group on Soil Classification of the German Soil Science Society, 1997).

Table 2.2 Stream types covered by our study reaches (acc. to the official German stream and river type classification system (Pottgiesser and Sommerhäuser, 2004).

Main category	**Sub-category**
Alps and Alpine foothills	1.1 = Small and mid-sized rivers
	2.1 = Small rivers in the alpine foothills
	2.2 = Mid-sized rivers in the alpine foothills
	3.1 = Small rivers in the Pleistocene sediments of the alpine foothills
	4 = Large rivers in the alpine foothills
Central highlands	5 = Small coarse substrate dominated siliceous
	7 = Small coarse substrate dominated calareous highland rivers
	9 = Mid-sized fine to coarse substrate dominated siliceous highland rivers
	9.1 = Mid-sized fine to coarse substrate dominated calcareous highland rivers
	9.2 = Large highland rivers
	10 = Very large gravel-dominated rivers
Central plains	15 = Mid-sized and large sand and loam-dominated lowland rivers
	20 = Very large sand-dominated rivers
Ecoregion independent streams	11 = Small organic substrate-dominated rivers
	21 = Lake outflows
Catchment size class:	
Small river:	10 - 100 km^2
Mid-sized river:	100 - 1,000 km^2
Large river:	1000 - 10,000 km^2
Very large river:	> 10,000 km^2

2.2.2 Factors affecting water residence time

In this chapter we evaluate the average discharge, drainage area, river width, length, slope, stream type, and sediment composition as potential

predictive factors for WRT in the selected river reaches (Table 2.1). Parameters are averaged over the reach between the upstream and downstream stations to represent the mean situation of the selected river reach.

We introduced the nonmetric multidimensional scaling (NMDS) plots (Agarwal et al., 2007) to obtain an insight into the patterns of hydromorphological conditions as well as WRT distributions for the studied river reaches. NMDS method provides as a useful tool in environmental assessment while integrating different forms of dataset no matter it is continuous monitoring data, discrete parameter, binary data or binomial category dataset. We used the Gower's generalized coefficient of dissimilarity approach (Gower and Legendre, 1986) to standardize the continuous variables against the discrete ones to get standardized Euclidean distance for the NMDS plots.

2.2.3 Spatial distribution model: Boosted Regression Trees (BRT)

The main aim of applying BRT modelling in this paper is to model spatial distribution of WRT with features of nonlinearity and interactions among multiple predictive variables (Elith and Leathwick, 2016). When the model is fitted, it simulates the variation of the 'distribution' of WRT under environmental scenarios. A measure of relative importance (in percentage) is calculated in the model to facilitate comparisons of term-wise contributions. In addition, partial dependence plots and fitted link functions for each variable were produced. Fitted BRT models were obtained by the sum of all trees multiplied by the learning rate (Elith et al., 2008):

$$f(x)=g[\sum iTi(x)] \qquad \text{(Eq. 2.1)}$$

where f is the fitted model, x is the independent variable, T_i are the individual

learners, and *g* is the link function that grows optimum trees.

In order to set up the BRT training model, the monitored and measured dataset of predictive variables described in section 2.2 was used for all selected river reaches. According to monitored discharge (Q), water level (D), and the average river width (B), baseline flow velocity (V) for the training model is solved by the basic relationship of hydrodynamics (Q=A*B*D). Then, the WRT values that were used for the training modelling were derived from the mean velocity between two gauging stations and the distance apart. Due to the length and scale-dependent attributes of water residence time, the average flow velocity is expressed as hour per kilometer instead of traditional time metric of hours. Calculations for BRT model were all performed in R (R Core Team, 2016) by using the package 'dismo' (Hijmans et al., 2016) and 'gbm' (Greg Ridgeway with contributions from others, 2015).

The error of the prediction is calculated using the Root Mean Squared Errors (RMSE):

$$RMSE = \sqrt{\frac{\sum_{i=1}^{n}(WRT_{pred} - WRT_{obs})^2}{n}} \quad \text{(Eq. 2.2)}$$

where WRT_{pred} is the predicted water residence time (h/km) and WRT_{obs} is the original calculated value according to observation at the river reach of *i*, and *n* is the number of studied river reaches.

2.2.4 Travel time of hydraulic waves method

The travel time or passage time of the peaking concentration for a conservative solute has been well established in studying the residence time and longitudinal dispersion of pollutants (Graf, 1986). Water residence time applied here is defined as the time lag between the observed discharge time series of the paired upstream and downstream gauging stations.

Cross-correlation techniques are often used to determine the relationship between two time series, which is based on the theory of linear time-invariant

system. In order to minimize the negative effects of white noise in the time series and the discharge magnitude distinctness, the peaks and valleys in the time series are detected firstly with values and locations out of the original dataset. Secondly, the cross correlation functions for each pair of 'peaking-time-series' are calculated to find out the maximum correlation and corresponding time lag as the water residence time for this river reach (Figure 2.2A).

Apart from determining the residence time by using the upstream and downstream hydrologic time series, we also analysed the average widths of each hydraulic waves ('hydro-width' hereafter) as an indicator of the damping ratio in this study (Figure 2.2B). The damping ratio (also called Q factor), a dimensionless measurement of system oscillation, is calculated as the peak locations divided by the width (Siebert, 1986). For the hydrologic transportation system, the implications of transit storage or dead zones are disclosed through the 'shape' of the hydrograph. The hydro-width on monthly basis for each river reach is the average widths of paired upstream-downstream hydrograph of corresponding month. Hydro-widths are calculated based on 15mins intervals and final results are converted into the unit of hours for illustration. Calculations are all made through Signal Processing Toolbox in MATLAB (MathWorks, 2016). Calculations are made through the Statistics and Machine Learning Toolbox in MATLAB (MathWorks, 2016).

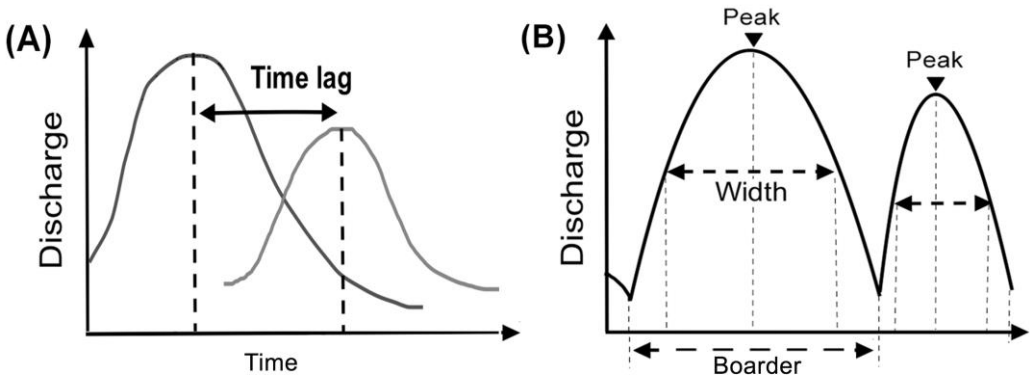

Figure 2.2 Schematic diagram of the discharge time series of the upstream input and downstream output with time lags between peaks.

2.3 Results and discussion

Elaboration of the results starts with spatial dissimilarity of the geomorphological and hydrological factors for studied river reaches, followed by the results of relative importance of variables calculated by the BRT model. Furthermore, we discussed the spatial distribution of estimated WRT under long-term annual average discharge conditions as well as during the extreme hydrological month of flood and drought.

2.3.1 Governing factors for water residence time

Multidimensional Euclidean distance between the studied river reach representing the varying channel hydro-geomorphology is showed in the Nonmetric multidimensional scaling (NMDS) plot (Figure 2.3). The colored river reaches according to their classification of stream types showed clustering patterns in accordance with the river size. Exceptions are the ecologically independent streams including lake outlets (type 21) and small organic substrate-dominated rivers (type 11). Spatial distributions of predictive factors for selected river reaches are illustrated in supplementary materials (Figure A1 - A3).

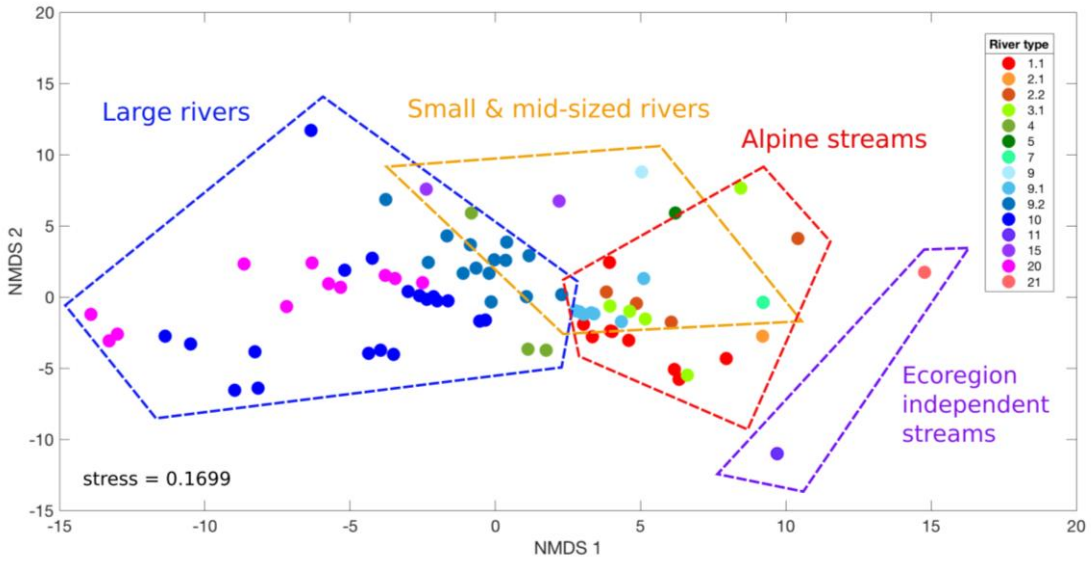

Figure 2.3 Dissimilarities of the studied river reach in the Nonmetric Multi-Dimensional Scaling (NMDS) ordination space according to hydro-geomorphic attributes.

Fitted BRT models were obtained by the sum of all trees multiplied by the learning rate of each predictive variables. The fitted model accounted for 54.53% of the mean total deviance of the monitored dataset (1-mean residual deviance / mean total deviance = 1-(23.546/40.751) = 0.4222). The optimal fit was achieved with the following variable setting: interaction depth =10, tree complexity = 10, learning rate = 0.001, bag fraction = 0.5 and cross-validation = 10-folds, optimal number of trees = 1680. For this fit, the training data correlation coefficient was 0.668, and cross-validation correlation coefficient was 0.614.

The predictive variable of mean discharge represented the most influential variable (57.42%) in the BRT model, followed by slope (21.54%) and the sum of drainage area (15.64%). Mean river width and river types together only contributed by less than 4% to the model. Similarly, substrate classes did not significantly influence water residence time (less than 2% contribution to the model). Especially, the substrates of clay, peat bog and fen showed no statistical contribution (Table 2.3). Although the latter predictive variables have little or no importance in our study, we did not exclude them from the set of the

predictive variables dataset, as they potentially may gain some importance in analyses of other datasets.

Table 2.3 The relative influence of predictive variables of river hydro-geomorphology as computed from the fitted BRT model on water residence time.

Variable	**Short name**	**Relative importance (%)**
Mean discharge (m^3/s)	Qmean	57.42
Slope (m/m)	Slope	21.54
Drainage area (km^2)	Area	15.64
Mean river width (m)	Width	2.41
River type	RType	1.25
Substrate_Sand (%)	Sand	0.70
Substrate_Loam (%)	Loam	0.69
Substrate_Silt (%)	Silt	0.34
Substrate_Clay (%)	Clay	0
Substrate_Peat bog (%)	Peat bog	0
Substrate_Fen (%)	Fen	0

In order to see how each predictive variables vary in shaping the simulated WRT, we bring the partial dependence plot (Figure 2.4) to show the relative influence of the leading eight variables on WRT after accounting for the average effects of all other variables in the boosted regression trees model. In each y-axis of the predictive factors, fitted function is showed in its greatest generality on the scale of link function (see Eq. 2.1).

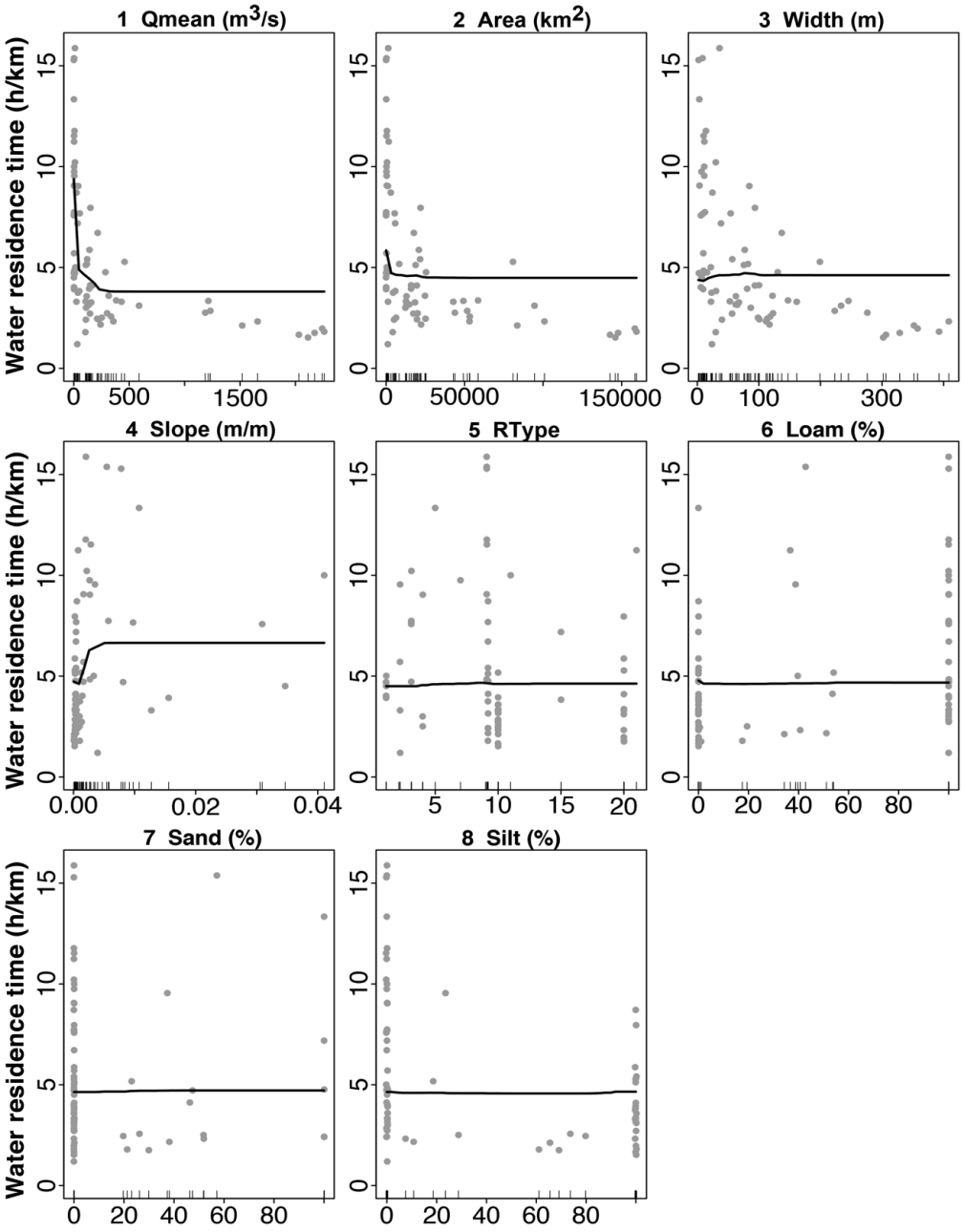

Figure 2.4 Partial dependence plots showing the dependence of residence time depends on hydro-geomorphologic variables after accounting for the average effects of the other predictors in boosted regression tree analysis. Each point represents an observed value for one quadrat with rug plots at the bottom of each panel. Y-axes are predicted values of the fitted functions. All panels are plotted on the same scale for comparison. Variable abbreviations are given in Table 2.3.

Influence of the mean discharge and drainage areas shows different magnitude of negative influence on WRT. River width of more than 100 meters

shows little influence on the variation of WRT. Longitudinal slope of riverbed is found to have a positive relationship with WRT, which is controversial with the common sense that rivers with larger slope has faster flow velocity. This is revealed by the less dominant position of slope in comparison with discharge and river width. The effects of river topography and soil composition appear to be largely mediated by their interactional influence with river hydrology distribution.

2.3.2 Interactional effects of predictive variables

Getting to know the interactional effects among predictive variables would facilitate the empirical estimation of WRT with available information of interested rivers. Among all the predictive variables, river hydrology ranks the first place of relative importance together with slope in shaping the variation of water residence time; and the drainage area is the usually in empirically linear relationship with the mean discharge (Bergstrom et al., 2016):

$$Q = \gamma A \qquad \text{(Eq. 2.3)}$$

where Q is the discharge in river reach, A is the contributing drainage area, and γ is the regression constant. Therefore, hydrological variations in the river reach have to be the paramount element of discussion.

The 2-dimensional partial dependence plot in Figure 2.5 shows the interactional effects between river discharge and drainage area. The results conform to the linear relationships as described in Eq. 2.3. Another important geomorphological factor is the river width that has great contribution to the distribution of WRT. Figure 2.6 shows the interactions between river width and drainage area, with predicted value of WRT in our studied river reaches. Furthermore, the river type classification, which represents generalized geomorphic and topologic attributes, could somehow simplify the process of WRT estimation especially under limited data availability conditions. The interactional effect between river type and the mean discharge is expressed in

Figure 2.7. For a river reach with known substrate class and river topology, water residence time under different discharge levels can be estimated.

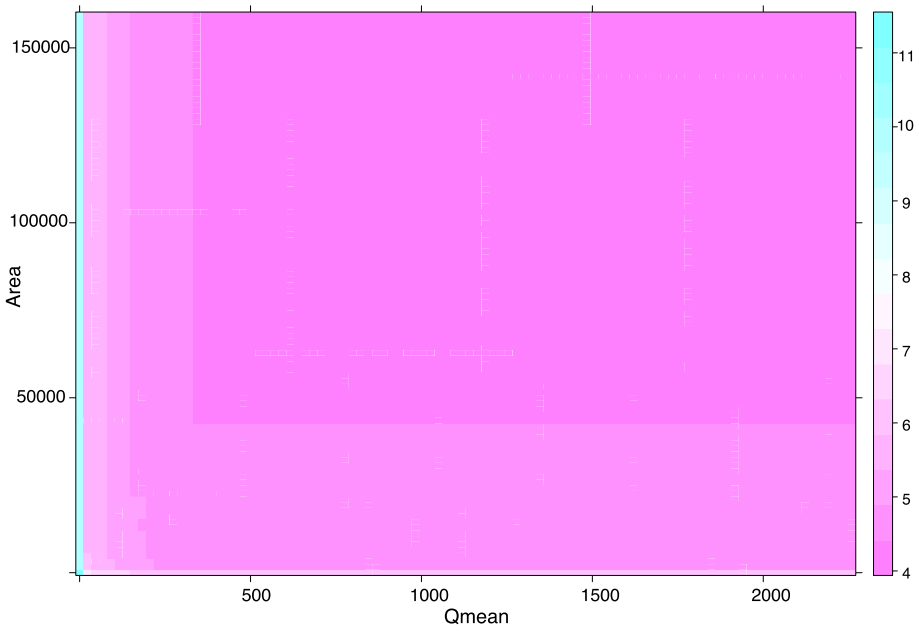

Figure 2.5 Two-dimensional interaction effects between the mean discharge (x-axis) and drainage area (y-axis). Colored scales are the estimated water residence time (h/km) accordingly.

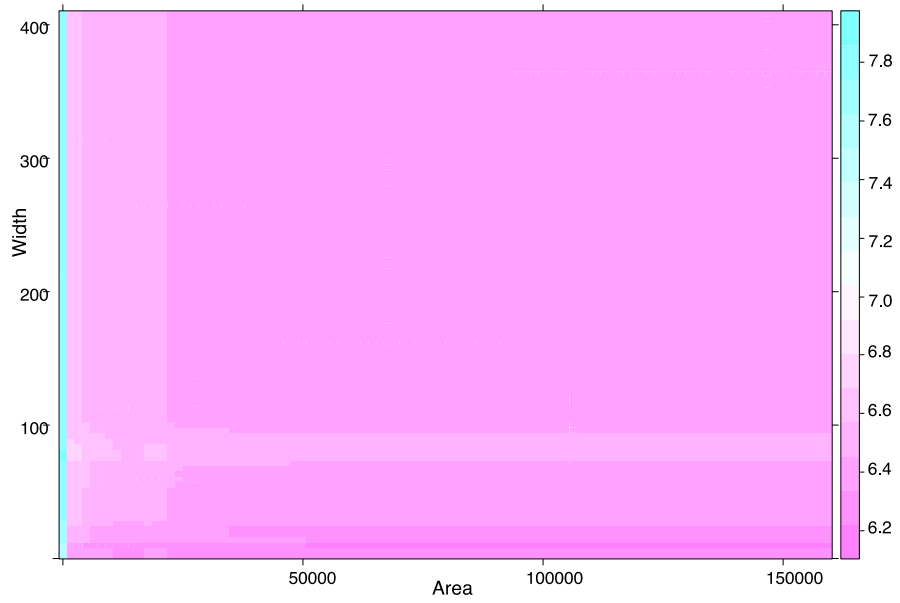

Figure 2.6 Two-dimensional interaction effects between the drainage area (x-axis) and river width (y-axis). Colored scales are the estimated water residence time (h/km) accordingly.

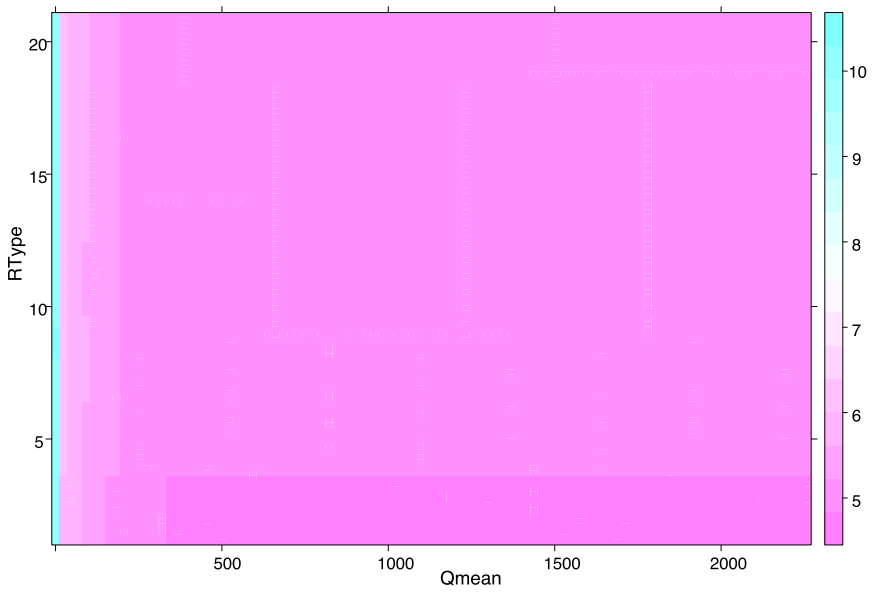

Figure 2.7 Two-dimensional interaction effects between mean discharge (x-axis) and the river type (y-axis). Colored scales are the estimated water residence time (h/km) accordingly.

2.3.3 Spatial distribution of predicted water residence time

2.3.3.1 Water residence time under annual average discharge

Water residence time for studied river reaches are estimated for the average discharge conditions during 2008-2013. While the hydrological and geomorphological conditions are widely scattered, the calculated WRT (h/km) for studied river reaches showed more synchronized distributions at stretches of large and very large rivers (river type 9.2, 10, 15, 20) that are featured by high level of discharge. Water residence time distribution at smaller rivers is more distracted due to distinct topologic features (Figure 2.8).

Scattered from the Euclidian distance to the spatial dimension, water residence time for studied river reaches are more directly observed for all river reaches (Figure 2.9). River reaches with the highest discharge rates showed annual average WRT of less than 4h/km. In general, a deduction in river discharge showed a property of longer WRT. However, this induction is not strickly comparable among different river reaches, especially, those with very

different geomorphological features.

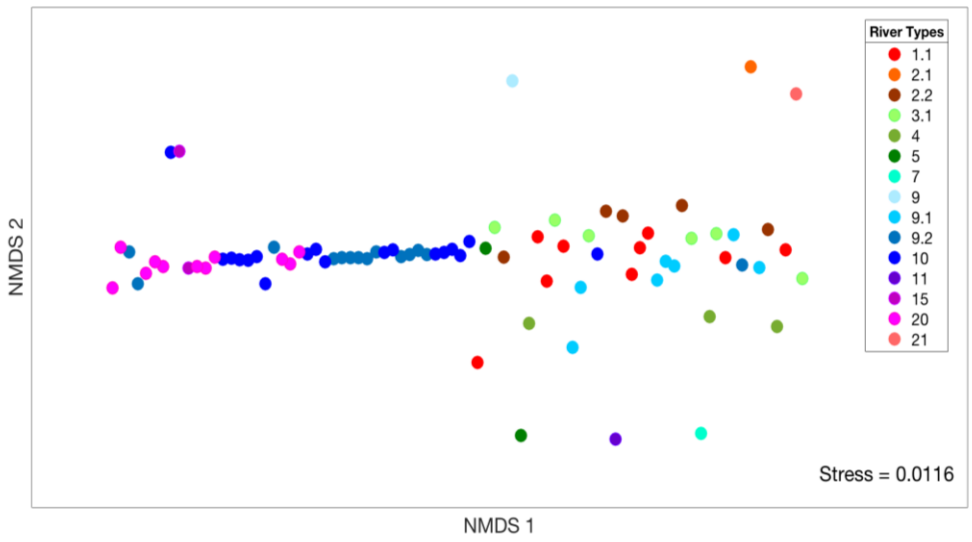

Figure 2.8 Dissimilarities of the calculated WRT (h/km) in the Nonmetric Multi-Dimensional Scaling (NMDS) ordination space.

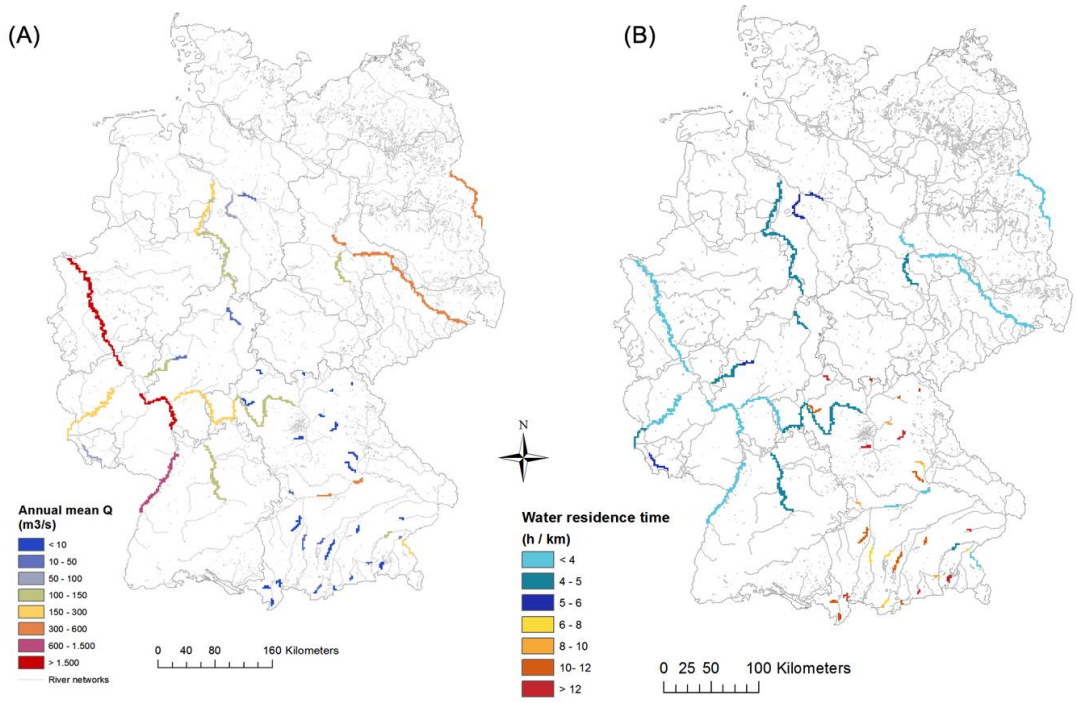

Figure 2.9 Spatial distribution of (A) annual mean discharge conditions during 2008-2013; (B) predicted water residence time (h/km) for studied river reaches.

Comparing the results of BRT model with that of the observed values showed a higher deviation between 1h/km (Figure 2.10). Poor model performance under low flows demonstrated need for further testing and data collection to support the inclusion of additional biogeochemistry processes. Site-specific uncertainties might arise from unknown flow paths and mixing dynamics significantly affect management strategies and expectations.

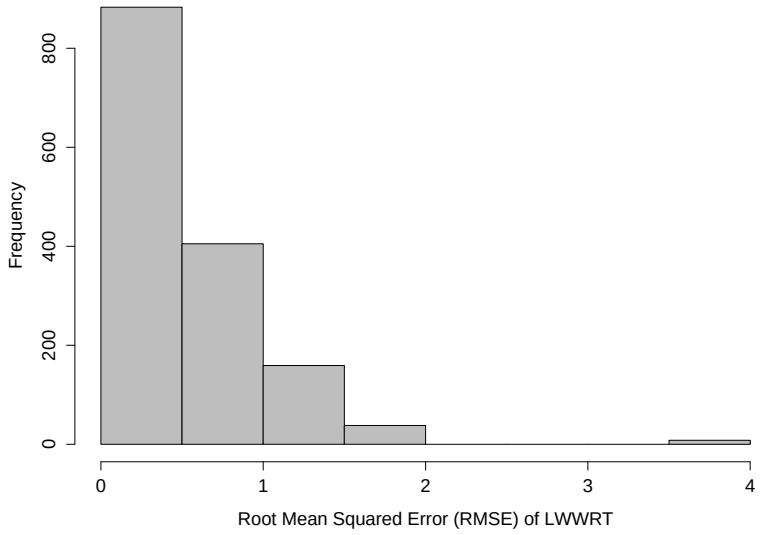

Figure 2.10 Frequency distribution of RMSE of predicted length weighted water residence time (h/km) against observed values across all sites.

Another widely applied way of measuring water residence time is by introducing solutes and measured residence time and flow velocity within specific river reach. In this study, we applied the empirical equation of $t = aQ^{-b}x^{c}$ proposed by Graf (1986), in which t represents the water residence time, Q is the discharge, x is the traveled distance in downstream direction, and a, b, c are the coefficients. By comparing the results of WRT, which are estimated through the BRT model and through the empirical equation, respectively, the calculated flow velocity for the same studied river reaches showed a decreased linear relationships with discharge in both correlation coefficients and the slopes (Figure 2.11). Possible explanations could be that in this study, the BRT model is built to explain variables through multiple boosted regressions by including the nonlinear interactional effects among

predictive variables. A lower tendency of linear relationship for the smaller discharge levels below 500 m^3/s has a potential to indicate geomorphological influence manifested at small rivers and non-bankfull conditions. This prediction is in conformity with the partial dependency analysis of each variable in section 2.3.2 that an overall consideration of all predictive variables at varied levels are needed by applying the systematic or network approach (Dumont et al., 2005).

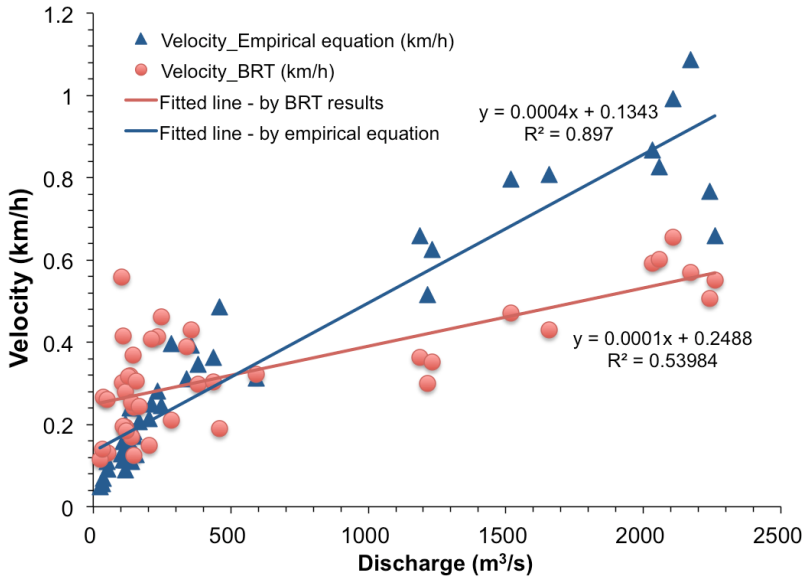

Figure 2.11 Spatial distribution of (A) annual mean discharge conditions during 2008-2013; (B) predicted water residence time (h/km) for studied river reaches.

2.3.3.2 WRT distribution under hydrologic extremes

The response between water residence time and discharge is complex, especially for distinct geomorphic sites. In order to facilitate more intuitive understanding, we did paralleled studies for the extreme hazard case of the flood event in June 2013 and the driest month of November 2011 in Germany. The May/June 2013 flood was the most severe large-scale flood events in Germany during the last 6 decades (Merz et al., 2014). Compared with the flood events in June 2013, the median discharge in November 2011 is 80.23% lower with the estimated water residence time is 20.73% (0.17 hours) longer per kilometer (Figure 2.12). Spatial variation is showed through the bivariate

map of mean discharge and water residence times. The contrasting effect is more clearly observed in the Elbe river basin where the most severe floods occurred (Figure 2.13).

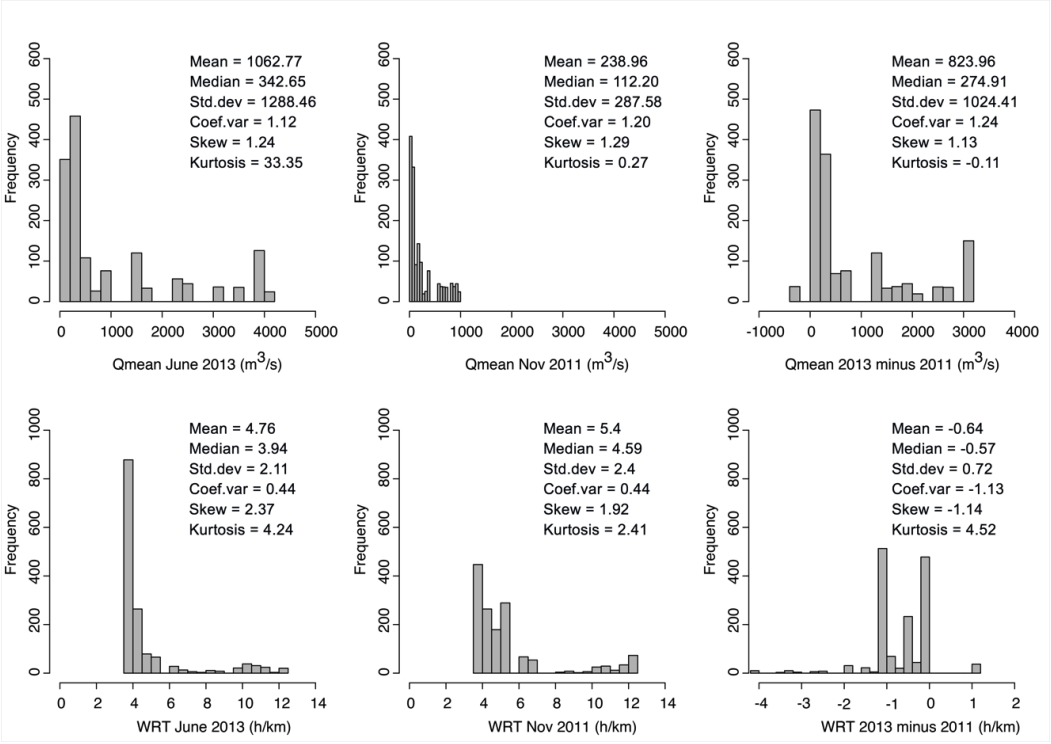

Figure 2.12 Statistical comparison of the mean discharge (in cubic meters per second) and corresponding water residence time (in hour per kilometer) in June 2013 (left), November 2011 (middle), and the difference between them (right), respectively.

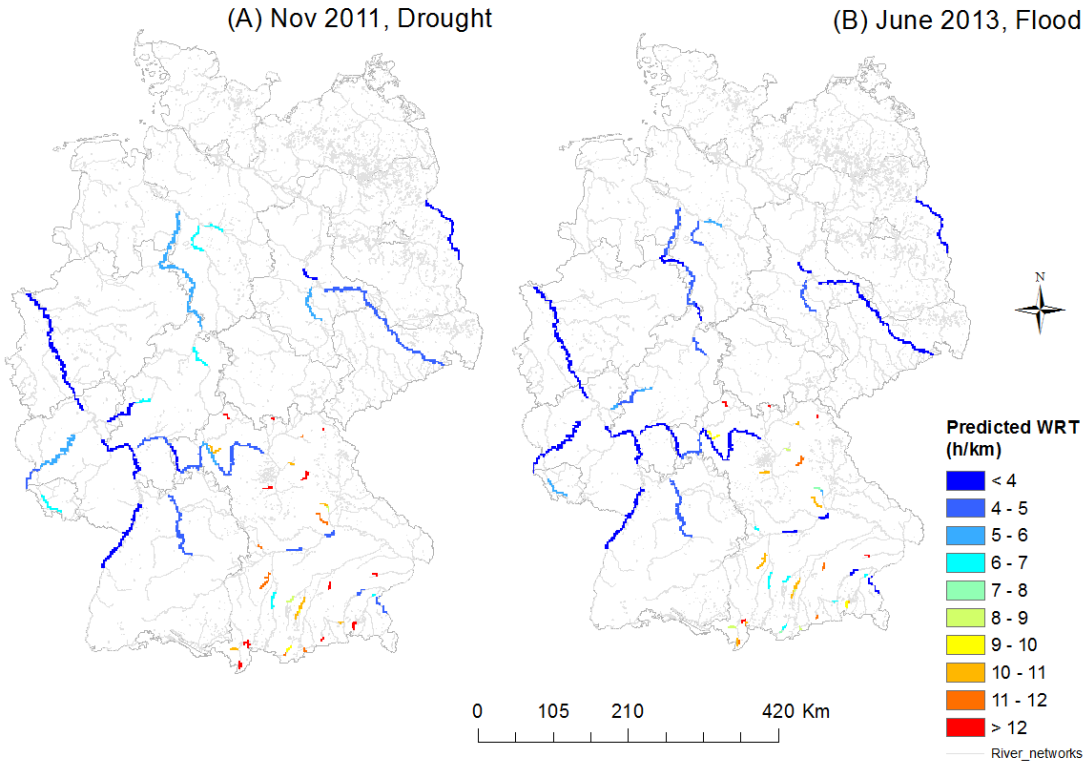

Figure 2.13 Spatial distribution of predicted water residence time (h/km) for (A) droughts during November 2011; and (B) floods during June 2013.

2.3.4 Impact of groyne fields on water residence time

River groynes (also called wing dams) are often constructed at the river bank with rocks or woods to prevent from ice jamming and lateral soil erosion by limiting the movement of water flow and sediments (Yossef, 2002). Due to simple construction, long-term durability and major functions, groyne fields (GF) are very widely applied in the lowland rivers of Germany. At present there are approximately 6900 groynes, covering 92% of the banks along the Middle Elbe River section (Schwartz, 2006). Because of the considerable reduction of water depth and flow velocity relative to the main stream, the prolonged retention time of water in the GF has important functions for the nutrient uptake dynamics and phytoplankton growth (Engelhardt et al., 2004; Guhr et al., 2000; Ockenfeld and Guhr, 2003). Investigation of hydraulic waves attenuation and water residence time in the specific hydrodynamic system at groyne fields is of great importance in water quality monitoring on nutrients and phytoplankton. Describing the specific hydraulic characteristics of flow velocity and residence time patterns in GF is the key to understanding the ecological significance of these retention zones.

Among our studied area, there are 14 out of 82 river reaches are characterized by groyne fields. Distribution of water residence time at these fields are linked to the variables and factors as we discussed above, however, looking at the shapes of hydrograph helps telling the different attributes of attenuation, which reveals ecological significance for nutrient retention. In order to exclude the influence of distinct scales, river reaches from the Alps, Alpine stream and central highlands in Bavaria (in total 39 reaches) are not considered for the comparison. Among the rest 43 river reaches of comparable discharge level, two groups of 14 river reaches with groyne fields and 29 free-flowing rivers are compared.

We plot the cumulative distribution functions of the mean hydro-width (in

hours) for the two groups (Figure 2.14). The empirical cdf plot shows that the probability level of hydro-width less than 90% are up to 44.41 hours at groyne fields, compared with that of only 21.42 hours at free-flowing rivers. There is very little chance (< 2.5 %) that the probability of hydro-width in free-flowing rivers will be less than one hour and there is also small chance (< 5%) that it could be as high as 33.71 hours. The groyne fields showed pronounced wider hydro-width than the free-flowing rivers: with 59.37% (87.57 hours) larger maximum value and more than 2 folds' (4.73 hours) at the median level. Not surprisingly, the estimated water residence time for GFs showed higher probabilities below 1.5 h/km in comparison with the free flow rivers (Figure 2.15).

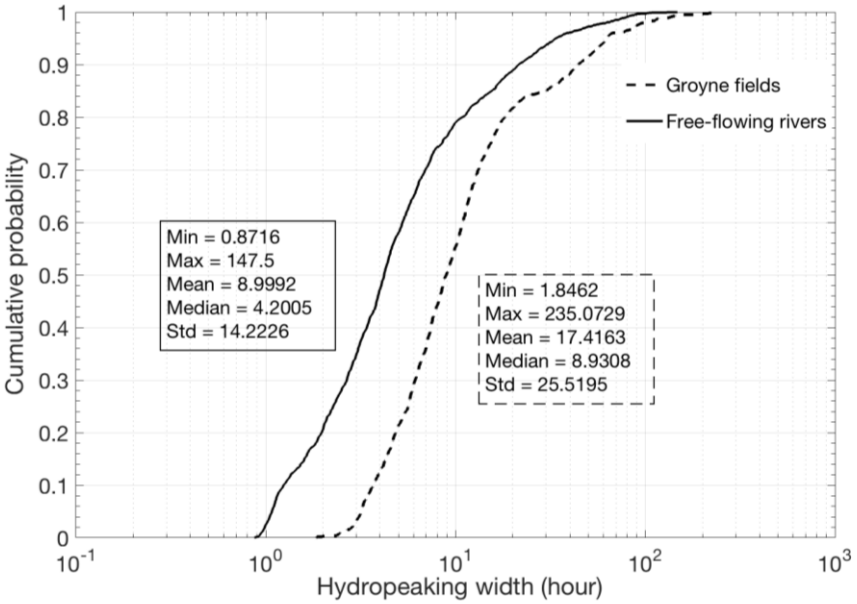

Figure 2.14 Cumulative probability plots of the average hydraulic waves half-prominence widths (in hours) at river reaches with groyne fields and the free-flowing ones.

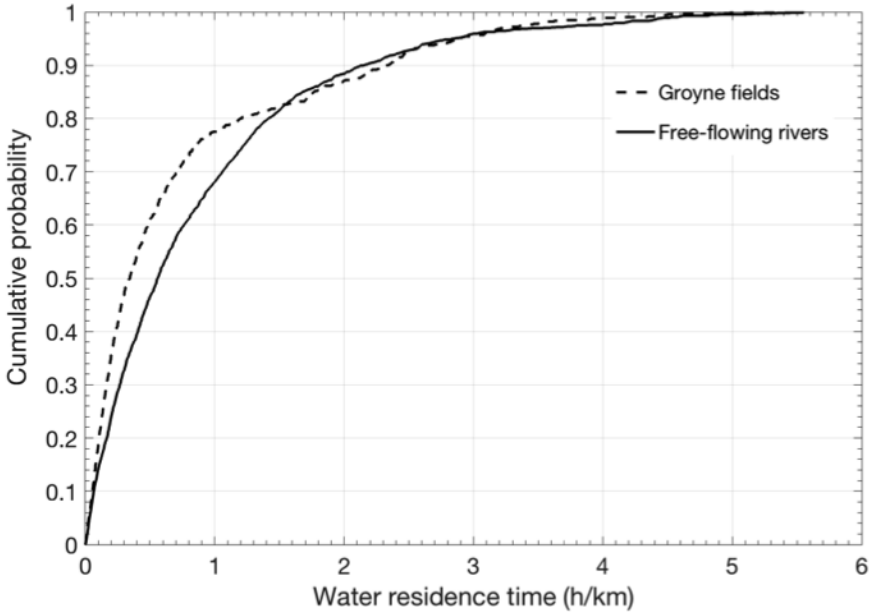

Figure 2.15 Cumulative probability plots of the estimated water residence time (h/km) for river reaches with groyne fields and the free-flowing ones.

2.4 Conclusions

Understanding the dynamics of in-stream water residence time could not only assist with water quality modelling in relation with nutrient retention, but also water management practices. Through application of the BRT model for estimating WRT in river networks, we identified that river discharge weights the most compared with river topologic and geomorphic attributes. We conclude that the BRT approach has the potential to be used for addressing how timescales of the hydrological cycle change at different scales. The results relative importance of geomorphological features provides implications for river restoration appraisals on runoff processes.

It is meaningful to investigate the retention time endpoints to identify threshold mechanisms by which potential of land use changes, drought or flood, and climatic stressors that affect water body condition, aquatic nutrient availability, and watershed integrity. The spatial distribution model contributes to an advanced methodology in WRT estimation in between of complex

deterministic process models and empirical statistical models, and can be applied to study areas of diversified scales. In combination with developed nonlinear spatial statistics could be another trend in solving hydro-geophysical or even social economic distribution related questions.

Acknowledgements

This part of work has been carried out within the SMART Joint Doctorate program “Science for the MAnagement of Rivers and their Tidal systems” funded by the Erasmus Mundus program of the European Union. The authors thank the Bavarian State Office for the Environment for providing hydrological dataset for Bavaria; and the ITZBund for providing hydrological monitoring dataset for Germany (www.pegelonline.wsv.de).

Chapter 3

Temporal-spatial propagations of hydropeaking: lessons learned from an alpine river basin

Abstract

Intermittent hydropower operation results in strong hydropeaking effects downstream, which are often associated with frequent changes in the water level and discharge dominated by geomorphologic conditions. Hydropeaking strongly influence the highly dependent biological communities and the ecological processes, especially in the most vulnerable alpine rivers in the mountainous areas. In order to grasp the realm of hydropeaking impacts, better understandings are needed in terms of temporal and spatial variation of the hydropeaking waves. In this work, long-term variations of the hydropeaking were analysed through applying the sub-daily indicators of hydropeaking characterization. Furthermore, we proposed a conceptual framework in terms of longitudinal spatial propagation of hydropeaking that transported to the downstream river reach. Hydrological and geomorphological contributions to the hydropeaking variation at different scales are analysed and discussed for the upper Rhone river basin in Switzerland. Results revealed that the key controlling geomorphologic factors of hydropeaking propagation within the homogeneous section is river width, slope, and the roughness coefficient. The study suggests a broader view on the potential hydropeaking management implications through analyzing the longitudinal propagation.

Keywords: Hydropeaking; Longitudinal propagation; Alpine rivers

3.1 Introduction

Substantial changes in the hydrological and thermal regimes in the hydropower-regulated catchments are processes that will take place on both global and regional scales (Milner et al., 2009). As a consequence of hydroelectric development and an extension of geomorphology variation, catchment hydrologic and thermal regimes will be altered significantly along the river reach. A period of higher discharge dynamics of hydropeaking (HP) (Zolezzi et al., 2009) will be followed by an interruption of hydrologic and ecological environmental conditions along the downstream river reach. High discharge rates from impoundments or hydropower production plants (HPP) result in disturbance of the thermo-structure and entrainment of nutrients into surface waters.

Hydropeaking as one of the most direct/important impacts from hydropower to aquatic ecosystems. Efforts have been done on the study of hydropeaking characterization and quantitative description of the variability since the last ten years (Sauterleute and Charmasson, 2014; Shuster et al., 2008; Zimmerman and Letcher, 2010). The most concerned issue was the hydro-ecological effects of hydropeaking upon the biological community and its habitat in the river downstream (Scruton et al., 2003; Tuhtan et al., 2012; Valentin et al., 1996; Young et al., 2011). However, the facets of hydropeaking itself are worth checking slowing down sometimes before rushing into the impacts and countermeasures analysis. Long-term variability of hydropeaking especially on different spatial scales in a hydropower-exploited river basin has not been well investigated so far. Studies on the total length and spatial distribution of affected river reaches are based on point data and result in “potentially affected reaches” (e.g. Tonolla, 2012). No model, not even simple ones that considering the physical effects that actually control hydropeaking waves propagation, has been developed and applied to this purpose so far.

Factors for the spatial propagation of hydropeaking are manifold: distance between the target gauging station and the hydropower plant outlet; physical obstructions along the stream channel; enrichment flows from the junctions and tributaries; and variations in cross-section geomorphologic settings (Hauer et al., 2013; Orlandini et al., 1998; Sauterleute et al., 2014). The alpine river systems are with typical features of the landscape with highly hydropower developments, receiving and distributing water resources that are most vulnerable to climatic and anthropogenic changes. Catchment characteristics of hydrological and geomorphological controls on the hydropeaking alterations are of particular interest to this question of flow regimes diversity and hydropower influence on the downstream rivers (Füreder, 2009).

In this paper we proposed the framework of analyzing longitudinal propagation of hydropeaking at spatial gradients of river segment, river reach and hydraulic unit. The approach based on long-term monitoring data and structural modelling can feature the temporal-spatial variations of hydropeaking with more detailed understanding from the major controlling factors of river hydromorphology. The results provide deeper insights into hydropower and water resources management by embracing the challenges of hierarchy in river landscapes.

3.2 Methods

Long-term patterns and particular short-term fluctuations are typically highly site-specific, depending on the local catchment area of the hydropower plant (Kumar et al. 2011). The propagation of flow in space and time through a mountainous stream networks is mainly complicated by three factors: junctions and tributaries, variation in cross section, and variation in resistance as a function both of flow depth and of location along the stream length (Orlandidi and Rosso, 1998). We proposed the framework of hydropeaking propagation to examine the study sites based on the steps of the following sub-sections.

3.2.1 Temporal variation characteristic

Schematic illustration of temporal variability is discussed through describing the sub-daily characteristics of hydropeaking. Sub-daily indicators for the magnitude of hydropeaking (HP1, dimensionless, Eq. 3.1) and the temporal rate of change (HP2, $m^3 \cdot s^{-1} \cdot h^{-1}$, Eq. 3.2) that developed by Carolli et al. (2015) are applied in this paper. The magnitude of hydropeaking (HP1) is affected by both the hydrological contribution from tributaries and the diffusion process of peak flows, while the value of HP2 is changed with the advection-diffusion process that controlled by geomorphologic settings (Figure 3.1).

$$\mathrm{HP1} = \frac{Q_{max} - Q_{min}}{Q_{mean}} = \frac{Q_p - Q_b}{Q_p + Q_b} * 2 \qquad \text{(Eq. 3.1)}$$

$$\mathrm{HP2} = \frac{\Delta Q}{\Delta t} = \frac{Q_k - Q_{k-1}}{t_k - t_{k-1}} \qquad \text{(Eq. 3.2)}$$

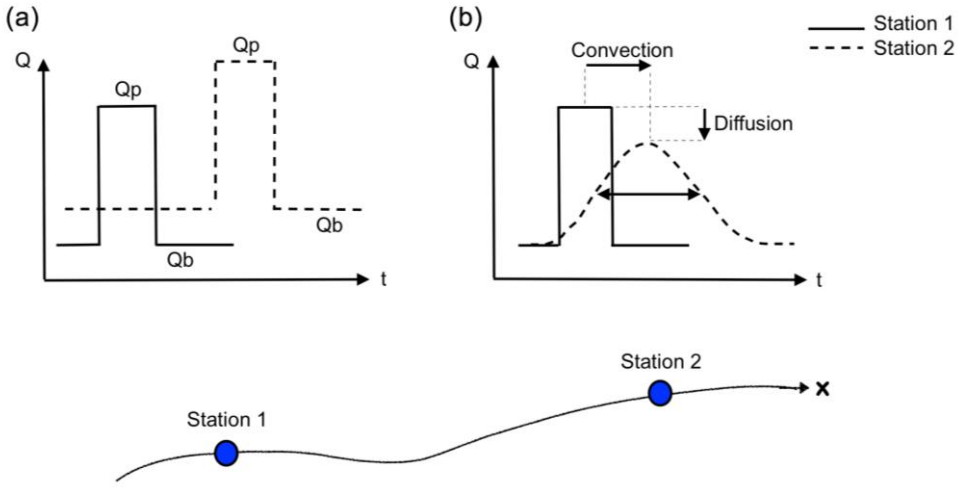

Figure 3.1 Schematic plots of the controlling factors of hydropeaking variation: (a) Impacts of incoming hydrologic contributions on the increased magnitude of hydropeaking (vice verse situation in case of water abstractions); (b) Hydraulic controls on hydropeaking diffusion and convection attributes by geomorphology settings. Station 1 and 2 is the upstream and downstream gauging station of the same river reach, respectively.

3.2.2 Spatial propagation factors analysis

Spatial perception into hydropeaking propagation and its main controlling factors begins with an overview of the landscape with physical obstruction of river connectivity, followed by an evaluation of hydrologic alterations by tributaries contribution, and geomorphologic controls on the hydraulic diffusion processes. The fate of hydropeaking is shaped by the traded-offs of these three aspects that consist of the spatial propagation framework.

3.2.2.1 Landscape heterogeneity and river segmentation

Geophysical obstructions such as hydropower dams, weirs, major impoundments, lakes and other landscape factors could directly interrupt the river connectivity. Sudden change of river width (i.e. river restoration practice) would affect the magnitude and variability of the diffusivity coefficient, resulting in different hydrological processes. In line with these considerations, careful geophysical observations are needed before locating the end point of homogeneous river segments as the first analytical unit.

3.2.2.2 Hydrologic controls on river reach unit

Based on the theory of continuity equation and simplified momentum equation, hydropeaking flows brought by the intermittent hydropower release is diffused and attenuated along the way to downstream river sections. However, large quantity of external inflows e.g. natural confluence or abrupt poured water into the river mainstream would create dilution effects to the flow regime and temperature regime. Getting to understand the longitudinal distribution of hydropeaking flows in the main stream cannot ignore the enrichment from tributaries.

The amount of the incoming discharge from tributaries (and sub-tributaries) to the main streams at each junction point is estimated through Drainage-Area-Ratio Method (Emerson et al., 2005) where no runoff data are

available. Calculations are made using the known discharge information of the same time period for the corresponding main stream by Eq. (3.3):

$$Q_L = Q_0 * (A_L / A_0)^{\Phi} \quad \text{(Eq. 3.3)}$$

in which Q_L is the estimated streamflow from ungagged tributary; Q_0 is the known discharge of the gauged main river reach; A_L and A_0 is the drainage area of tributaries and mainstream accordingly. In widespread practice, the exponent ϕ=1 (Emerson, 2005), therefore the calculation is a direct proportion of stream flow per unit area (km^2).

Instead of increased amount of discharge only, significant hydrological perturbation is identified when the magnitude of hydropeaking (HP1) is below threshold value ($HP1_{Threshold}$, Eq. (3.4)) based on the situation of non-hydropeaking affected stations. Critical contribution of discharge is calculated by Eq. (3.5), above which the dilution effects of tributaries are noticeable. On the other hand, the interference effects brought by tributaries could be neglected until the next junction point of significant hydrological alteration calls the end of the selected secondary-level river reach.

$$HP1_{Threshold} = HP1_{P75} + 1.5 \cdot (HP1_{P75} - HP1_{P25}) \quad \text{(Eq. 3.4)}$$

$$Q_{Threshold} = (HP1_{Threshold} \cdot Q_{mean}) + Q_{min} \quad \text{(Eq. 3.5)}$$

where P_{25} and P_{75} subscript is the 25^{th} and 75^{th} percentile value, respectively, Q_{mean} is the mean discharge of the main stream, Q_{min} is the minimum discharge accordingly.

3.2.2.3 Geomorphologic controls on hydraulic unit

The signatures of geomorphology prominent in river's cross-section width *B*, slope *s* and manning's roughness coefficient *n* are the most direct and determinant geomorphological parameters of the spatial hydropeaking propagation. Followed by the up-to-bottom scaled classification of the landscape homogeneous segment and of the hydrological alteration in the

river reach, the trail of hydropeaking is further delineated on the scale of hydraulic unit based on the application of one-dimensional hydrodynamic advection-diffusion model. Hypotheses are made as non-uniform and unsteady flows in the temporal and spatial aspects under the background that the propagation of hydropeaking waves in an open channel flow with longitudinal slope *s* that receives water discharge of different temperatures released from a hydropower plant. Hydrodynamic waves are simulated according to the simplified Saint-Venant equation. In the absence of sources or sinks, and constant diffusion coefficient, the 1-dimensional hydrodynamics in a rectangular channel is described using the simplified advection-diffusion equation (Eq. 3.6-3.7):

$$\frac{\partial D}{\partial t} + c\frac{\partial D}{\partial x} = k_w \frac{\partial^2 D}{\partial x^2} \quad \text{(Eq. 3.6)}$$

$$k_w = \frac{Qk^2 R_h^{4/3}}{2BU^2} \quad \text{(Eq. 3.7)}$$

where *D* is the water depth; *U* is cross-sectional averaged velocity; *c* is the celerity of hydrodynamic waves; t is time; x is the longitudinal distance along the flow paths; k_w is hydrodynamic diffusivity; *Q* is the discharge; k is the Gauckler-Sticker coefficient; R_h is the hydraulics radius; *B* is the river width; *U* is the cross-section averaged velocity. Boundary conditions are the known hydrological (Q_0 and Q_n) and geometric parameters at these two stations, respectively.

Hydrodynamics are represented by the hydropeaking waves front celerity and the height of water levels characterization. Understanding the characteristic time T_{dec} and distance L_{dec} where the hydropeaking waves begin to decay due to the dramatic decrease of the flow height is important for the hydropower and water resources management. According to Toffolon et al. (2010), simplified analytical solution of the longitudinal 1-D hydrodynamics is represented by Eq. 3.8. The time at which the maximum depth becomes smaller than the initial value D_p indicates the start of the decay is represented

by time (Eq. 3.9) and distance (Eq. 3.10):

$$D(x,t,x_0) = D_0 + \frac{\Delta D}{2}\left\{ erf\left[\frac{x'-c_f(t'-T_{hp})}{\sqrt{4k_{wt}(t'-T_{hp})}}\right] - erf\left[\frac{x'-c_f t'}{\sqrt{4k_{wh}t'}}\right]\right\} \quad \text{(Eq. 3.8)}$$

$$T_{dec} = T_{hp} + \frac{k_{wm}}{2}\left(\frac{l_w^*}{c_p-c_f}\right)^2\left[\sqrt{1+\left(\frac{2(c_p-c_f)L_{hp}}{l_e^* l_w^* k_{wm}}\right)^2}-1\right] \quad \text{(Eq. 3.9)}$$

$$X_{dec} = T_{dec} * c_f \quad \text{(Eq. 3.10)}$$

where x and t is the hydropeaking traveling distance and time; D_0 is the base flow depth; ΔD is the difference between the peak depth D_p and D_0; x' and t' is the spatial and temporal difference between the location where the release starts (initially set x'=x, t'=t); c_f is the front celerity; Diffusivity for head (k_{wh}), tail (k_{wt}) and the mean value, respectively; k_{wh}, k_{wt}, and k_{wm} are the hydrodynamics diffusion coefficients for head, tail and the mean of them, which are calculated through Eq. (3.7), respectively; T_{hp} is the release duration; L_{hp} is the whole wavelength where the decay starts.

$$L_{hp} = l_e^*\sqrt{k_{wh}t'} + l_e^*\sqrt{k_{wt}\left(t'-T_{hp}\right)} \quad \text{(Eq. 3.11)}$$

in which l_e^* and l_w^* are the dimensionless parameters. According to Toffolon et al. (2010), l_e^*=3.29 represents a 1% reduction of the step height function F. Thus when it comes to the 50% of F, l_e^*=2.3262. l_w^* is defined as below:

$$l_w^* = \frac{(c_p-c_m)^2}{(k_{wt}-k_{wm})(t'-T_{hp})} \quad \text{(Eq. 3.12)}$$

Thus, based on the analytical solution of hydrodynamic waves, the time and distance where the hydropeaking waves start to decay is obtained as geomorphological controlled unit of longitudinal diffusion.

3.3 Study area and database

The Rhone River, covering a basin area of 98,000 km^2, rises from the Rhone Glacier in Valais of the Swiss Alps at an altitude of 2150 meters. Complex hydropower regulation systems have produced strong hydropeaking

effects to the river networks. In this paper, we selected 7 major gauging stations in the upper and middle Rhone River basin in Switzerland (Figure 3.2). Long-term records of river discharge with 10-min resolution are collected for 35 years during 1980-2014. Geomorphology parameters of the stations are illustrated in Table 3.1. Along the river section of all the 7 gauging stations in the main stream, the change of elevation covers around 1400 meters since the first station in the headwater mountainous valley, flowing through 200 kilometers and reached the inlet of Lake Geneva in the lowland areas.

Hydropower plants (HPP) of 'storage-type' with impoundment are considered as physical obstructions here. Those of run-off hydropower plants are not taken into account instead. There are two small HPP with installed power capacity below 10MW in the downstream section near Porte du Scex, and four large HPP above 200MW (Table 3.2).

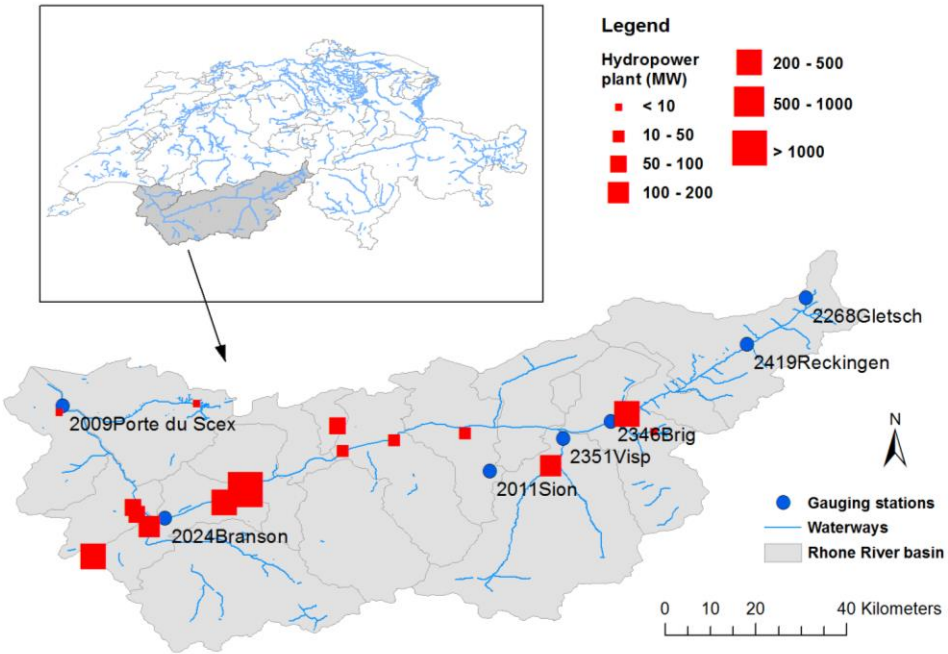

Figure 3.2 Rhone river basin in Switzerland and selected gaging stations (blue dots) and hydropower plants (red box, sized by the built power) from the upstream (Gletsch) to downstream (Porte du Scex) river networks. Labeled are the station code and name in accordance with Table 3.1.

Table 3.1 Geomorphology and flow regimes of the studied gauging stations. Surface area is the total area above each selected gauging station up to the nearest next one, including all sub-tributaries passing through. Distance is calculated by taking the first station 2268 as starting point.

ID	Name	Coordinates (CH1903/LV03)	Station elevation (m a.s.l)	Catchment mean elevation (m a.s.l)	Glaciation (%)	Surface area (km^2)	Average Discharge (m^3/s)	Distance from headwater (km)
2268	Gletsch	670810/ 157200	1716	2719	52.2	36.95	5.8	0
2419	Reckingen	661910/ 146780	1311	2306	17.5	193.00	20	16.1
2346	Brig	641340/ 129700	667	2370	24.2	655.99	249	32.9
2315	Visp	634030/ 125900	659	2660	29.5	300	24	43.9
2011	Sion	593770/ 118630	484	2310	18.4	1759.93	222	76.01
2024	Branson	573150/ 108300	457	2250	16.8	745.99	249	101.75
2009	Porte du Scex	557660/ 133280	377	2130	14.3	840.96	287	135.08

Table 3.2 Hydroelectric development schemes along the Upper and Middle Rhone River. (Data source: statistics on hydropower plants (WASTA) (Swiss Federal Office of Energy). Note: only the HPP of storage type are listed here.

ID	WASTA no.	Name	Location	Coordinate (WGS 84)		Distance to rivers (km)	Operation since	Power (MW)	Production (GWh)
				Lat	Lon				
Hydropower plant released to mainstreams									
1	509000	Vouvry	Vouvry	46.33624	6.88154	1	1902	7.5	6.12
2	502800	Turtmann	Turtmann	46.29543	7.68600	2	1925	21.5	70.1
3	503700	St-Léonard	St-Léonard	46.26057	7.44474	0.2	1956	34	93
4	503400	Navisence	Chippis	46.28130	7.54640	0.2	1908	50	290
5	507500	Miéville	Vernayaz	46.14638	7.02890	0.2	1950	60	110.4
6	507200	Vernayaz (CFF)	Vernayaz	46.13337	7.03592	0.5	1927	92	240
7	507300	La Bâtiaz	Martigny	46.10989	7.06176	0.5	1978	170	415
8	507400	Riddes	Riddes, Ecône	46.15747	7.20914	0.3	1956	225	667.8
9	505100	Nendaz	Riddes	46.18305	7.25151	0.05	1960	384	224
10	501200	Bitsch (Biel)	Bitsch (Biel)	46.33371	8.00760	0.2	1969	331	556
11	504950	Bieudron	Riddes	46.18300	7.25144	0.5	1999	1260	1780
Hydropower plant released to tributaries									
12	508700	Diablerets	Les Diablerets	46.35304	7.15459	11	1957	5.2	15.2
13	506800	Châtelard-Vallorcine	Vallorcine	46.05094	6.94912	10	1978	210	410
14	501375	Ganterbrücke	Ried-Brig	46.29790	8.06083	7	1990	5	23.2
15	503500	Croix	Croix/Ayent	46.30820	7.43417	6	1957	64	147
16	501800	Stalden (KWM)	Stalden	46.23033	7.85713	5.5	1965	180	518.4

3.4 Results

3.4.1 Temporal variation of hydropeaking

Long-term variations of hydropeaking over the 35 years in this pre-alpine river basin are plotted in Figure 3.3. In order to observe the effects of hydropeaking more clearly, seasonal comparisons of winter (December, January, February) and summer (June, July, August) are plotted for HP1 and HP2, respectively. Given the specific conditions of the Alpine Rivers with major snow melting effects as in spring and complicated heatwaves effects from air temperature or flooding effects that frequently occurred in summer, hydrodynamic waves are 'disturbed' with compounded effects. In this case, the magnitude of hydropeaking indicated by HP1 is distinctly observed in winter. The sub-daily change of temporal frequency is closed linked with the fluctuation of energy market of higher demands in summer and winter. The value of HP2 continued to decrease since 2001, reached the lowest level in 2009, slightly rebounded in 2010 and kept dropping until now.

A further examination of the seasonal variations of hydropeaking indicators showed more clear patterns of inter-annual difference among the hydropeaking affected ('peaked') and non-hydropeaking ('unpeaked') stations (Figure 3.4). Monthly variations of HP1 and HP2 values for the peaked stations are in line with the 35-year variations showed in Figure 3.3, while the HP1 and HP2 values for unpeaked stations remained a low level with a small increment with the higher precipitation during summer. For hydropower plants in the alpine regions, precipitations as well as melting snow and ice are the main drivers determining the seasonal generation (and storage) potential (Barry et al., 2015). In Switzerland, the seasonality of the water flows shows a general pattern with high inflows during summer months and low levels in the winter months (FOEN 2014b). Over many years, this hydrological pattern and the

consumption patterns have been quite stable and have led to storage levels with peaks during September and October and low levels in March and April (SFOE 2015).

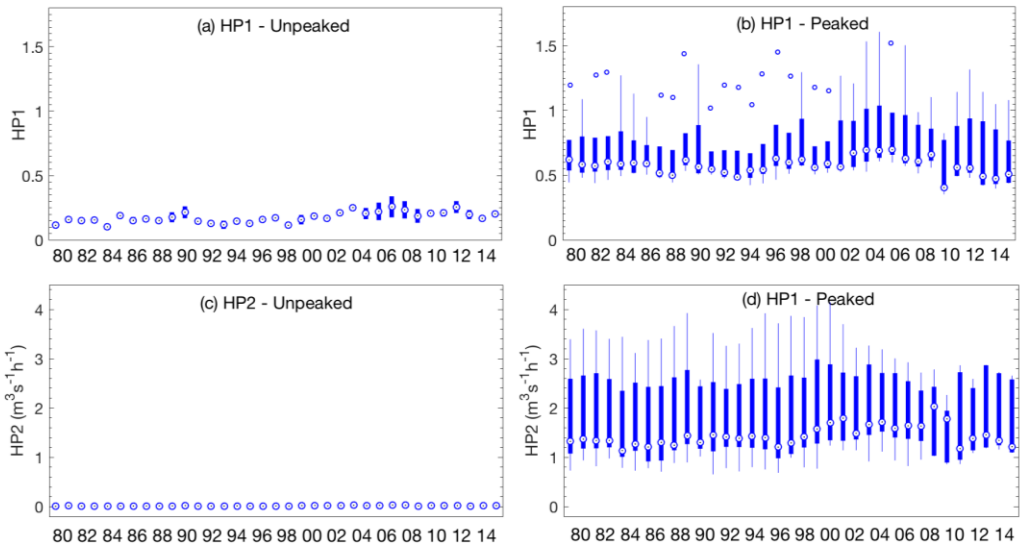

Figure 3.3 Boxplot of HP1 (a, b) and HP2 (c, d) variations of the peaked gauging stations and unpeaked stations during 1980-2014. Axes for the unpeaked and peaked stations are aligned at the same magnitude for easier comparison.

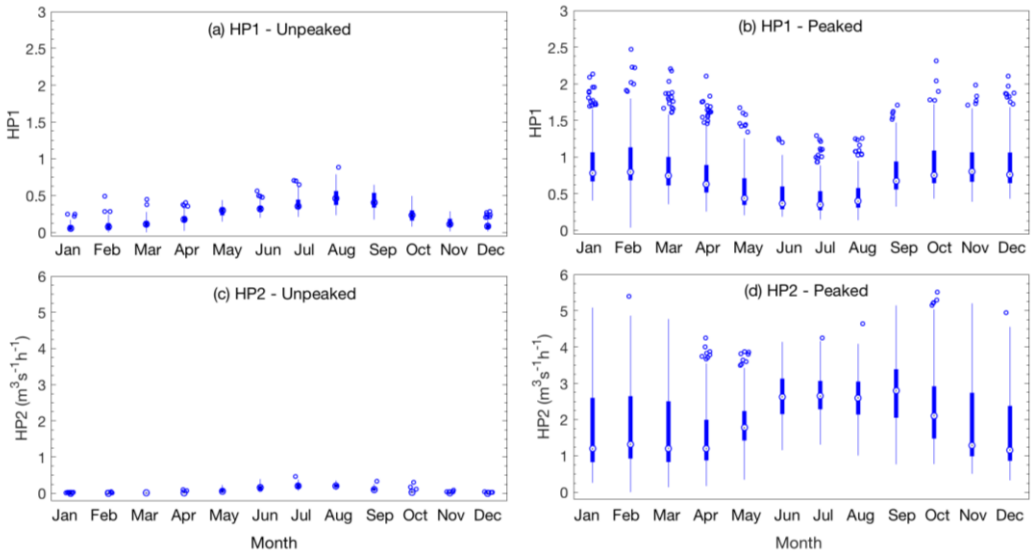

Figure 3.4 Inter-annual variations of the HP1 (a, b) and HP2 (c, d) indicator values for the unpeaked stations (n=2) and peaked ones (n=5) over the 35 years of 1980-2014. Axes for the unpeaked and peaked stations are aligned at the same magnitude for easier comparison.

3.4.2 Spatial variation of hydropeaking

The longitudinal variation of hydropeaking indicators are analysed for each station along the main stream (Figure 3.5). From the first station in the upstream to the second one (2268 - 2419), there are subtle changes of HP1, which correspond to the little hydrological contribution in Figure 3.6. In this section, hydropeaking propagation is dominated by the hydraulic advection-diffusion process with increased HP2 indicators. The second segment (2419 - 2346) shows both hydrologic and hydraulic control with increased two indicators. The third segment (2346 - 2351) is strongly dominated by hydropower activities within a small distance from the upstream station. Both HP1 and HP2 indicators are strongly altered. The fourth segment (2351- 2011) shows decreased HP1 while maintaining the same level of HP2 variability. It is dominated by geomorphic hydraulic process. The last two segments (2011 - 2024, 2024 - 2009) are affected by small hydrologic factors and increasingly dominated diffusion processes.

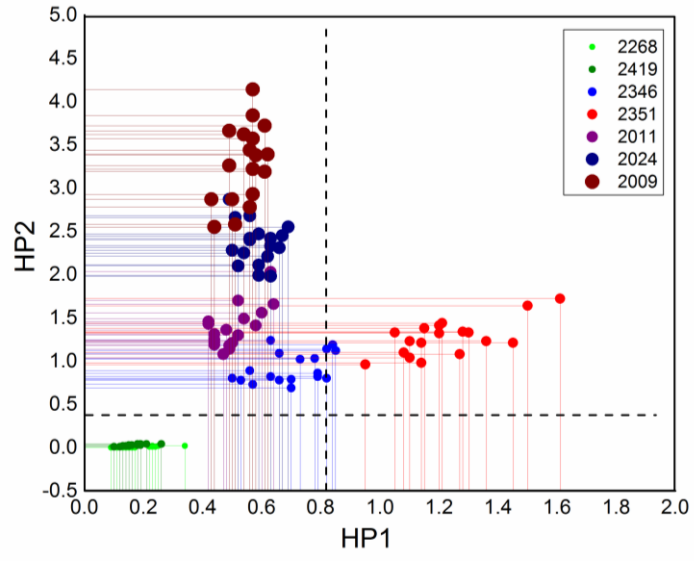

Figure 3.5 Scatter plot of hydropeaking indicators and thresholds (HP1: x-axis; HP2: y-axis) for the seven stations of 35-year values. Size of the colored bubbles are increasing with the distance of the head water (smaller in the upstream and bigger in the downstream).

In order to understand thus distributions of hydropeaking indicators displayed in Figure 3.5, we examined the main river reaches and 7 major gauging stations in the river basin based on the three-level framework of spatial propagation of hydropeaking described in part 3.2.2.

3.4.2.1 Landscape segmentation analysis

The first step of selecting analytical units considers the geomorphology obstructions of lakes, weirs, and dams along with the six major segments divided by seven gauging stations (Figure 3.6). Except from the first segment between station 2268 and 2419, there are hydropower stations above each gauging stations. The mainstream of the studied river basin was divided into 13 segments on the physical obstruction level. To be noted, only hydropower plants, which belong to the type of storage that is constructed with impoundment such as dams or weirs, are considered here as physical obstructions that destroy the river connectivity. Detailed information of the hydropower plants are listed in Table 3.2.

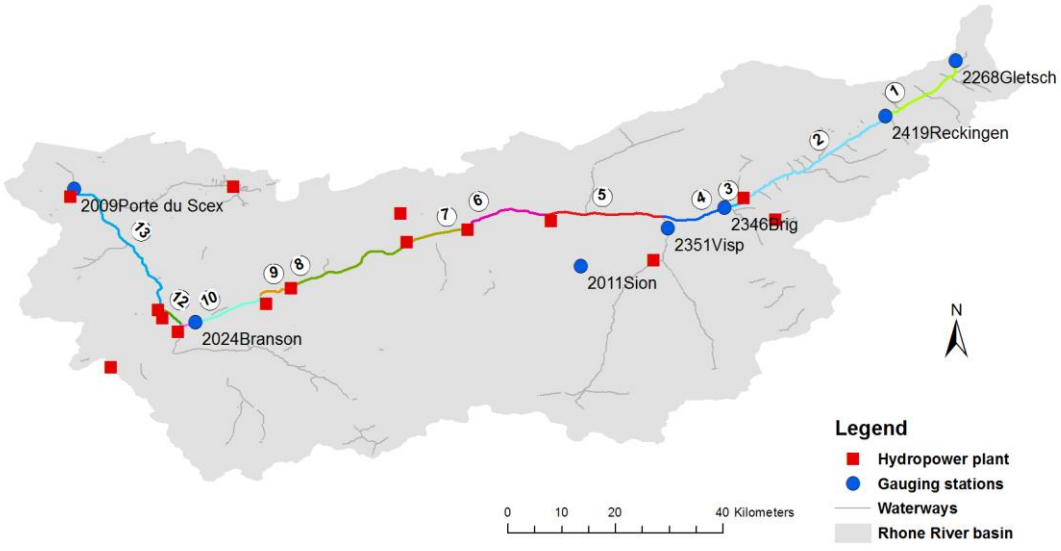

Figure 3.6 Landscape segmentation results of the main stream based on geophysical obstructions. Labled and colored lines are river segements divided by hydropower plants and gauging stations.

3.4.2.2 River hydrology-controlled river reach

An overall check of the hydrograph at the 7 gauging stations is followed by the hydrological classification of river reaches based on the river segments derived in Figure 3.7. In general, river discharge at the gauging stations showed an increasing trend along the main stream except for the station 2351 at Visp due to the interception by a large storage hydropower plant in the upstream.

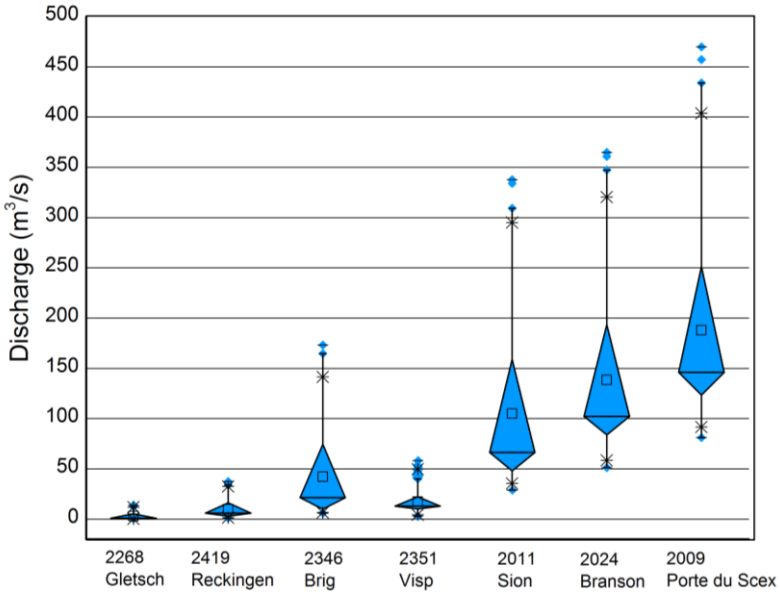

Figure 3.7 Boxplot statistics of daily river discharge during 1980-2014 at gauging stations in the main stream: gauging stations from the upstream in the left to the downstream in the right.

Further illustrations of the hydrograph for all the stations during 1980-2014 are plotted from Figure 3.8 to Figure 3.14. The unpeaked stations at Gletsch and Reckingen where shows natural flow variations have low values of hydropeaking indicators below thresholds (Figure 3.8 - 3.9). Special attentions are given to the highly altered flow regimes at Visp (Figure 3.11) where both HP1 and HP2 are above the threshold. From Sion to Porte du Scex (Figure 3.12 - 3.14), the magnitude of hydropeaking remained at the same level but the temporal change of frequency was increased, same with distribution in Figure 3.4.

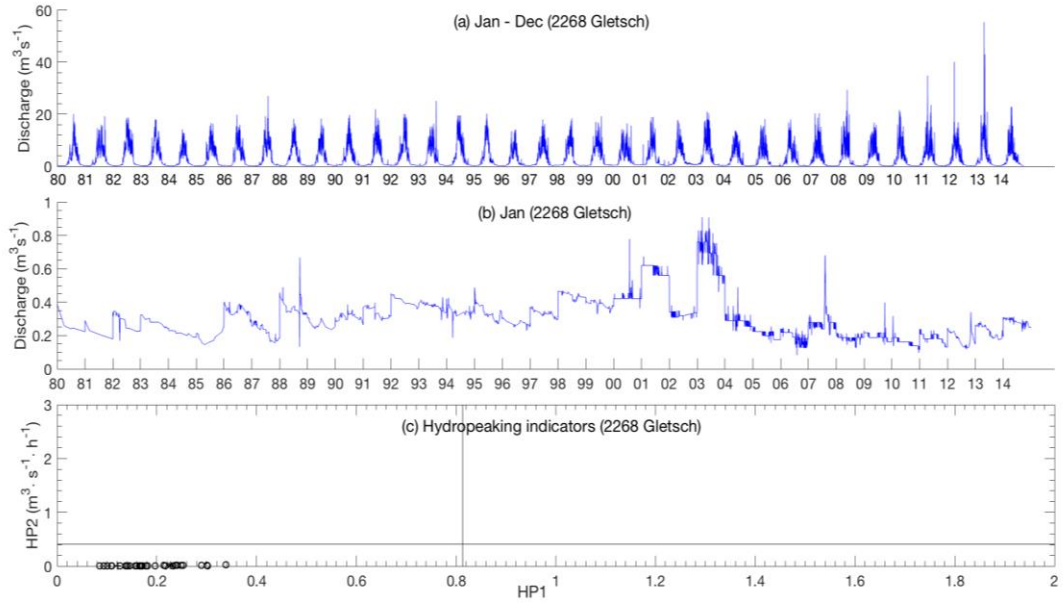

Figure 3.8 Hydrograph of gauging station at Gletsch (ID = 2268): (a) Daily discharge of the whole year during 1980 – 2014; (b) Daily discharge of January only during 1980 – 2014; (c) Distribution of HP1 and HP2 values.

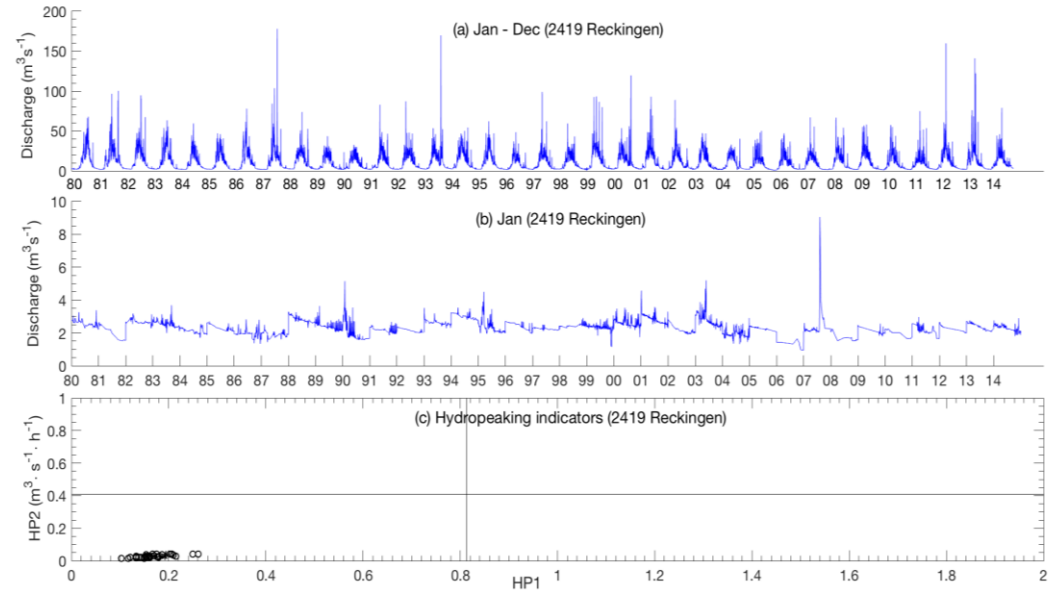

Figure 3.9 Hydrograph of gauging station at Reckingen (ID = 2419): (a) Daily discharge of the whole year during 1980 – 2014; (b) Daily discharge of January only during 1980 – 2014; (c) Distribution of HP1 and HP2 values.

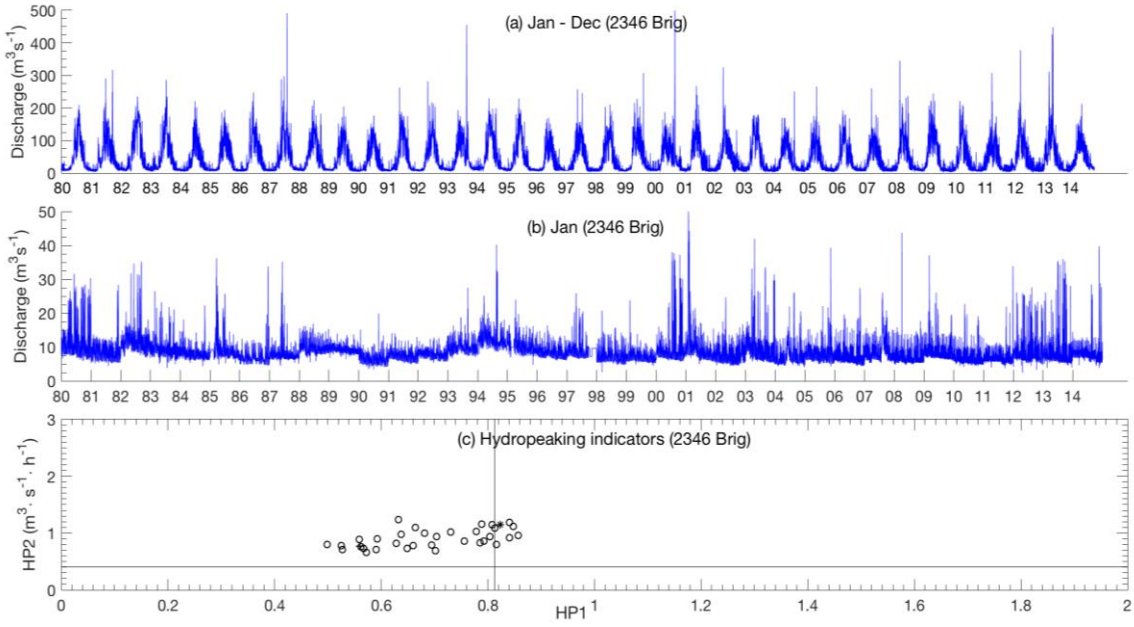

Figure 3.10 Hydrograph of gauging station at Brig (ID = 2346): (a) Daily discharge of the whole year during 1980 – 2014; (b) Daily discharge of January only during 1980 – 2014; (c) Distribution of HP1 and HP2 values.

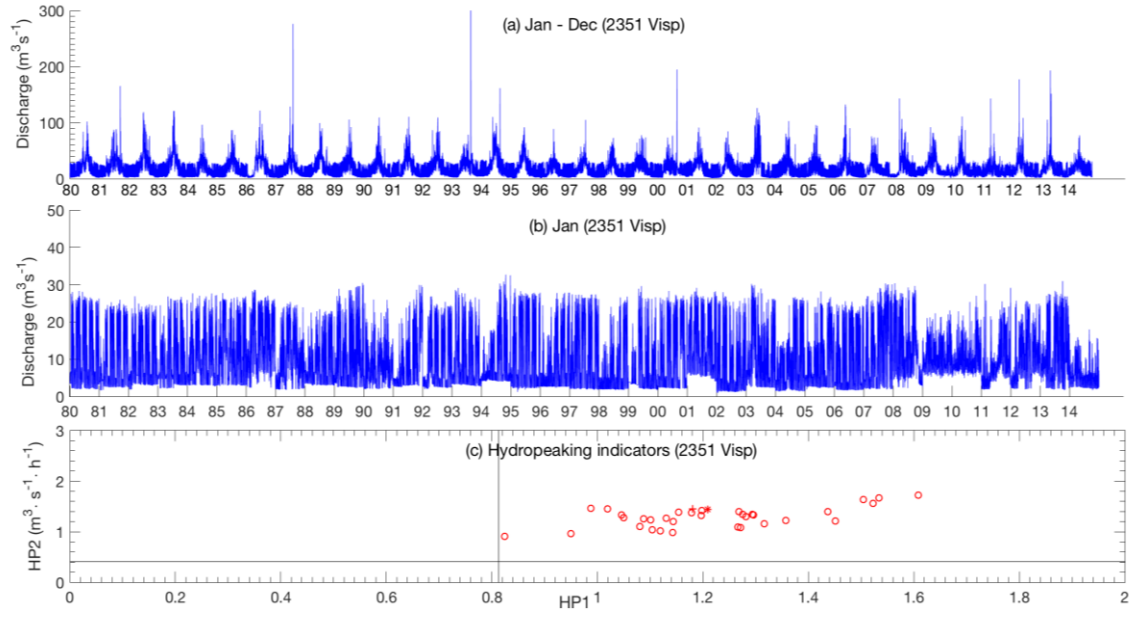

Figure 3.11 Hydrograph of gauging station at Visp (ID = 2351): (a) Daily discharge of the whole year during 1980 – 2014; (b) Daily discharge of January only during 1980 – 2014; (c) Distribution of HP1 and HP2 values.

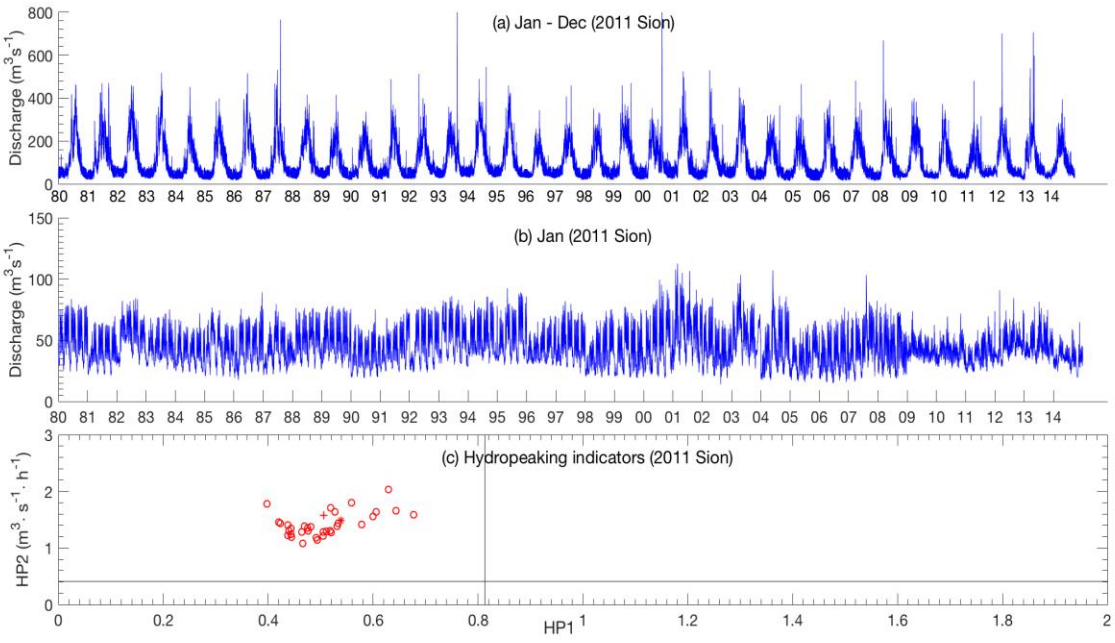

Figure 3.12 Hydrograph of gauging station at Sion (ID = 2011): (a) Daily discharge of the whole year during 1980 – 2014; (b) Daily discharge of January only during 1980 – 2014; (c) Distribution of HP1 and HP2 values.

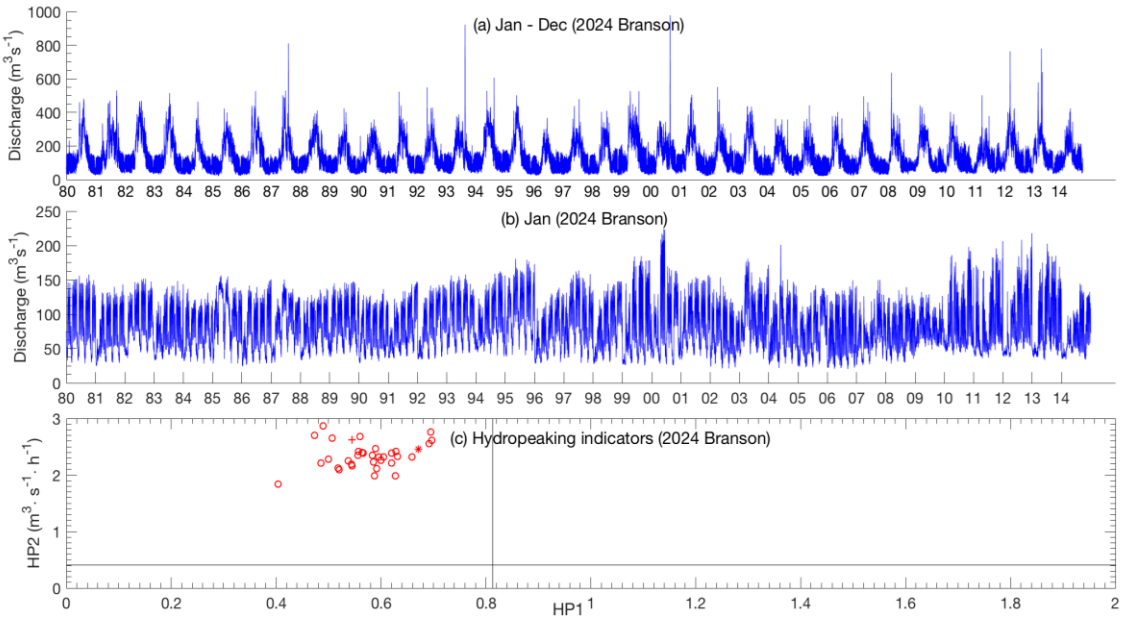

Figure 3.13 Hydrograph of gauging station at Branson (ID = 2024): (a) Daily discharge of the whole year during 1980 – 2014; (b) Daily discharge of January only during 1980 – 2014; (c) Distribution of HP1 and HP2 values.

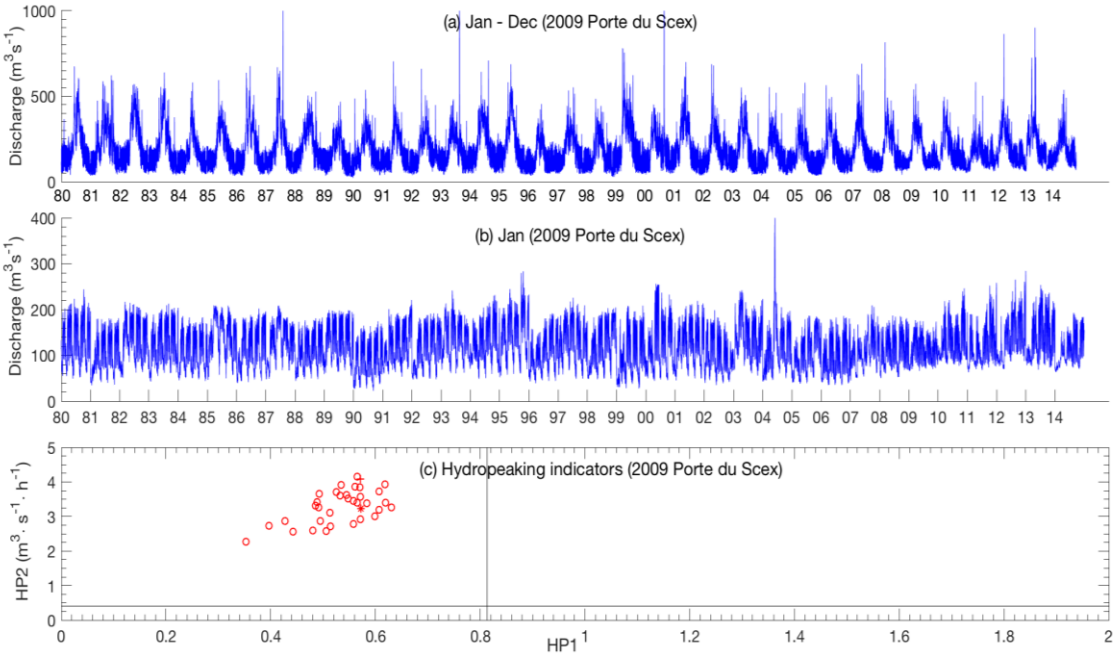

Figure 3.14 Hydrograph of gauging station at Porte du Scex (ID = 2009): (a) Daily discharge of the whole year during 1980 – 2014; (b) Daily discharge of January only during 1980 – 2014; (c) Distribution of HP1 and HP2 values.

Analyses of hydrological contribution by tributaries are performed within each physically divided segment in section 3.4.2.1. A sub-section is created in case of significant hydrological alteration occurs (Eq.3.3 - Eq.3.5) at certain junction point. Hydrology-controlled river reaches result with 5 more sub-sections thus 18 river reaches are divided as the secondary level (Figure 3.15).

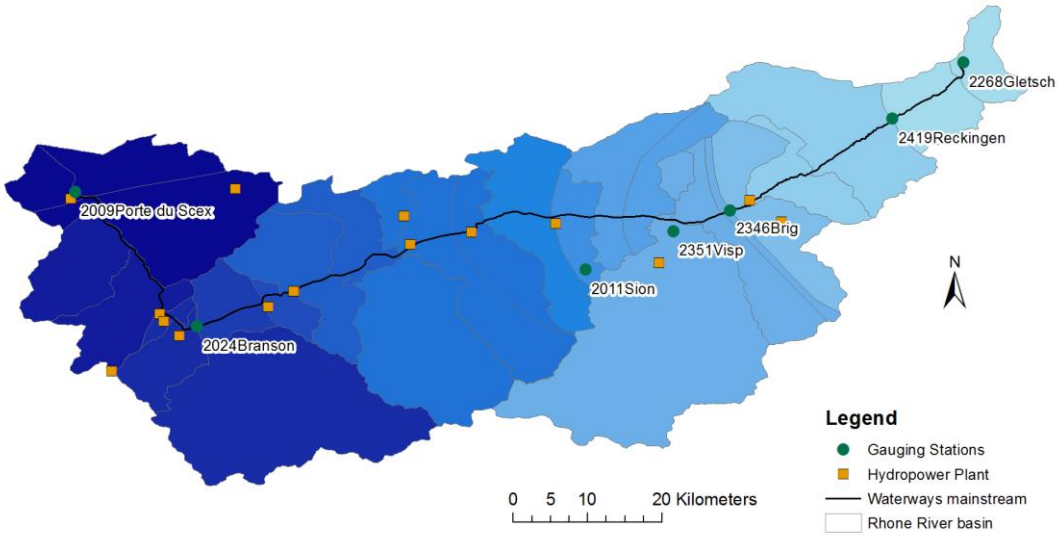

Figure 3.15 Hydrologically controlled river basin classifications based on the significant hydrologic control on the magnitude of hydropeaking. Seven major gauging stations are labeled with code and name. Yellow squares are the storage hydropower plants.

3.4.2.3 Geomorphology-controlled river reach

Together with the diffusion coefficient, the reduction in the amplitude of hydrodynamic square waves is affected by geomorphologic parameters as well as by the variations of water depth and river discharge. By taking the examples of hydrograph in January, results of geomorphologic controlled distance (X_{dec}) and time (T_{dec}) are solved for stations with hydropeaking impacts. Results of the hydropeaking affected gauging stations (except unpeaked stations of 2268 and 2419) and their subsequent river reaches are compared to provide an idea of spatial variations with geomorphological characteristics (Table 3.3).

Although having the same duration of hydropeaking release, station 2351 and 2024 resulted with very different values of T_{dec} and X_{dec}. The time and distance where the hydropeaking waves start to decay is a combination effects of hydrodynamics. The results of explanatory regression analysis for the ordinary least squares (OLS) model showed that the positive variables on the X_{dec} include drainage area of the gauging station (***, $p<0.01$) and the height of square waves (***, $p<0.01$); negative variables include the manning's

coefficient (**, p<0.05) and river width (***, p<0.01). The value of drainage area is correlated with river width and mean discharge (adjusted R-squared = 0.7822).

Table 3.3 Geomorphic parameters and solved time and distance of decay for each gauging stations in the main stream: base flow (Q_0), peaking flow (Q_p), hydropeaking release duration (T_hp), and time (T_{dec}) and distance (X_{dec}) where hydropeaking waves start to decay.

ID	Name	Slope	Width (m)	Manning's n	Q_0 (m^3/s)	Q_p (m^3/s)	T_hp (h)	T_{dec} (hours)	X_{dec} (km)	X_q (km)
2268	Gletsch	0.0252	13.56	0.04	0.26	0.59	-	-	-	15.48
2419	Reckingen	0.0383	18.83	0.03	1.95	3.01	-	-	-	15.25
2346	Brig	0.0017	28.2	0.05	8.72	23.79	8.83	14.2464	103.742	8.89
2351	Visp	0.0041	35.01	0.02	3.62	27.2	11.66	12.1732	148.65	4.97
2011	Sion	0.0011	61.3	0.023	30.55	72.08	6.66	40.0895	270.74	19.94
2024	Branson	0.0024	49.5	0.023	40.49	142.6	10.66	38.0687	444.87	12.97
2009	Porte du Scex	0.0049	77	0.1	65.6	199.5	11.66	17.6063	410.943	13.60

In comparison with the hydrological controlled river sub-basins in Figure 3.15, a classification of the geomorphological controlled river basins is derived after each gauging stations based on the distance that hydropeaking waves start to decay (Figure 3.16). The first two gauging stations in the upstream are colored with full distance to the downstream stations, as they are free from hydropeaking effects.

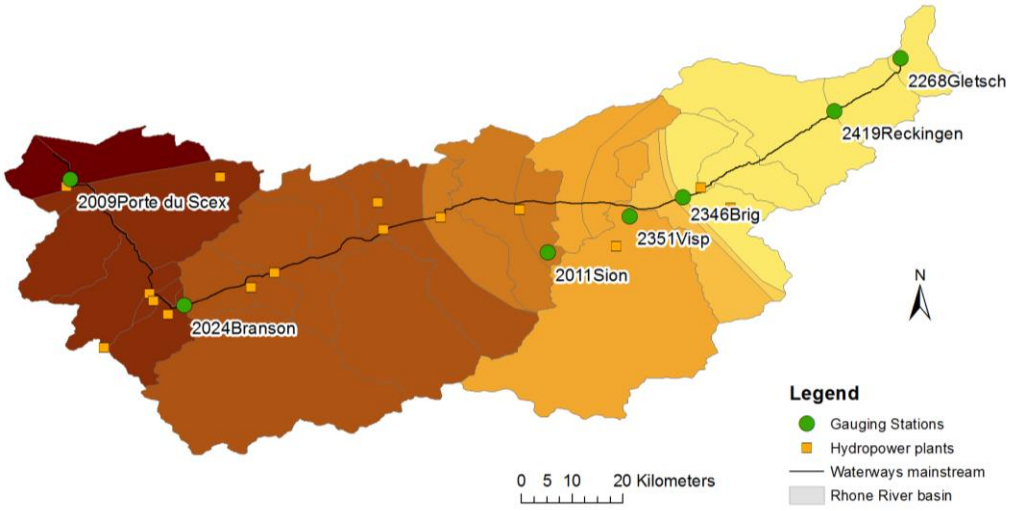

Figure 3.16 Morphologically controlled river basin classifications based on the significant geomorphic control on the hydropeaking waves attenuation. Seven major gauging stations are labeled with code and name. Yellow squares are the storage hydropower plants.

3.5 Discussion

3.5.1 Trade-offs of the two controlling factors

In order to highlight the river reaches with hydrological and geomorphological controlling factors, respectively, a hot spot analysis (Getis-Ord Gi* statistic) is performed through the Hot Spot Analysis tool (Spatial statistics toolbox, ESRI 2016). The hotspot analysis uses vectors to identify the locations of statistically significant hot spots and cold spots in data. Comparing the hot spot map of the main stream for these two controlling factors (Figure 3.17 and Figure 3.18), the headwaters in the upstream (above station 2346 at Brig) are controlled by natural flows of hydrological contributions from tributaries, while the lower river reach is more prominent in geomorphological controls on the kinematic hydraulic waves. The river reaches in the middle river basin that are with no significant prominence are subjected to geophysical obstructions by intensive hydropower interruptions. Improving the availability of the dataset of the gauging stations and hydropower plants along these river reaches could help improve the

understanding of the distance of hydropeaking propagation in the middle part. The results of hot spot analysis are in conformity with the spatial variability of hydropeaking indicators of HP1 and HP2 in Figure 3.4.

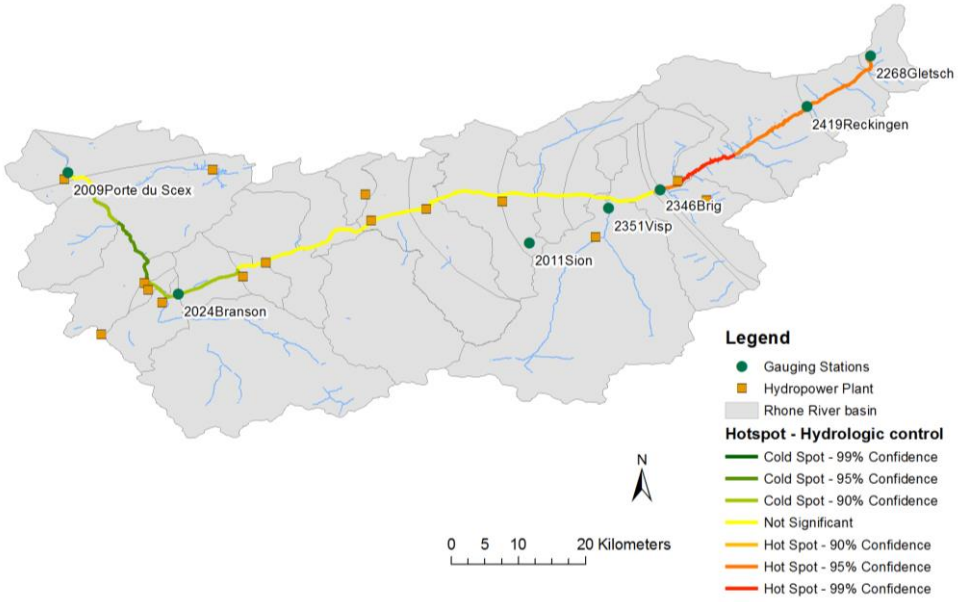

Figure 3.17 Hotspot analysis of hydrologically controlled river reaches. A color gradient is used to indicate distance of increasingly higher confidence under hydrological control.

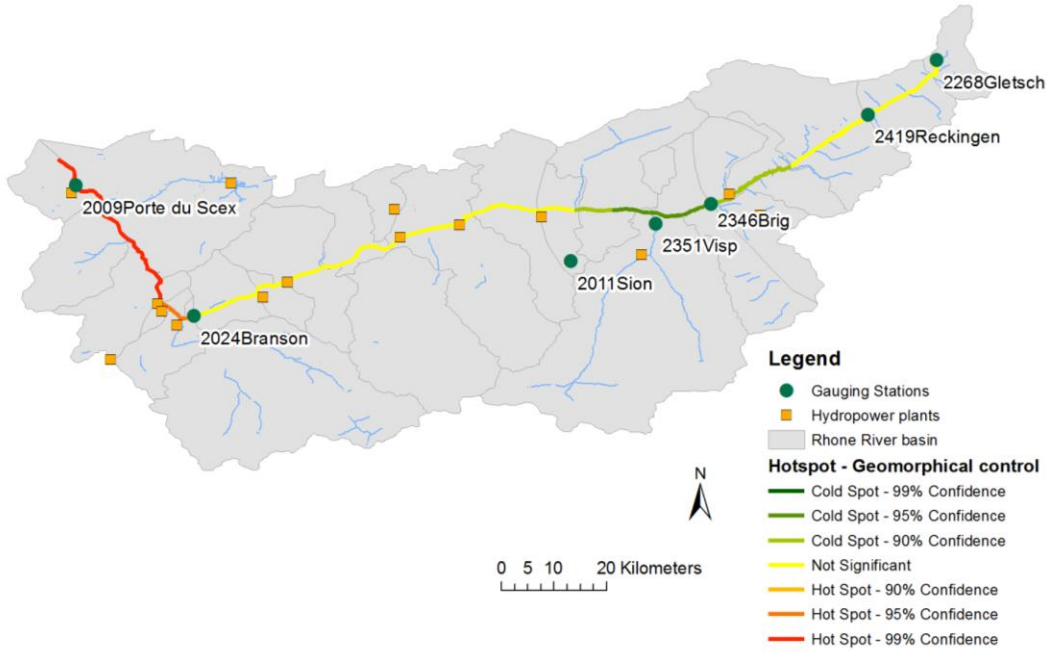

Figure 3.18 Hotspot analysis of the geomorphologically controlled river reaches. A color gradient is used to indicate distance of increasingly higher confidence under geomorphological control.

3.5.2 Hydropeaking variability in relation with the energy market

Hydropower is considered as compensation to the intermittent renewable generation from solar and wind. The electricity generation in Switzerland is characterized by 56% of hydropower production (Abrell, 2016). From the 1990s, hydropower production in Switzerland varied with several peaks of increasing and falling down around every ten years (Figure 3.19). A similar trend is observed for the hydropeaking indicators' variation in Figure 3.3. Although these statistics of electricity production is for the whole country, it represents some peeks for the Rhone River basin as well.

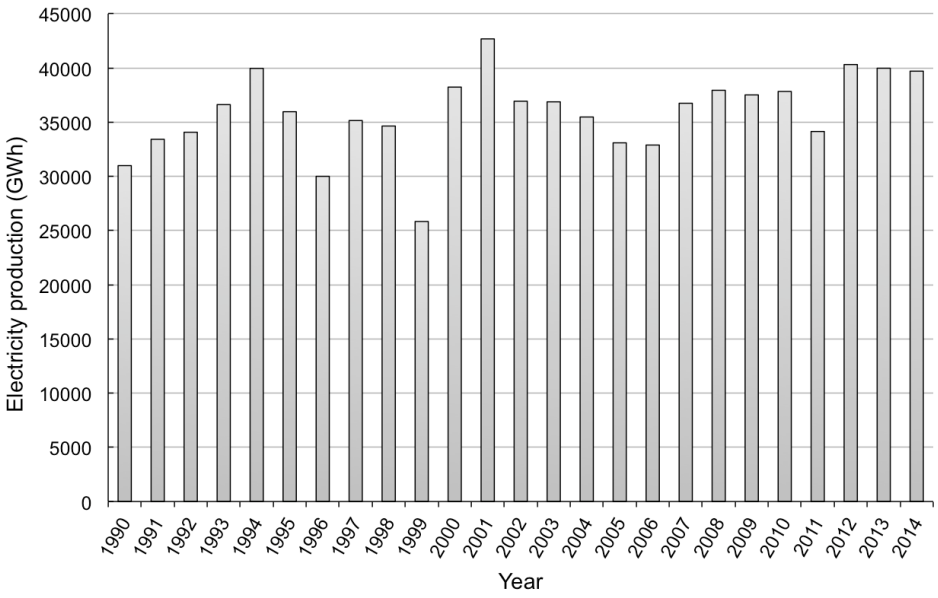

Figure 3.19 Statistics of electricity production by hydropower (GWh) in Switzerland, from 1990 to 2014. (Data source: International Energy Agency http://www.iea.org/statistics/).

3.5.3 Thermopeaking variability under hydropeaking effects

Temporal and spatial implications of hydropeaking on river thermal regimes are displayed as altered daily oscillations of water temperature with irregular patterns, which is referred to as thermopeaking effects (Zolezzi et al., 2011). To get a visual understanding of these contrasting

hydro-thermopeaking effects, an example observation for the sub-daily hydrographs and temperature graphs are illustrated for the representative peaked gauging station 2019 and unpeaked station 2135 in Switzerland (Figure 3.20). As mentioned before, in order to show the hydropeaking effects more clearly, we take the dataset in January for illustration. In line with the sunrise and warmed up air and water temperature, the natural patterns of river water temperature showed regular daily oscillations at unpeaked stations. However, the variations of water temperature under hydropeaking effects are amalgamated with the square waves of hydropeaking. Further detailed analyses of the thermopeaking effects for hydropeaking affected stations and un-affected stations in the alpine rivers are discussed in Chapter 4.

Apart from the example illustration in January, full display of river water temperature variations over the 35 years along with the distribution of thermopeaking indicators (see the methods part in Chapter 4) are plotted for the gauging station 2011 at Sion (Figure 3.21) and station 2009 at Porte du Scex (Figure 3.22).

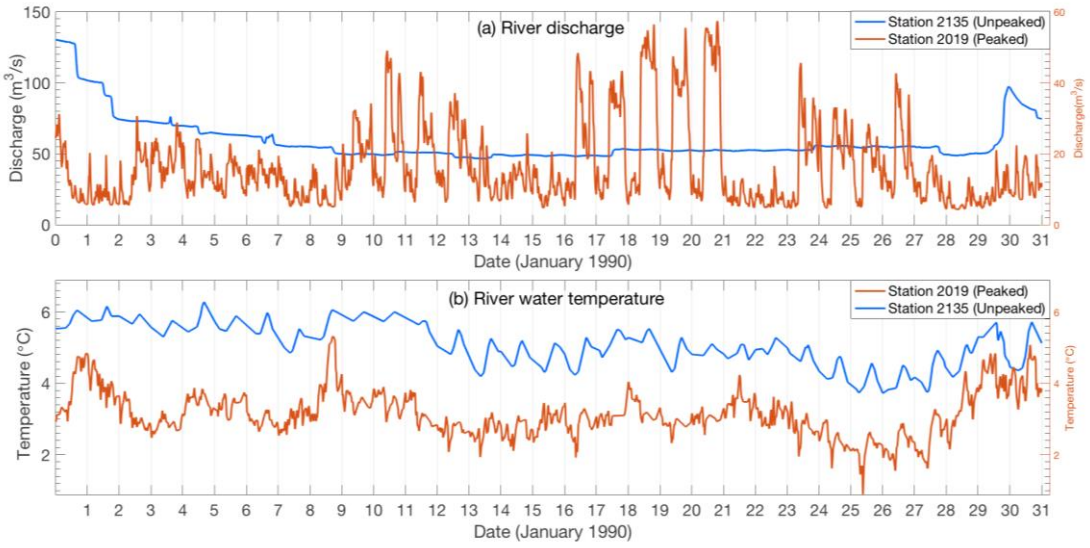

Figure 3.20 Comparison of sub-daily variation of (a) river discharge and (b) river water temperature for representative unpeaked station (ID = 2019, blue) and peaked station (ID = 2135, orange) during January 1990.

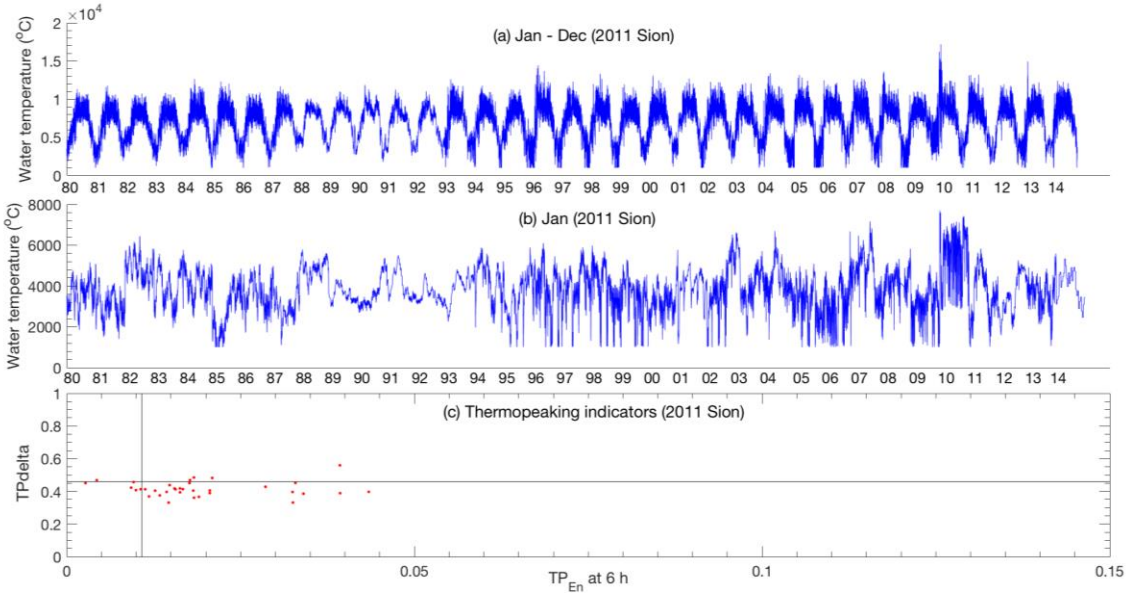

Figure 3.21 River water temperature at gauging station of Sion (ID = 2011): (a) Sub-daily water temperature of the whole year during 1980 – 2014; (b) Sub-daily water temperature of January only during 1980 – 2014; (c) Distribution of sub-daily water temperature rate of change (TPdelta), and the frequency of sub-daily temperature fluctuations (TPEn). Vertical and horizontal lines are the threshold value calculated according to Vanzo et al. (2016).

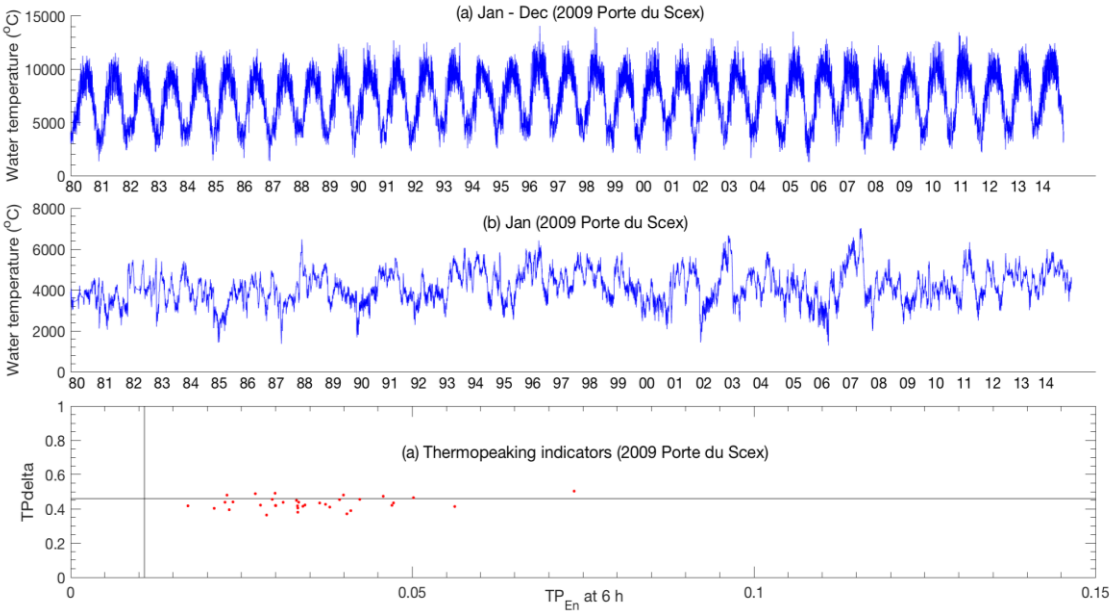

Figure 3.22 River water temperature at gauging station of Porte du Scex (ID = 2009): (a) Sub-daily water temperature of the whole year during 1980 – 2014; (b) Sub-daily water temperature of January only during 1980 – 2014; (c) Distribution of sub-daily water temperature rate of change (TPdelta), and the frequency of sub-daily temperature fluctuations (TP_{En}). Vertical and horizontal lines are the threshold value calculated according to Vanzo et al. (2016).

3.5.4 Implications for the local-scale management

Floodplain management is considered as cost-effective option to attenuate flood peaks and to lower nutrient loads along river corridors (Natho and Venohr, 2014). Understanding the controlling factors of hydropeaking propagation and its spatial ranges is of great importance for hydropower management practices and for assessing the impacts on riverine ecosystems. Identifying the major geomorphological factors for hydropeaking propagation would assist with river restoration activities (Schirmer et al., 2013), which results in modification of geomorphology and corresponding controlling effects on hydropeaking.

In the further analysis, a combination of the open data server with our framework of the hydropeaking propagation analysis by creating the impact summary map in GIS platforms (ESRI, 2011). This interactive map highlights who and what has been impacted by hydropeaking and shows the effects and potential impact, and most importantly, its location, and the infrastructure, businesses, population, households, biodiversity in and around area of the hydropower plant. The analysis allowed identifying regions with high proportions of hydropeaking impacts. In this case, it would be highly useful for the management practices and the public communities.

3.6 Conclusions

Given the enormous amount of natural and human-affected riverine systems in the Alpine areas, it is important to understand the mitigation effects of hydropeaking waves along the river. As a further exploration of the human implications on nutrient transportation as discussed in the second chapter of the thesis, application of hydropeaking analysis would benefit the understandings of flood control or nutrient transport mechanisms of key water quality indicators.

Based on the advection-diffusion theory, hydrodynamics waves are simulated and characterized along the river mainstream of a hydropeaking-affected river. We analysed the hydrological and geomorphological controlling factors for the longitudinal propagation of hydropeaking, as well as the time and longitudinal distance where the hydropeaking waves start to decay for the seven major gauging station in the Rhone River basin in Switzerland. Geomorphology homogeneity of the drainage area, river width, and the manning's roughness coefficient are identified as the most fundamental parameters during the river hydrodynamic processes.

This research provides a methodology for characterization of artificial hydrological regime alterations within a variety of geological and climatic settings. The developed and discussed framework of hydropeaking propagation in the highly regulated pre-alpine rivers provides a reliable description of the dynamic processes and controlling factors of hydropeaking waves on the river reach scale. The application of this new methodology will build essential information for assessing the hydropower development of the alpine river systems through stream hydrologic and geomorphological variations.

Acknowledgements

This part of work has been carried out within the SMART Joint Doctorate program “Science for the MAnagement of Rivers and their Tidal systems” funded by the Erasmus Mundus program of the European Union. The authors thank the Swiss Federal Office of the Environment (BAFU) to provide stream-flow data and river water temperature dataset analysed in this Chapter.

Chapter 4

Response of water temperature to extreme heatwaves under hydropower regulation in the alpine rivers

Abstract

During the past 30 years, two major heatwaves in 2003 and 2006 in Europe have broken the highest temperature records of the past 500 years. We analysed the potential response of several river sections that are subject to hydropeaking and thermopeaking effects by intermittent water releases from hydropower stations, and of river sections without these effects. Thermopeaking in alpine streams is known to intermittently cool down the river water in summer and to warm it up in winter. We analysed the response of river water temperature to air temperature during heatwaves for 19 gauging stations across Switzerland, using a 30-year dataset at 10 minutes resolution. Stations were classified into an 'unpeaked and a 'peaked' group according to four statistical indicators of hydropeaking and thermopeaking pressure. The peaked stations were subject to a reduced temporal variability of river water temperature, as well as to weaker equilibrium relationship towards air temperature changes, compared with the unpeaked stations. Such behavior is reflected by peaked stations showing a much weaker response to heatwaves compared to the unpeaked ones. To be noted, this 'cooling effect' created by the hydro-thermopeaking is more outstanding in 2003 and 2006 under heatwaves. Analysis of continuous duration of thermal stressful events for typical cold eurythermal fish species (brown trout) showed improved environments at peaked stations during heatwaves. While the presence of hydropower operations in high-mountains with hypolimnetic water release may

locally mitigate the adverse effects of heatwaves on downstream river ecosystems, the present results add to the complexity of artificial physical template associated with flow regime regulation in alpine streams.

Keywords: Hydropeaking; Thermopeaking; Heatwaves; Thermal habitat; Alpine rivers.

4.1 Introduction

Meteorological observations of the last hundred years indicate considerably accelerating climate warming (Crowley, 2000; Schar et al., 2004). Summer heatwaves are predicted to become more frequent and extreme in Europe, in line with trends already observed in recent decades (Barriopedro et al., 2011; Rebetez et al., 2009). The heatwaves in 2003 and 2006 were spot with the maximum air temperature anomalies increased by more than 19℃ They had extensive magnitude and spatial scales, with worries of adverse impacts over large areas (IPCC, 2007). It is expected that summer heatwaves will return with more frequency and magnitude in Europe during this century (Della-Marta et al., 2007; Meehl and Tebaldi, 2004), which may result in severe adverse effects on human health (Fischer and Schär, 2010) as well as on aquatic ecosystems (Hari et al., 2006).

Previous studies on the effects of climate change on river water temperature (RWT) have shown significant increase of WRT compared to historical average values in the last decades (Bourqui et al., 2011; Chen et al., 2012; Null et al., 2013; Sinokrot et al., 1995). This warming has been attributed to rising air temperature (AT) (Edinger et al., 1968; Webb & Nobilis et al., 1995) and extreme heatwave effects caused by global climate change (Hammond et al., 2007). River ecosystems are subjected to several major pressures arising from climate change (Chen et al., 2007), as peaked hydrology, accelerated biochemical metabolism, and increasing human uses such as damming or water abstraction, which are expected to severely affect aquatic biodiversity

and ecosystem functions (Praskievicz et al., 2009). Thereby, the stream sensitiveness to the warming temperature - especially extreme heatwaves - has not been well understood so far (Luce et al., 2014). Heatwaves may indeed result in extreme temperatures, which may severely affect populations of cold-stenotherm aquatic biota (Hari et al., 2006; Yates et al., 2008), which may respond to extreme high temperature by cessation of growth, inability to reproduce successfully, or even die-off.

Increase of RWT in individual rivers may differ considerably, as it is influenced by river size, channel depth, flow velocity, and other variables (Arismendi et al, 2012). Additionally, RWT is influenced by human alterations of river systems, especially by the construction of reservoirs (David et al., 2000) and related dam operations. In the European Alps, 79% of the river reaches are influenced by hydropower operations (Truffer, 2010). In most countries of the European Alps the hydropower production potential has already largely been exploited, covering a fundamental share of the national electricity production in several countries, up to 57% in Switzerland (Crettenand, 2012). Thereby, in order to meet peak demands for electricity especially during the working time of energy-intense industries or private demands, hydropower operations create modifications of flow and water temperature through intermittent flow releases occurring mostly at daily and sub-daily frequency, which are referred to as ‘hydropeaking’ (e.g. Moog et al., 1993) and ‘thermopeaking’ effects (Zolezzi et al., 2011).

Thermopeaking is related to reservoirs with hypolimnetic releases, which typically causes a reduction of downstream RWT in summer, and increase in winter. Hence, it has been suggested that reservoirs with hypolimnetic relaease may partially offset RWT increase associated with climatic factors in downstream river sections (Null et al., 2010), and thus somehow paradoxically may contribute to support the survival of cold-stenotherm fish, as salmon during summer (Yates et al., 2008). However, such potential effect does not

seem to have been quantified so far in relation to a set of target river reaches.

The present Chapter aims to make an attempt in this direction and specially intends to address the following questions: (1) to quantify the effects of selected summer heatwaves on the water temperature of a set of alpine river reaches; (2) to determine the difference in thermal response to heatwaves between river reaches affected by hydro- and thermaopeaking, and those that are not affected by intermittent power plant releases; (3) to quantitatively suggest one potential ecological implications of such different response for fish physical habitat. We answer these questions by investigating the hydro-thermopeaking characteristics in a set of Swiss alpine rivers and by characterizing their water temperature responses, with the special attention paid to the year 2003 and 2006 heatwave events that had significant signatures in European especially in alpine riverine systems (Beniston, 2004; Fischer, 2014; Rebetez et al., 2009).

4.2 Material and methods

4.2.1 Study area and dataset

The study is based on a multi-decadal and high temporal resolution dataset of river streamflow, RWT and AT time series of 10-min resolution covering 19 gauging stations in the Swiss Alps during 1984-2013 (Table 4.1). These stations span an elevation range of the catchments from 262 until 1645 m a.s.l, with a percentage of glaciers in the catchment from 0 to 21%. Air temperature records measured at 2 m height at the meteorological stations of Zurich, Basel, and Geneva were collected and further averaged to obtain a representative AT time series for Switzerland due to the similar elevations above sea level of the three stations (Beniston et al., 2004; Kuglitsch et al., 2009).

Table 4.1 Geographic information of the 19 gauging stations for both discharge and water temperature with outcomes of the hydropeaking (HP) and thermopeaking (TP) classification (Section 2.2).

Code	River	Reach	Station elevation (m a.s.l.)	Mean catchment elevation (m a.s.l.)	Drainage area (km²)	Glaciation (%)	Coordinates (CH1903/LV03)		Group
2425	Kleine Emee	Emmen	431	1050	477	0	664220	213200	Unpeaked
2016	Aare	Brugg	332	1010	11726	2	657000	259360	Unpeaked
2029	Aare	Brugg -aegaerten	428	1150	8293	2,9	588220	219020	Unpeaked
2044	Thur	Andelfingen	356	770	1696	0	693510	272500	Unpeaked
2070	Emme	Emmenmatt	638	-	443	-	623610	200430	Unpeaked
2091	Rhein	Rheinfelden	262	1039	34526	1,3	627190	267840	Unpeaked
2135	Aare	Bern-Schonau	502	1610	2945	8	600710	198000	Unpeaked
2143	Rhein	Rekingen	323	1080	14718	0,57	667060	269230	Unpeaked
2415	Glatt	Rheinsfelden	336	498	416	0	678040	269720	Unpeaked
2462	Inn	S chanf	1645	2466	618	10,1	795800	165910	Unpeaked
2009	Rhone	Porte du Scex	377	2130	5244	14,3	557660	133280	Peaked
2011	Rhone	Sion	484	2310	3373	18,4	593770	118630	Peaked
2019	Aare	Brienzwiler	570	2150	554	21	649930	177380	Peaked
2056	Reuss	Seedorf	438	2010	832	9,5	690085	193210	Peaked
2084	Muota	Ingenbohl	438	1360	316	0,08	688230	206140	Peaked
2085	Aare	Hagneck	437	1380	5104	4,5	580680	211650	Peaked
2174	Rhone	Chancy	336	1580	10323	8,4	486600	112340	Peaked
2372	Linth	Mollis	436	1730	600	4,4	723985	217965	Peaked
2473	Rhein	Diepoldsau Rietbrucke	410	1800	6119	1,4	766280	250360	Peaked

4.2.2 Classification of peaked and un-peaked stations

Every analysed gauging station has been subject to a preliminary screening with the aim to detect the presence of ‘hydropeaking’ (in short, HP) and ‘thermopeaking’ (in short, TP) phenomena at each station. To this aim the characterization methods recently proposed by Carolli et al. (2015) for hydropeaking and by Vanzo et al. (2015) for thermopeaking have been employed. These methods prescribe two HP indicators (HP1 and HP2 represents statistical measurements of the magnitude and rate of change for sub-daily streamflows, respectively) and two TP indicators (sub-daily RWT rate of change and relative importance of sub-daily thermal oscillations), which are built as quantitatively comparable metrics among streams of different size and hydro-morphological characteristics. The methods also define one peaking threshold for each of the indicators, with reference to a large number of hydrometric and RWT gauging stations that are certainly unaffected by upstream intermittent releases from hydropower plants. All these thresholds are observed to fall within a relatively narrow range of values, at least for streams belonging to alpine cold temperate climatic regions, so that they can be considered ‘quasi-universal’. Thermopeaked stations are necessarily hydropeaked, while hydropeaking is not a sufficient condition for thermopeaking.

Each station is eventually classified as peaked or un-peaked station depending on its HP and TP indicators falling above or below their corresponding threshold (Table 4.1, last column). Only one ‘un-peaked’ station was included that showed hydropeaking but no thermopeaking effects due to the mitigating influence of an incoming tributary downstream of the hydropower release. Two example stations with typical features of each group are showed in the lower panel of Figure 4.1 (a) and (b).

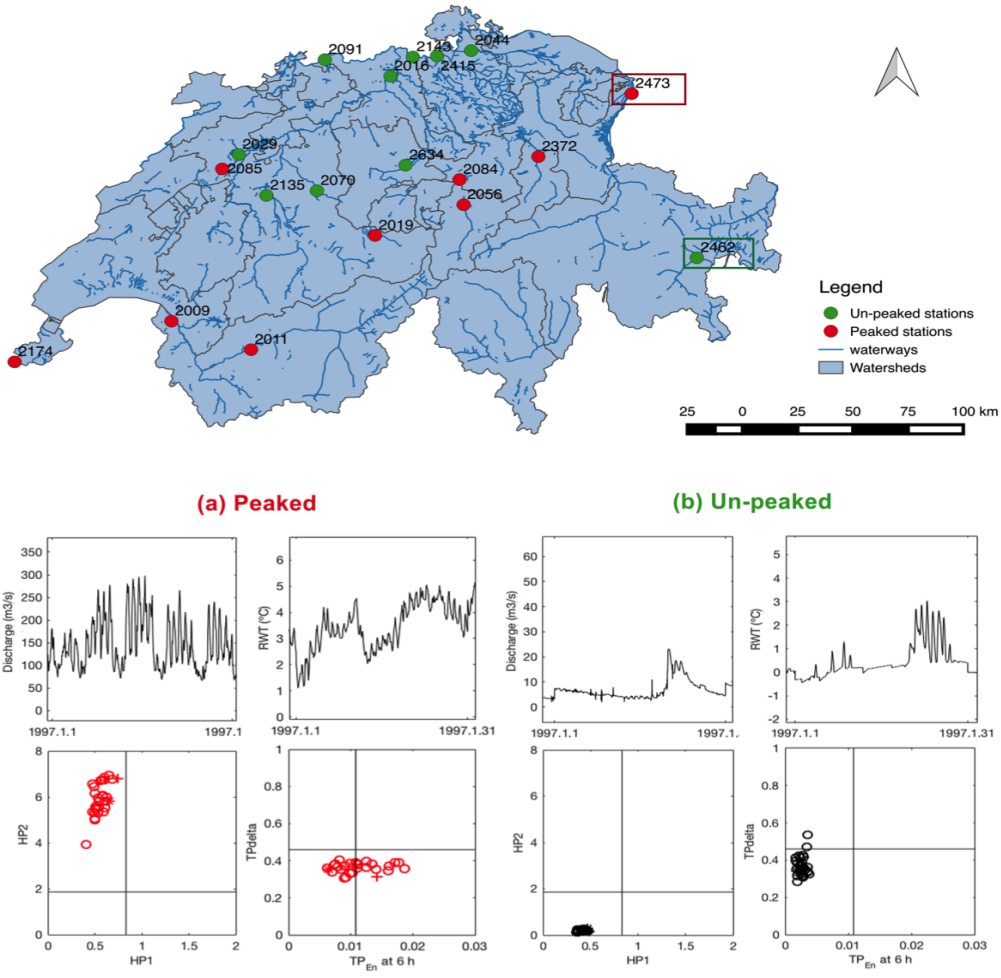

Figure 4.1 Map of Switzerland with locations of the analysed gauging stations of two groups (red: peaked stations; green: un-peaked stations). Stations are denoted with the same code reported in Table 4.1. Two examples of the hydrograph and thermograph for January 1997 are illustrated in the lower panels for (a) peaked station (2473) and (b) un-peaked station (2462). In the same panels, the position of the two stations in the (HP1, HP2) and in the (TP1, TP2) parameters space over the 30-year period is reported.

4.2.3 Temperature variability analysis

Monthly and daily maximum AT and RWT temperature and their anomalies were computed from the original observation dataset in order to analyse the temperature dynamics for the two pre-classified groups at different temporal scales. Special attention was given to the summer months when heatwaves usually occur. More specifically, the 2003 heatwaves spread

throughout the whole summer months (June-July-August, subsequently referred to as JJA) with the highest temperature values from June to mid-August; the 2006 heatwaves only occurred during July (Rebetez et al., 2009).

Statistical analysis for investigating the variability of maximum, minimum and mean air and water temperature were performed at different time scales (daily, monthly, seasonal, and yearly). Another metric measuring the accumulated heat budget in the form of degree-days (Cesaraccio et al., 2001), has been calculated based on the 10-mins RWT time series, to indicate total amount of heat during each monthly period, such quantity being directly correlated with the mean RWT.

For each of these site-specific dataset, temperature anomalies are computed as the differences between the measured values and the standard baseline value, which is the historical average value of the consecutive 30-year period (1984-2013 in this paper) (WMO, 1989).

4.2.4 Correlation and time-lag analysis

In order to account for the RWT response to AT, simple linear regression models ($y=a*x+b$, coefficient a is the slope and b is the y-intercept) were performed monthly over 30 years with daily maximum RWT as response variable and AT as explanatory variable for each station. Pearson's correlation coefficient (r) and p value was also computed.

Cross-correlations between RWT and AT were analysed to evaluate the synchronization or time lag between the rising air temperature and river water temperature. The representative time lag (tlag) between the two 'input' (AT) and 'output' (RWT) signals is chosen as the one yielding the highest cross-correlation coefficient between the two time series (Olden et al., 2001).

$$tlag=n*\Delta t \qquad \text{(Eq. 4.1)}$$

where Δt is the sampling frequency, n is the number of time intervals corresponding to the highest cross-correlation. In this case, the Δt is 1/6 hour with dataset resolution of 10mins.

4.2.5 Ecological thermal stress evaluation

To investigate one of the potential ecological impacts of extreme heatwaves, a simple analysis on the thermal habitat vulnerability for fish, especially during species growth period, has been proposed. To this aim, the brown trout (*Salmo trutta*), typical cold stenotherm has been chosen as representative species in the examined Alpine region. The upper temperature growth limit for the brown trout is considered 19.5°C(Elliott and Hurley, 2001). Daily maximum temperature above this critical threshold will interrupt the period of growth for brown trout and create harmful effects (Olden et al., 2001). Thus, an analysis of the continuous duration and frequency of thermal events exceeding this threshold has been performed separately for peaked and un-peaked stations, and focusing on their characteristics during the two examined heatwaves in 2003 and 2006.

On monthly scale, exceedance days were calculated as the total number of days within each month that the daily maximum temperature is higher than the baseline threshold. Then the session of maximum consecutive days when the exceedance value is higher than zero are counted as persistence days in that month. Besides such cumulated metric, also the continuous duration of individual thermal events characterized by RWT falling above the considered ecological threshold has been computed referring to the UCUT (Uniform Continuous Under Threshold) methodology (Parasiewicz et al., 2012). Thermal stressful events may indeed become seriously harmful or even lethal when being of long continuous duration, besides their frequency.

4.3 Results

4.3.1 RWT variability of peaked and un-peaked stations

The analysis of RWT variability yielded analogous results in terms of all the three examined variables (minimum, mean and maximum daily RWT). Therefore we chose to show the results for daily maximum AT and RWT in this paper. Statistical distributions of summer daily maximum temperature of 30 years (1984-2013) for all stations are shown in Figure 4.2. Maximum RWT values of the un-peaked group are correspondent to the heat waves in year 2003 and 2006 as it appears in the air temperature distributions (Figure 4.2a). In all months, and also in the summer period (June to August), the peaked stations showed significantly lower mean standardized values compared to un-peaked ones, and a larger standard deviation. As an example in June, the peaked stations showed 18.68% lower mean standardized RWT values and a 17.3% larger standard deviation (p<0.01, confidence interval=0.05) compared to un-peaked stations. The higher variability of peaked stations is systematically associated with an expansion of the distribution of the daily RWT max values towards the lower end, coherently with the reduction of the mean, in comparison with the unpeaked stations. This reflects a generalized and significantly different (p<0.01, confidence interval=0.05) cooling tendency of intermittent hydropower release.

This behavior has immediate consequences during the two heatwaves in years 2003 and 2006, which are almost invariably associated with the highest three RWT values on record for un-peaked stations, while they disappear from these values in the case of peaked stations (Figure 4.2b, c). This suggests a highly reduced impact of extreme heatwaves on the RWT records due to the hydro-thermopeaking effects.

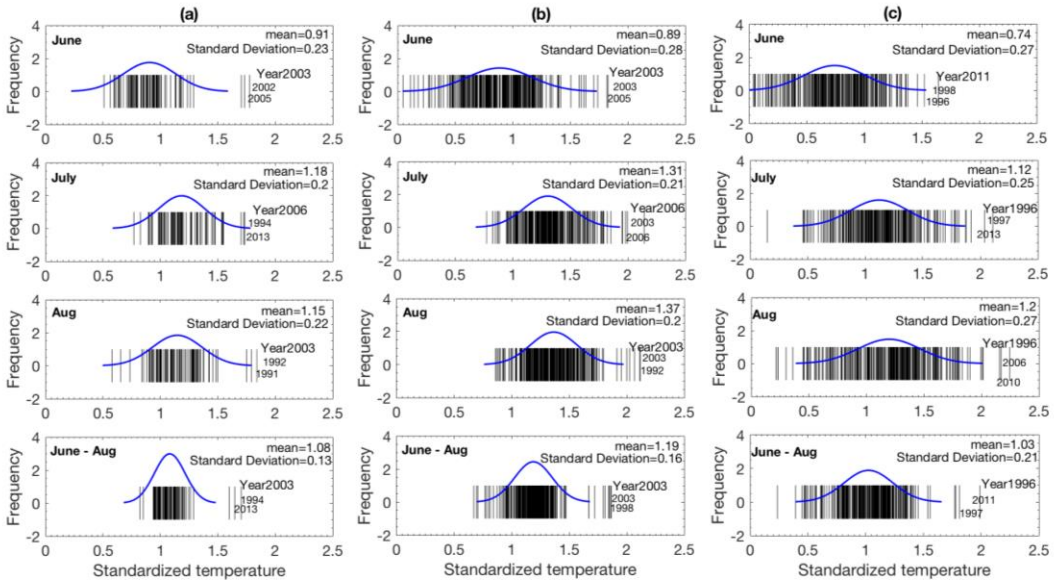

Figure 4.2 Statistical distribution of the daily maximum temperature in June, July, Aug, and June-Aug as a whole summer period over the 30 years (1984-2013), respectively. Columns represent (a) averaged AT for meteorological stations at Basel, Geneva and Zurich; (b) RWT for all the un-peaked stations; (c) RWT for all the peaked stations. All dataset are standardized by subtracting the mean value and divided by the standard deviation before extracting the mean value for each selected month period. Within each panel is the rug plot of monthly mean value of 30 years, with the three highest values labeled by the corresponding year. Fitted Gaussian distribution (blue curves) with the mean value and standard deviation is given for each panel.

Monthly-accumulated heat budget for the analysed rivers at the chosen gauging stations are computed from RWT time series in terms of degree-days, which measure the level of heating effects to the river systems. In Figure 4.3, degree-days anomalies for the summer months (JJA) were computed for all the stations of the two groups throughout 30 years. Results indicate that below the water release point, the hydro-thermopeaking affected stations showed 56.04%, 56.03% and 43.24% lower mean degree-days anomalies and 25%, 11.38% and 37.9% of standard deviation (p<0.01, confidence interval=0.05) in June, July and August, respectively compared with the unpeaked stations.

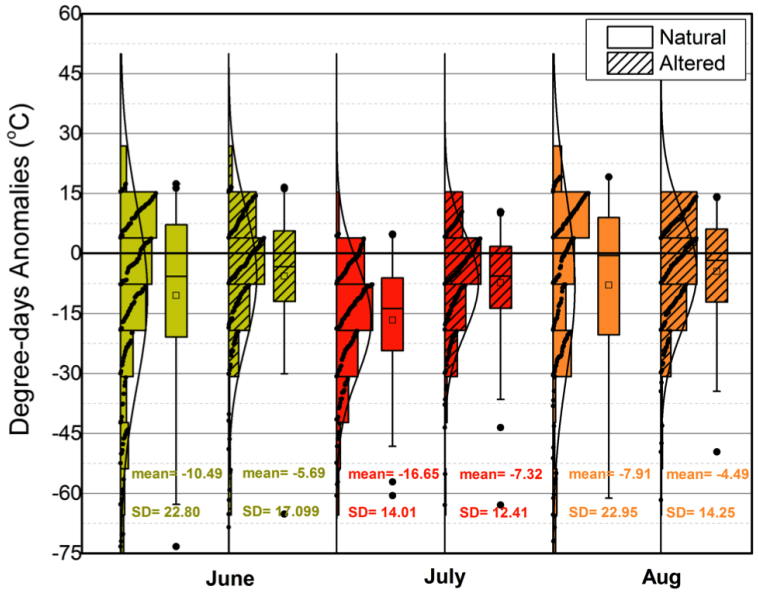

Figure 4.3 Degree-days anomalies of summer months from June to August (JJA) throughout 1984 to 2013 for the whole dataset considered. Anomalies are calculated relative to the deviation of the 30-year (1984-2013) baseline, and normal distributions are shown, respectively. Boxplots are shown for unpeaked stations (solid color) and peaked stations (filled pattern) for June, July, and August, respectively.

4.3.2 Correlation analysis in response to heatwaves

Figure 4.4 shows a representative example of the relation between AT and RWT for one peaked and one unpeaked station. In the unpeaked station both the slope of the linear regression and the coefficient of determination are higher compared to the peaked one. Such behavior is actually representative of a broader ensemble of analysed stations. Figure 4.5 synthesizes the results of linear regression analysis between AT and RWT for all the analysed stations during heatwave months, and also highlights differences between heatwaves years 2003, 2006 and the other ones. In contrast with the unpeaked groups, the peaked stations showed decreased correlation in both coefficients of determination and fitted regression slopes for all the 30 years. Such difference in behavior appears to be more pronounced during heatwave years. For example, the difference in the median value of the r^2 coefficient between the

peaked and unpeaked stations (Figure 4.5A) increased from 0.236 (30.77%) in the 28 non-heatwave years to 0.354 (53.31%). Percentage values in brackets have been calculated as deviation from unpeaked stations, same as below. Analogously, the difference between the peaked and unpeaked stations in July increased from 0.245 (33.26%) in the 28 non-heatwave years to 0.358 (47.61%) in 2006. An analogous behavior is displayed by the slope of the linear regression in Figure 4.5B. In JJA 2003, the difference between the median values of such slope distributions between unpeaked and peaked stations, was 0.291 (54.19% of the median value of the peaked stations), while reducing to 0.08 (30.77%) in JJA of non-heatwave years; the same quantities attain values of 0.291 (54.19%) in July 2006 and 0.21 (41.18%) in July of non-heatwaves years. In summary, the peaked stations showed a noticeable effect in diminishing the homogeneity of the relatively high linear correlation that can be observed between river water temperature and air temperature, and this effect is more evident under heatwaves.

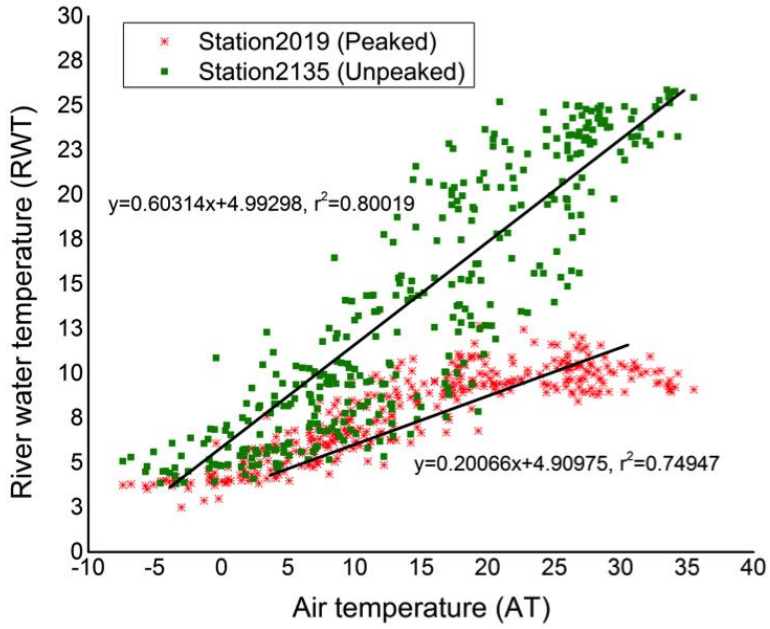

Figure 4.4 Scatter plot of AT and RWT for one representative peaked station (2019, red) and one representative unpeaked station (2135, green) in the Aare river catchment. Linear regression and related coefficient are reported.

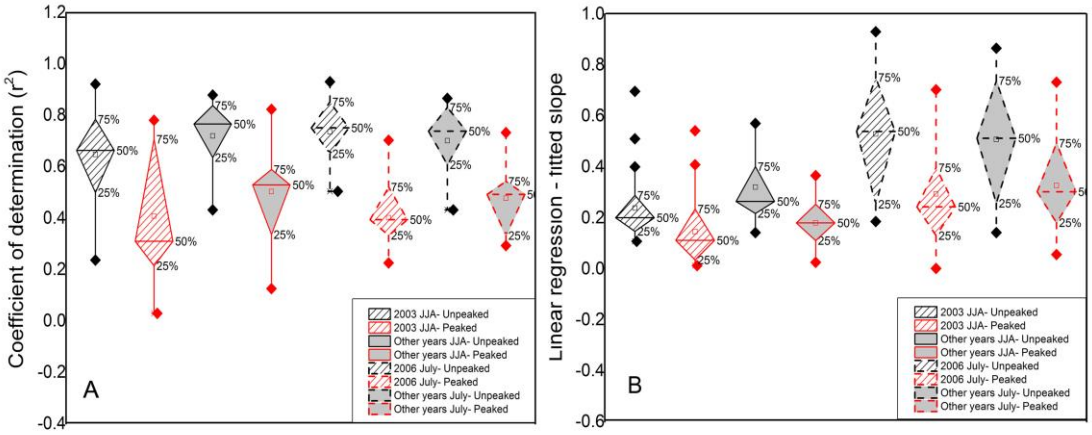

Figure 4.5 Results of linear regression analysis between daily maximum AT and RWT. Distributions of: (A) coefficient of determination (r^2); (B) Slope of fitted linear regression. Results are compared between the unpeaked stations (black) and peaked stations (red) in JJA of 2003 (solid lines), July 2006 (dotted lines), and the corresponding period in the rest 28 years, respectively.

4.3.3 Adaptation period for river water temperature

The instantaneous response of RWT to variations in AT is known to be characterized by an adaptation process related to the exchange of heat fluxes between air and water and to the thermal capacities of both means: this determines a time lag in the RWT adaptation to AT. We have investigated whether the peaked and unpeaked stations may be characterized by differences also in terms of such adaptation time and which could have been the effect of heatwaves on such delay. To this aim we analysed the time lag by using the lagged cross correlation analysis between the 10-min resolution AT and the corresponding RWT for the two mega-heatwaves events in 2003 and 2006 as well as other years, Figure 4.6 compares the median values and the range of variability of these time lags: invariably, RWT at peaked stations (in red) showed longer (larger range) adaptation time lags in response to the rising air temperatures in summer. The effect of the heatwaves years (slashed-line filled), contrary to the previously analysed variables, is instead controversial. For JJA of 2003, their mean time lag showed statistically

minored difference between the two station groups due to absolute warming up by all river sections, compared with the non-heatwaves years (solid fills). For July only, the difference of mean time lag between peaked and unpeaked stations dropped 48.51% from 38.28 minutes in non-heatwaves years to 19.71 minutes in 2006. Potential reason for that could be the physical interpretation of this difference of observed behavior as the time lag of RWT is dependent on occasional cases such as the clouds cover that can be highly variable among the different stations, or the specific time pattern of the hydropower plant.

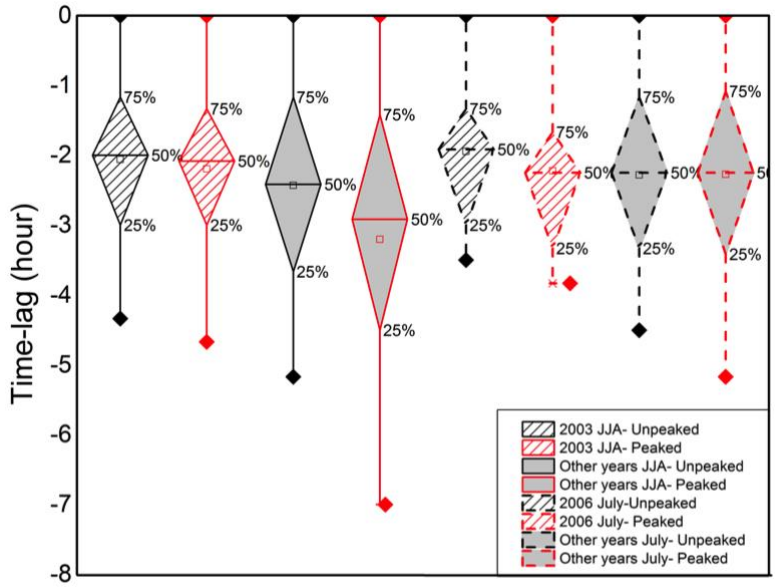

Figure 4.6 Statistics comparison of the time lag between the “input” time series of AT and “output” RWT in at peaked stations (red) and unpeaked stations (black). Solid and dotted contours represent JJA months and July, respectively. Lagged time of the cross correlation functions are calculated on 10-min resolution but expressed as the number of hours here.

4.3.4 Ecological threshold exceedance

The observed differences in heating effects between hydro-peaked and unpeaked stations in summer months may imply yet unknown ecological effects. We made a first attempt to address this question by assuming a RWT upper limit of 19.5°C which can be considered for the brown trout, a typical fish species in the examined Alpine streams, and investigating differences in exceedance of such threshold among peaked and unpeaked stations, and

between heatwave and non-heatwave years during the summer months. Figure 4.7 shows the monthly average number of exceedance days over this critical ecological threshold for all stations of each group. Against the background of AT exceedance days over the same threshold (Figure 4.7a), the peaked stations (Figure 4.7b) showed a distinctively smaller number of exceedance days compared to the peaked stations (Figure 4.7c; $p< 0.01$, significantly different at confidence level 0.05), such difference outstanding more during summer, and taking values of 88.14%, 79.83% and 77.4% in June, July and August, respectively (Figure 4.7d).

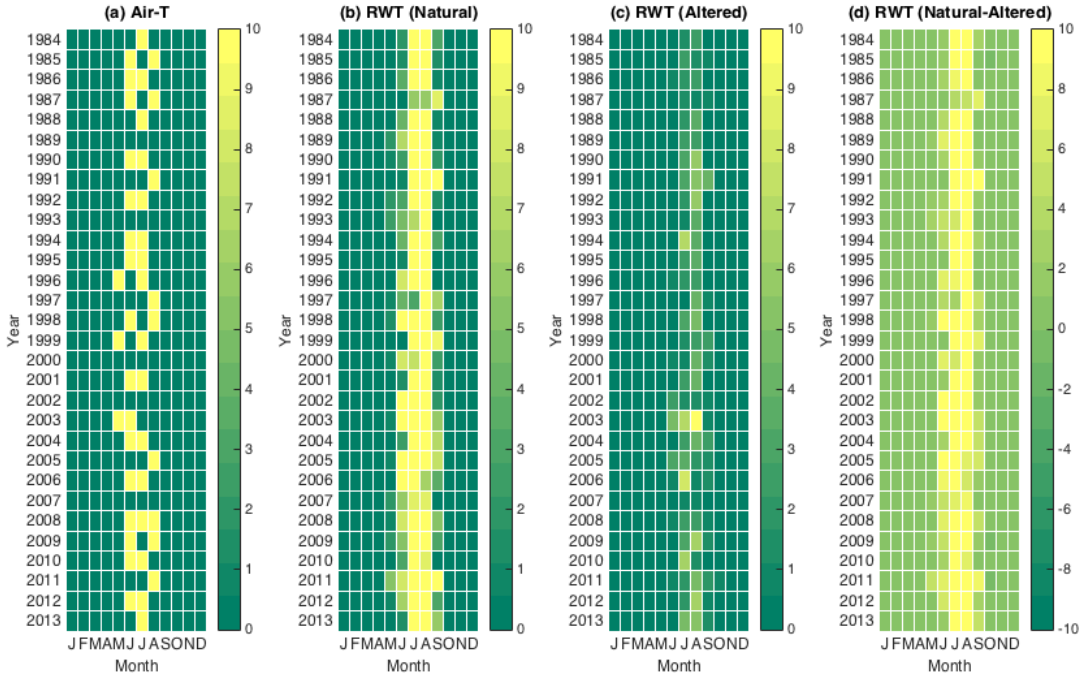

Figure 4.7 Number of exceedance days over the upper limit of temperature threshold for brown trout. Monthly average exceedance days for (a) AT averaged three meteorological stations; (b) RWT at unpeaked stations; (c) for RWT of peaked stations, and (d) difference between these two groups, calculated as number of exceeded days for the unpeaked group minus the peaked group accordingly.

In 2003, the exceedance days of the unpeaked stations in the most heated months JJA were 19.7, 23.5 and 28.2 days on average. However, the exceedance days in the peaked stations were considerably less, being 4.6, 7.2 and 10.2 days, (i.e., by 76.65%, 69.36% and 63.83%, respectively; $p< 0.01$,

significantly different at confidence level 0.05). In July 2006, the effect of the heatwave was less attenuated by peaking operations, with such difference being 3.48 days, with likely less harmful consequences for the fish. Overall, intermittent hydropower releases have been observed to induce a mitigation of extreme heatwave effects on brown trout thermal growth thresholds by reducing the number of exceedance days over such critical high temperature.

To quantify the possible loss or gain of thermal habitat for brown trout, we combined two variables of number of exceedance days and the duration of each exceedance event. Statistics of the exceedance events with their continuous duration days over 2003, 2006, and the 28 non-heatwaves years are calculated and compared between the peaked and unpeaked station groups (Figure 4.8). The probability of long-term exposure to high temperature showed more clearly deviation between the peaked stations and unpeaked stations with the increasing of continuous duration days. Under the same probability, the peaked stations were found to have less heat-exceeded days. This beneficiary brought by the hydro-thermopeaking effects was more obvious in the heatwaves years especially under high duration of extreme thermal exposure.

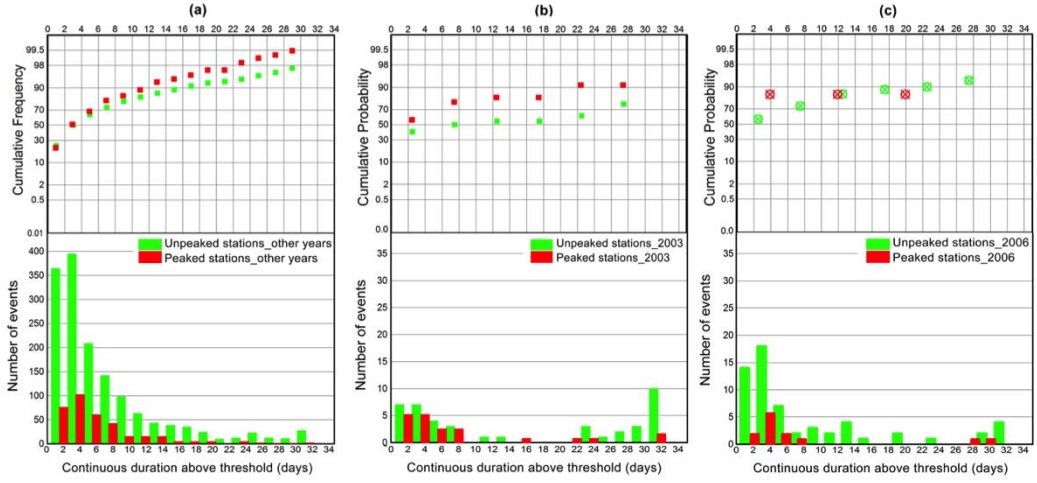

Figure 4.8 Continuous exceedance events when the maximum daily temperature was above the tolerance threshold of 19.2ºC. Histograms of the continuous exceedence duration days are calculated for all the peaked and unpeaked stations in (a) non-heatwaves years, (b) 2003 and

(c) 2006. The corresponding cumulative frequencies of events are in the upper figure.

In light of the thermal habitat conditions evaluation, the above events of continuous exceedance days are used to create the Uniform Continuous Under Threshold (UCUT) curves that were illustrated by Parasiewicz (2008). Instead of looking at low flow conditions, we modified the UCUT curves for river thermal regimes as Uniform Continuous Above Threshold (UCAT) curves applied for the habitat suitability evaluation of cold stenotherm.

The UCAT curves describe the duration and frequency of significant thermal events that continuous durations days of RWT is above the brown trout growth threshold. The cumulated exceedence days of each continuous duration day, which ranged from 1 to 31 days, are counted per year and divided by the total number of heat period we assume. Horizontal difference (e.g. right shifts) of the curve at the same continuous duration depicts an increase in the frequency of occurrence. The smaller the frequency of duration, the less RWT is above the upper growth limit, which means higher thermal habitat suitability is available for brown trout. This allows the evaluation of habitat suitability at a range of thermal regimes using suitable temperature duration days, which could be used for managers to determine the habitat thermal bottlenecks.

In Figure 4.9, the peaked stations (in red) showed steep curves with low changes and consistent small magnitude of frequency compared with all the unpeaked stations (green) in corresponding years. Under the same climatic background, a temperature-indicated habitat suitability beneficiary is discovered in the river sections with hydro-thermopeaking peaked sites.

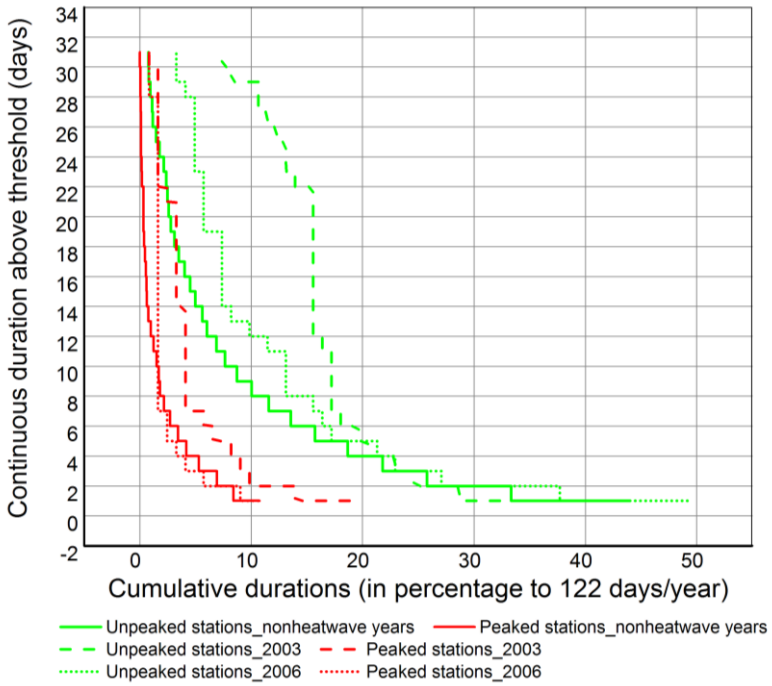

Figure 4.9 The Uniform Continuous Above Threshold (UCAT) curves for the thermal habitat of brown trout. Each curve represents the cumulative duration and frequency of the number of events when RWT is higher than the upper growth limit for a continuous duration days depicted on the y-axis. The x-axis is proportioned as percentage compared with the total number of considered heat days (June to September, 122 days) per year.

4.4 Discussion

4.4.1 Extreme heatwave events mitigation by hydropower

Results of the present study indicate that in a set of selected alpine rivers, river thermal regulations associated with hydropeaking and thermopeaking in summer months could result in cooling and lagged effects on the thermal response of the recipient streams to changing air temperature. Effects of climate change on the hydrology (Beniston, 2012; Middelkoop et al., 2001; Jasper et al., 2004) and temperature of rivers in the Alps have been investigated on both experimental and modelling level (Caissie, 2006; Hari et al., 2006; Null et al., 2013; Toffolon and Piccolroaz, 2015). However, little were demonstrated such effects as warming of river water due to other human impacts possibly combined climate-induced effects (Gobiet et al., 2014).

Results described in the present Chapter are consistent with existing work on the thermal dynamics of rivers (Piccolroaz et al., 2016), which suggests that hydropower-regulated rivers may have a more resilient behavior with respect to variations in air temperature if compared with other types, non-regulated rivers, that are discovered to behave more reactively. A similar concept was previously demonstrated by Null et al. (2013), through a modelling study of reservoir operations and releases into downstream water bodies, explicitly focused on assessing whether dams may mitigate the effects of climate changes on stream temperatures. Their study suggests that, at weekly timescale, during summer months, reservoir releases should result in cooling the recipient stream, though such effect may be dampened further downstream still in relation to temperature warming trends associated with climatic effects.

The present analysis moves from these acquisitions and, differently with respect to previous analyses, it focuses on another element of climatic changes, e.g. the occurrence of heatwaves for which an increase in the temporal frequency in the Alpine area is forecasted. A second distinctive feature of the present study is that the analysis is conducted at a much finer time scale, i.e., sub-daily scale, through the analysis of a high temporal resolution RWT dataset. This is a key requirement for the scope of the analysis because the cooling effect by released hypolimnetic water from the reservoir is typically associated with the intermittent flow releases that respond in real-time to the peaking demands from energy market, for which hydropower is a privileged power source. Released hypolimnetic water that causes cold thermopeaking in summer months because it is known to be cooler than the water of the receiving stream in summer, and similarly it becomes warmer in winter (Carolli et al., 2008, Zolezzi et al., 2011).

Hydropower regulation produces large weakening influence on the equilibrium relation between RWT and changing air temperature. Moreover, it

is interesting to be noted that the mitigated impacts of extreme heated air temperature on the peaked stations of RWT is affected of smaller magnitude but bigger range of time intervals for RWT to be warmed up by AT on both annual and inter annual scales. This agrees with the findings of the statistically wider distribution of RWT anomalies against the unpeaked station observations.

4.4.2 Implications for cold-stenotherm river habitat

One of the most important relevance of the results of the present study is related with their ecological implications. Heatwaves lasting for several days may severely affect the integrity especially of the alpine river ecosystems, causing unusually long warm periods that may determine intolerable thermal stress for the aquatic biota. In alpine streams, in particular, typical fish species are adapted to habitats characterized by cool temperature levels and only exhibit limited tolerance towards warmer temperature. High temperature generated by heatwaves might be fatal for river biota that adapted to live in cold river water (cold-stenotherm organisms) in case that the temperature exceeds threshold levels tolerated by those organisms.

Temperature threshold of stream fish (e.g. salmonid or trout) varies somewhat from the duration time and fluctuation of the extreme temperature that the organism is exposed to (Kevin et al., 2007). The duration time and the number of temperature over-exposure events affect the thermal habitat for specific species.

As such events are threshold-based, and considering that several fish species in the Alpine rivers are documented to live very close to the upper limit of their thermal survival range (Hari et al., 2006), even small increases in RWT may result into large increments of the duration of harmful thermal events for the examined fish species (the brown trout, salmo trutta in this case).

Our results indicate that in the absence of heatwaves, unpeaked stations

already exhibit much longer duration of thermal stressful events for the considered species. When heatwaves occurred in 2003 and 2006, the continuous duration of such events considerably increased, especially in the long summer heatwaves of 2003, with maximum increases for events of the order of one week. It has been argued that climate-induced warming trends of river water temperature in mountainous regions may trigger a migration of cold-stenotherm organisms in upstream direction (Hari et al., 2006). Our results point out an additional effect that may impose conditions of fish migration in the alpine rivers, because of a tendency to move towards artificially and intermittently cooled riverine habitats may be hypothesized as well. Such hypothesis would however need to be carefully verified, because, depending on channel morphology, river reaches subject to hydropeaking may on the other hand present high stranding risk (Vanzo et al., 2015) or reduced food supply for fish from macroinvertebrates because of increased catastrophic drift (Bruno et al., 2010).

4.4.3 Management implications and further research needs

The projected increase of frequency and duration of heat waves in the future may represent an additional threat to the already vulnerable river ecosystems. Debates are increasingly being developed (e.g. Bruder et al., 2016) about how to effectively conjugate the need of renewable energy production from hydropower with the need to mitigate its impacts on freshwater ecosystems. The results of our analysis seem to suggest a paradox: hydro- and thermopeaking may protect cold stenotherm aquatic biota from the adverse effects associated with the projected increase in heatwaves. Does this mean that more storage power plants should be built and operated to protect fish in Alpine streams? The cooling water in summer released from reservoirs can be used to mitigate the detrimental effects of climate change, which has already been suggested by Yates et al. (2008) in the modelling application of California’s Sacramento Valley in the U.S.A has never been demonstrated in

the Alpine rivers. Clearly, however, the mitigation effect of reservoirs on Alpine rivers of heat waves represents only one of the numerous effects of reservoirs operation on rivers. As hydropeaking has multiple known adverse effects on the integrity and connectivity of river ecosystems, it is of course not straightforward to consider intermittent flow releases as ideal agents of thermal mitigation purposes, as their other adverse effects clearly outweigh the potential mitigation effects. The present results add some complexity to the existing picture of biophysical processes occurring in hydropower-regulated Alpine streams. At the same time, more specific implications should be explored in the near future.

The presented analysis has, in principle, a very restricted spatial focus, because the analysed data are collected at-a-station. Previous research has shown that effects of hydropower operation on thermal regimes can continue for periods of several weeks after the regulation events have ceased (Dickson et al., 2012). Thus information at river reach- or segment-scale would be needed to assess how long are actually the river sections for which our considerations apply. An analysis on the line of the one proposed in Chapter 3 is therefore needed in relation to the characteristics spatial and time scales of thermopeaking propagation in specific case studies, which will allow to quantify which can be the actual length, connectivity and spatial distribution properties in the catchment of those reaches where the detected thermal protection from heatwaves by thermopeaking would occur. At the same time, the hydromorphology of these rivers has extensively been modified by humans, because of their huge potential to provide a variety of ecosystem services, like hydropower production, multipurpose water supply, cultural and recreational activities.

Finally, when considering climatic effects on river ecosystems as a whole, it has to be kept in mind that besides temperature, climate change also influences river runoff dynamics, and specific analyses already have been

conducted for mountains and snowy regions such as Himalaya Rivers (Kaltenborn et al., 2010). Alpine rivers are among the most vulnerable river systems towards climate change, as runoff is thereby much determined by snowfall and presence of glaciers. The reduced summer river temperatures may not apply to rivers that experience periodic influence from glaciers and groundwater spills (Dickson et al., 2002). In our study, however, special attentions are given to the extreme heatwaves in summer, during which glacial impacts are not so prominent as in winter and early spring. From a point view of hydropower management on riverine ecosystems, alterations in river thermal regimes for glacier-affected rivers may need further examinations within a specific context.

4.5 Conclusions

Alterations by human activities under climate changes to the aquatic environment are unavoidable ‘sweet burdens’ under disputes. This Chapter applies methods and applications to quantify the river thermal regime impacts by human regulated intermittent hydropower production activities in the Swiss alpine rivers. Through sub-daily hydropeaking and thermopeaking analysis for widespread gauging stations, we quantified to which extent water temperature in the alpine rivers showed predictable warmed-up trends at all river sections in summer but specific “human-perturbed” lagged-response to air temperature with reduced magnitude of increment with water temperature. Such effect is mostly amplified during heatwaves but not for all parameters of the correlation. During heatwaves, especially in case of long lasting continuous above threshold events, the sub-daily thermopeaking effects brought by regularly peaked hydrological regimes create beneficiary environment for cold-stenotherm river biota within a spatially hydro-geophysical characterization related distance.

These hydro-thermopeaking alterations to the downstream river sections

are discovered as somehow mitigation path to increased thermal habitat suitability by providing reduced water temperature oscillation ranges. The results provided important understanding for the effects of heatwaves and add to the complexity of climatic effects on water temperatures in river systems regulated by hydropower production activities. As an apparent paradox, human interference is discovered as potential mitigation measures in response to extreme climatic events. The outcomes of this study should be viewed in their implication for the temporary selection of thermally protected areas within regulated river systems under the projected increase of heatwave frequency in Alpine areas.

Acknowledgements

This part of work has been carried out within the SMART Joint Doctorate program “Science for the MAnagement of Rivers and their Tidal systems” funded by the Erasmus Mundus program of the European Union. The authors thank the authorities who provided the data for all the analysis: Stream-flow data and river water temperature time series for the Switzerland river sites were provided by the Swiss Federal Office of the Environment (BAFU). The Federal Office of Meteorology and Climatology MeteoSwiss provide air temperature records.

Chapter 5

General conclusions

In this chapter a summary of the relevant conclusions arising from all the previous chapters is given. Afterwards, the particular conclusions are jointly reviewed to answer the research questions posed in Chapter 1 of the thesis. Furthermore, some implications of the study results for river management are presented. Finally, some recommendations for further research are given.

This doctoral thesis focuses on the analysis of selected aspects of the river hydrological and thermal regimes of recognized ecological significance. The developed research is built on the three main elements, as introduced in Chapter 1, and it focuses on their physical dimension, without explicitly analyzing their ecological implications in details. However, attempts to discuss some ecological implications are proposed in the discussion part of each analyzed research element at various stages.

5.1 Overview of the research elements

The selected topics investigate ecologically relevant flow and thermal regimes characteristics at different spatial and temporal scales, following an arrangement that is graphically illustrated in Figure 5.1. Here, markers refer to the three thematic chapters of the thesis, while colors denote the ranges of time and space scales at which the results of each Chapter have its main implications.

The research questions in the thesis are addressed in a way of ‘downscaling’ order. In Chapter 2, the research element of water residence time is elaborated on the temporal scale of multi decades, though it is based on reach-scale information. It has the foremost implications on river ecology by

linking nutrient retention time in streams at larger spatial and temporal scales. While applied to few representative catchments. It can set the basis for a country scale analysis and can be relevant at longer time scales associated with climate variability.

Research questions involved with hydropeaking are the most detailed element throughout the whole thesis. In Chapter 3, hydropeaking variability, which is characterized by the sub-daily fluctuations of river discharge at each gauging station, is analyzed spatially for the propagation along the river reach, river segment, and can be extended to the whole catchment; and temporally during seasonal, yearly, and multi-decadal, through the analysis of a 35 years high-resolution dataset. Also for this Chapter, results can have implications at larger spatial scales, because the method can provide a simple, yet quantitative approach to calculate the length of all river reaches subject to significant hydropeaking flow alteration even at country level. Considering the analysis that is subsequently developed in Chapter 4, results of Chapter 3 may have implications at larger time scales associated with climatic changes, because hydro- and thermos-peaked river reaches are much less responsive than unpeaked reaches to climatic extremes represented by heatwaves.

In Chapter 4, the analyses of hydropeaking are performed from the sub-daily to multi-decadal scales for grouped gauging stations, and their validity is therefore strictly valid only at a very local (cross-section) level. Special focuses are given to monthly and seasonal scales when the summer heatwaves occurred, at which point the ecological implications related to thermal thresholds are manifested.

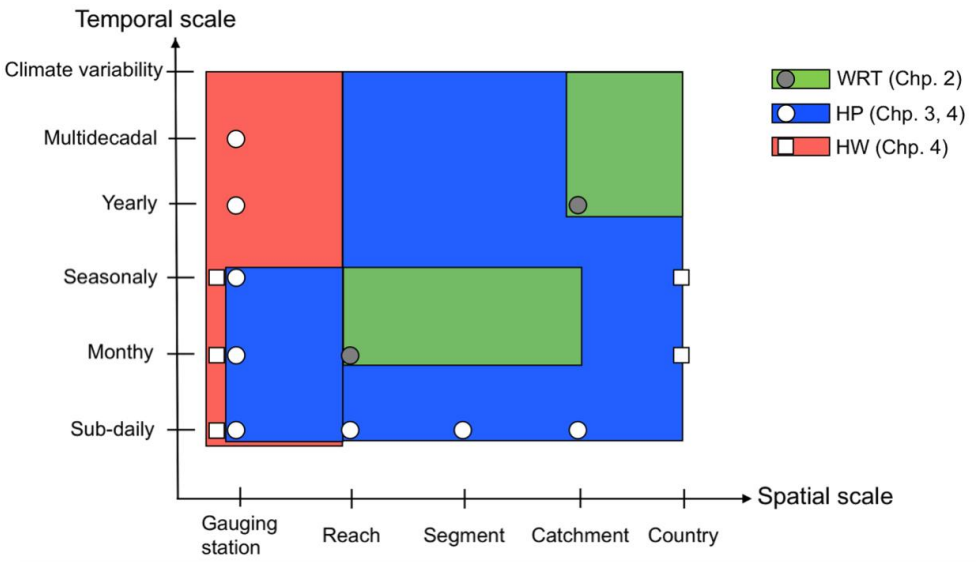

Figure 5.1 Temporal and spatial scales related to the three main research elements and their ecological implications presented in this thesis (Green: water residence time; Blue: hydropeaking; Red: heatwaves). Colored squares are the scale of ecological implications accordingly. The Bracket after each element states the chapter in which it is included.

5.2 Summary of chapter conclusions

Chapter 2 presents the development of spatial statistical approach for estimating the water residence time in river networks by applying the spatial distribution model of boosted regression trees (BRT). The approach is proved to be robust in results and fast application while considering the spatially heterogeneous attributes of hydromorphology in river reaches. More importantly, the approach filled the imbalance between the time-consuming process models and the over-simplified empirical estimations. At the scale of river networks, water residence time is primarily affected by river discharge, followed by river width and river channel slope. Geomorphological attributes are more influential on small rivers in the Alpine mountainous areas. By taking the example of river discharge during flood and drought events, the BRT modelling is useful for water residence time estimation under extreme hydrological scenarios.

Chapter 3 represents a quantitative attempt to investigate the temporal

and spatial variations of hydropeaking in a target catchment in the Alpine region. The hydropower-exploited Rhone River basin in Switzerland is chosen as a case study. The chapter proposes a framework to analyse in a simplified way the spatial propagation mechanisms of hydropeaking that are mainly controlled by river hydrology and hydraulics. The spatial propagation of hydropeaking was discovered to be controlled by channel geomorphological reach-scale parameters, though for typical parameter ranges of Alpine streams the hydrologic effect associated with lateral inflow from tributaries seems to represent a dominant mechanism for the attenuation of hydropeaking waves, at least in a river that is channelized and presents little morphological complexity. Based on the proposed framework, the length of river reaches that are affected by hydropeaking below hydropower stations can be determined. Such quantification of hydropeaking-affected river reaches offers a powerful tool to support catchment-, regional- or country-scale planning, assessment and impact analyses of hydropeaking and its related mitigation measures.

Chapter 4 investigates the potential mitigation impacts by hydropeaking and thermopeaking regulation on the warming of river water temperature associated with heatwaves. River water temperature in the Alpine rivers shows a reduced correlation with air temperature in ‘peaked’ river reaches and this somehow expected behavior is examined particularly under heatwaves that are projected to occur more frequently in the future in relation to climate change. Besides being warmed up in summer, river reaches with hydro- and thermopeaking showed specific “human-perturbed” lagged-response to air temperature with a reduced increment with water temperature. Such effect of hydropower regulation is more visible during heatwaves but not for all parameters of the correlation. The results provided a crucial understanding of the effects of heatwaves, and of the potential implications for freshwater fauna, under hydropower flow regulation determining intermittent, artificial flow

fluctuations. The study adds to the complexity of physical effects of hydropeaking, particularly in relation to the interplay with the effects of climatic extremes, and rises questions about possible tendencies towards species shifts in specific river reaches downstream the hydropower plant releases.

5.3 Implications for river management

Water residence time represents a key variable to identify threshold mechanisms that are sensitive to changes of land use, drought or flood, and climatic stressors that affect the status of water bodies, the availability of aquatic nutrients, and watershed integrity. Understanding the governing variables of in-stream water residence time could not only support water quality modelling that is influenced by nutrient retention, but also water management practices. The results underline the relative importance of hydromorphological features, which has clear implications to optimize the efficiency of river restoration effects on runoff processes.

Understanding the impacts and variations of hydropeaking and thermopeaking is of great importance to evaluate the effects of ecological impacts through hydropower production on river hydraulics. The results of Chapter 3 have their main relevance as a simple yet quantitative tool to support (i) the assessment of the actual length of hydropeaking affected reaches within a given area, and (ii) the design and location of most effective mitigation measures, with highest likelihood of reducing hydropeaking impact for longest river reaches, thus achieving an optimal ecological effectiveness.

The alterations of thermally peaked flows to river sections downstream of hydropower plant releases are discovered as paradoxically mitigating the thermal stress that could develop because of heatwaves in alpine streams, by providing reduced water temperature oscillation ranges compared to unpeaked stream reaches. The results of Chapter 4 add to the complexity of climatic effects on river water temperatures in systems regulated by

hydropower production activities. As an apparent paradox, human interference is discovered as potential mitigation measures in response to extreme climatic events. The outcomes of this Chapter should be viewed in their implication for the temporary selection of thermally protected areas within regulated river systems under the projected increase of heatwave frequency in Alpine areas. Depending on the actual length of regulated ('peaked') river reaches where the thermal protection would occur, some species may indeed tend to select temporary habitats as those protected areas during particularly intense and long-lasting heatwaves.

5.4 Recommendations for further research

Detailed recommendations for further research are already suggested in each of the three thematic Chapters of this thesis. A short summary of the main points in this respect is presented as below.

- In-depth studies of the linkages and translations between water residence time and nutrient retention time could explain in more details the biogeochemical processes and transitional storage at several scales.
- The spatial distribution modelling of water residence time could be refined by including river reaches that are subjected to hydropower regulations. A combination with the nonlinear spatial statistics could be another trend in solving hydro-geophysical or even social economic distribution related questions.
- Although lab and field experiments are both useful ways to examine habitat suitability related with temperature tolerance both in high constant and extreme environments, longer term biological data on differential fish habitat use in peaked river reaches during heatwave events would shed additional light on the anticipated possible

ecological effects of the different response of peaked and unpeaked river reaches to heatwaves.

- The computation of the actual length of such thermally protected river reaches should account for a more refined analysis of the potential effects of climatic changes on hydropower management, which is presently debated in the light of changes in the space-time distribution of future water availability in the Alps.

Bibliography

Abrell, J. (2016). The Swiss Wholesale Electricity Market.Emerson D., Vecchia A. and Dahl A., “Evaluation of drainage-area ratio method used to estimate streamflow for the Red River of the North Basin, North Dakota and Minnesota”, US Department of the Interior, US Geological Survey, (2005). http://pubs.usgs.gov/sir/2005/5017/.

Acreman, M. C., & Dunbar, M. J. (2004). Defining environmental river flow requirements? A review. Hydrology and Earth System Sciences Discussions, 8(5), 861-876.

Agarwal, S., Wills, J., Cayton, L., Lanckriet, G. R., Kriegman, D. J., & Belongie, S., 2007. Generalized Non-metric Multidimensional Scaling. In AISTATS, pp. 11-18.

Aguilera, R., Marcé, R., & Sabater, S., 2013. Modelling nutrient retention at the watershed scale: Does small stream research apply to the whole river network? J. Geophys. Res.: Biogeosci. 118(2), 728-740.

Alfieri, L., Perona, P., & Burlando, P. (2006). Optimal water allocation for an alpine hydropower system under changing scenarios. Water resources management, 20(5), 761-778.

Alonso, C., Román, A., Bejarano, M. D., de Jalon, D. G., & Carolli, M. (2017). A graphical approach to characterize sub-daily flow regimes and evaluate its alterations due to hydropeaking. Science of The Total Environment, 574, 532-543.

Ambrosetti, W., Barbanti, L., & Nicoletta, S. A. L. A. (2003). Residence time and physical processes in lakes. Journal of Limnology, 62(1s), 1-15.

Amoros, C., & Bornette, G. (2002). Connectivity and biocomplexity in waterbodies of riverine floodplains. Freshwater Biology, 47(4), 761-776.

Arismendi, I., Johnson, S. L., Dunham, J. B., Haggerty, R., & Hockman-Wert, D. (2012). The paradox of cooling streams in a warming world: regional climate trends do not parallel variable local trends in stream temperature in the Pacific continental United States. Geophysical Research Letters, 39(10).

Bakken, T. H., King, T., & Alfredsen, K. (2016). Simulation of river water temperatures during various hydro-peaking regimes. Journal of Applied Water Engineering and Research, 1-13.

Baron, J. S., Poff, N. L., Angermeier, P. L., Dahm, C. N., Gleick, P. H., Hairston, N. G., ... & Steinman, A. D. (2002). Meeting ecological and societal needs for freshwater. Ecological Applications, 12(5), 1247-1260.

Barriopedro, D., Fischer, E. M., Luterbacher, J., Trigo, R. M., & García-Herrera, R. (2011). The hot summer of 2010: redrawing the temperature record map of Europe. Science, 332(6026), 220-224.

Barry, M., Baur, P., Gaudard, L., Giuliani, G., Hediger, W., Romerio, F., ... & Weigt, H. (2015). The Future of Swiss Hydropower-A Review on Drivers and Uncertainties. Available at SSRN 2663879.

Benettin, P., J. W. Kirchner, A. Rinaldo, and G. Botter (2015), Modelling chloride transport using travel time distributions at Plynlimon, Wales, Water Resour. Res., 51, 3259-3276, doi:10.1002/2014WR016600.

Beniston, M. (2012). Impacts of climatic change on water and associated economic activities in the Swiss Alps. Journal of Hydrology, 412, 291-296.

Beniston, M., & Diaz, H. F. (2004). The 2003 heat wave as an example of summers in a greenhouse climate? Observations and climate model simulations for Basel, Switzerland. Global and Planetary Change, 44(1), 73-81.

Bergstrom, A., McGlynn, B., Mallard, J., & Covino, T., 2016. Watershed structural influences on the distributions of stream network water and solute

travel times under baseflow conditions. Hydrol. Process. 30: 2671–2685. http://dx.doi.org/10.1002/hyp.10792

Bourqui, M., Hendrickx, F., & Le Moine, N. (2011). Long-term forecasting of flow and water temperature for cooling systems: case study of the Rhone River, France. IAHS Publ, 348, 135-142.

Bouwman, A. F., Bierkens, M. F. P., Griffioen, J., Hefting, M. M., Middelburg, J. J., Middelkoop, H., & Slomp, C. P. (2013). Nutrient dynamics, transfer and retention along the aquatic continuum from land to ocean: towards integration of ecological and biogeochemical models. Biogeosciences, 10(1), 1-22.

Brown, L. E., & Hannah, D. M. (2008). Spatial heterogeneity of water temperature across an alpine river basin. Hydrological Processes, 22(7), 954-967.

Bruder, A., Tonolla, D., Schweizer, S. P., Vollenweider, S., Langhans, S. D., & Wüest, A. (2016). A conceptual framework for hydropeaking mitigation. Science of The Total Environment.

Bruno, M. C., Maiolini, B., Carolli, M., & Silveri, L. (2010). Short time-scale impacts of hydropeaking on benthic invertebrates in an Alpine stream (Trentino, Italy). Limnologica-Ecology and Management of Inland Waters, 40(4), 281-290.

Bruno, M. C., Siviglia, A., Carolli, M. and Maiolini, B. (2013), Multiple drift responses of benthic invertebrates to interacting hydropeaking and thermopeaking waves. Ecohydrol., 6: 511–522. doi:10.1002/eco.1275

Bunn, S. E., & Arthington, A. H. (2002). Basic principles and ecological consequences of altered flow regimes for aquatic biodiversity. Environmental management, 30(4), 492-507.

Bunt, C. M., Cooke, S. J., Katopodis, C. And Mckinley, R. S. (1999),

Movement and summer habitat of brown trout (Salmo trutta) below a pulsed discharge hydroelectric generating station. Regul. Rivers: Res. Mgmt., 15: 395–403.

Caissie D., 2006, The thermal regime of rivers: a review. Freshwater biology, 51(2006) 1389-1406.

Carolli, M., Bruno, M. C., Siviglia, A., & Maiolini, B. (2012). Responses of benthic invertebrates to abrupt changes of temperature in flume simulations. River research and applications, 28(6), 678-691.

Carolli, M., Maiolini, B., Bruno, M. C., Silveri, L., & Siviglia, A. (2008, June). Thermopeaking in an hydropower impacted Alpine catchment. In 4th ECRR Conference on River Restoration, Venice S. Servolo Island, Italy (pp. 789-796).

Carolli, M., Vanzo, D., Siviglia, A., Zolezzi, G., Bruno, M. C., & Alfredsen, K. (2015). A simple procedure for the assessment of hydropeaking flow alterations applied to several European streams. Aquatic Sciences, 77(4), 639-653.

Carslaw, D. C., & Taylor, P. J., 2009. Analysis of air pollution data at a mixed source location using boosted regression trees. Atmos. Environ. 43(22), 3563-3570.

Catalán, N., Marcé, R., Kothawala, D. N., & Tranvik, L. J. (2016). Organic carbon decomposition rates controlled by water retention time across inland waters. Nature Geoscience.

Ceola, S., Bertuzzo, E., Singer, G., Battin, T. J., Montanari, A., & Rinaldo, A. (2014). Hydrologic controls on basin‐scale distribution of benthic invertebrates. Water Resources Research, 50(4), 2903-2920.

Ceola, S., Hödl, I., Adlboller, M., Singer, G., Bertuzzo, E., Mari, L., ... & Rinaldo, A. (2013). Hydrologic variability affects invertebrate grazing on

phototrophic biofilms in stream microcosms. PloS one, 8(4), e60629.

Ceola, S., Pugliese, A., Castellarin, A., & Galeati, G. (2015, April). Impact of alternative environmental flow prescriptions on hydropower production and fish habitat suitability. In EGU General Assembly Conference Abstracts (Vol. 17, p. 681).

Céréghino, R., Cugny, P., & Lavandier, P. (2002). Influence of intermittent hydropeaking on the longitudinal zonation patterns of benthic invertebrates in a mountain stream. International review of hydrobiology, 87(1), 47-60.

Cesaraccio, C., Spano, D., Duce, P., & Snyder, R. L. (2001). An improved model for determining degree-day values from daily temperature data. International Journal of Biometeorology, 45(4), 161-169.

Change, I. P. O. C. (2001). Climate change 2007: Impacts, adaptation and vulnerability. Genebra, Suíça.

Chen, X., Fang, C., & Zhang, Y. (2012). Review on the Impact of Climate Change on Features of Hydrology and Water Resources. Clim Change Res Lett, 1, 96-105.

Crettenand, N. (2012). The facilitation of mini and small hydropower in Switzerland. Ecole Polytechnique Fédérale de Lausanne (EPFL). Thèse N° 5356.

Crook, D. A., Lowe, W. H., Allendorf, F. W., Erős, T., Finn, D. S., Gillanders, B. M., ... & Kilada, R. W. (2015). Human effects on ecological connectivity in aquatic ecosystems: Integrating scientific approaches to support management and mitigation. Science of the Total Environment, 534, 52-64.

Crowley, T. J. (2000). Causes of climate change over the past 1000 years. Science, 289(5477), 270-277.

Daufresne, M., Veslot, J., Capra, H., Carrel, G., Poirel, A., Olivier, J. M., &

Lamouroux, N. (2015). Fish community dynamics (1985–2010) in multiple reaches of a large river subjected to flow restoration and other environmental changes. Freshwater Biology, 60(6), 1176-1191.

Death RG, Fuller IC, Macklin MG. (2015). Resetting the river template: The potential for climate-related extreme floods to transform river geomorphology and ecology. Freshwater Biol. 60, 2477–2496. (doi:10.1111/fwb.12639)

Della-Marta, P. M., Haylock, M. R., Luterbacher, J., & Wanner, H. (2007). Doubled length of western European summer heat waves since 1880. Journal of Geophysical Research: Atmospheres, 112(D15).

Dickson, N. E., Carrivick, J. L., & Brown, L. E. (2012). Flow regulation alters alpine river thermal regimes. Journal of Hydrology, 464, 505-516.

Doyle, M. W., 2005. Incorporating hydrologic variability into nutrient spiraling. J. Geophys. Res.: Biogeosci. 110(G1).

Doyle, M. W., Stanley, E. H., & Harbor, J. M. (2003). Hydrogeomorphic controls on phosphorus retention in streams. Water Resources Research, 39(6).

Drummond, J. D., Bernal, S., Schiller, D. V., & Martí, E., 2016. Linking in-stream nutrient uptake to hydrologic retention in two headwater streams. Freshw Sci. 35(4), 000-000.

Dudgeon, D., Arthington, A. H., Gessner, M. O., Kawabata, Z. I., Knowler, D. J., Lévêque, C., ... & Sullivan, C. A. (2006). Freshwater biodiversity: importance, threats, status and conservation challenges. Biological reviews, 81(02), 163-182.

Dumont, E., Harrison, J. A., Kroeze, C., Bakker, E. J., & Seitzinger, S. P. (2005). Global distribution and sources of dissolved inorganic nitrogen export to the coastal zone: Results from a spatially explicit, global model. Global

Biogeochemical Cycles, 19(4).

Edenhofer, O., Pichs-Madruga, R., Sokona, Y., Seyboth, K., Matschoss, P., Kadner, S., ... & von Stechow, C. (2011). IPCC special report on renewable energy sources and climate change mitigation. Prepared By Working Group III of the Intergovernmental Panel on Climate Change, Cambridge University Press, Cambridge, UK.

Edinger, J. E., Duttweiler, D. W. & Geyer, J. C. (1968) The response of water temperatures to meteorological conditions. Water Resour. Res. 4(5),1137–1143.

Elith, J., & Leathwick, J., 2016. Boosted Regression Trees for ecological modelling.

Elith, J., Leathwick, J. R., & Hastie, T., 2008. A working guide to boosted regression trees. J Anim Ecol. 77(4), 802-813.

Elliott JM, Hurley MA (2001). Modelling growth of brown trout, *Salmo trutta*, in terms of weight and energy units. Freshwater Biology, 46, 679–692.

Emerson D., Vecchia A. And Dahl A., “Evaluation of drainage-area ratio method used to estimate streamflow for the Red River of the North Basin, North Dakota and Minnesota”, US Department of the Interior, US Geological Survey, (2005). Http://pubs.usgs.gov/sir/2005/5017/.

Engelhardt, C., Krüger, A., Sukhodolov, A., & Nicklisch, A., 2004. A study of phytoplankton spatial distributions, flow structure and characteristics of mixing in a river reach with groynes. J. Plankton Res. 26(11), 1351-1366.

Ensign, S. H., & Doyle, M. W. (2006). Nutrient spiraling in streams and river networks. Journal of Geophysical Research: Biogeosciences, 111(G4).

ESRI 2011. ArcGIS Desktop: Release 10. Redlands, CA: Environmental Systems Research Institute.

Fischer, E. M. (2014). Climate science: autopsy of two mega-heatwaves. Nature Geoscience, 7(5), 332-333.

Fischer, E. M., & Schär, C. (2010). Consistent geographical patterns of changes in high-impact European heatwaves. Nature Geoscience, 3(6), 398-403.

Füreder L., “Species traits in the alpine stream fauna: a promising tool for freshwater monitoring”, Proc. 4th Symposium of the Hohe Tauern National Park for Research in Protected Areas, Castel of Kaprun, (2009), pp 93 - 96.

George SD, Baldigo BP, Smith AJ, Robinson GR. (2015). Effects of extreme floods on trout populations and fish communities in a Catskill Mountain river. Freshwater Biol. 60, 2511–2522. (doi:10.1111/fwb.12577)

Geris, J., Tetzlaff, D., Seibert, J., Vis, M., & Soulsby, C. (2015). Conceptual modelling to assess hydrological impacts and evaluate environmental flow scenarios in montane river systems regulated for hydropower. River Research and Applications, 31(9), 1066-1081.

Gibson, G., 2000. Nutrient criteria technical guidance manual.

Gobiet, A., Kotlarski, S., Beniston, M., Heinrich, G., Rajczak, J., & Stoffel, M. (2014). 21st century climate change in the European Alps—A review. Science of the Total Environment, 493, 1138-1151.

Gottschalk, L., Krasovskaia, I., Leblois, E., & Sauquet, E., 2006. Mapping mean and variance of runoff in a river basin. Hydrol. Earth Syst. Sci. Discuss. 3(2), 299-333.

Gorla, L., Signarbieux, C., Turberg, P., Buttler, A., & Perona, P. (2015). Effects of hydropeaking waves’ offsets on growth performances of juvenile Salix species. Ecological Engineering, 77, 297-306.

Gower, J. C., & Legendre, P., 1986. Metric and Euclidean properties of dissimilarity coefficients. J CLASSIF. 3(1), 5-48.

Graf, J. B., 1986. Traveltime and longitudinal dispersion in Illinois streams (Vol. 2269). Dept. of the Interior, US Geological Survey.

Greenacre, M. Measures of distance between samples: non-Euclidean.

Greg Ridgeway with contributions from others, 2015. gbm: Generalized Boosted Regression Models. R package version 2.1.1. https://CRAN.R-project.org/package=gbm

Grizzetti, B., Bouraoui, F., Granlund, K., Rekolainen, S., & Bidoglio, G., 2003. Modelling diffuse emission and retention of nutrients in the Vantaanjoki watershed (Finland) using the SWAT model. Ecol. Model. 169(1), 25-38.

Guhr, H., Karrasch, B., & Spott, D., 2000. Shifts in the processes of oxygen and nutrient balances in the river Elbe since the transformation of the economic structure. Acta Hydroch. Hydrob. 28(3), 155-161.

Hammond, D., & Pryce, A. R. (2007). Climate change impacts and water temperature. Climate change impacts and water temperature.

Hari, R. E., Livingstone, D. M., Siber, R., Burkhardt-Holm, P., & Guettinger, H. (2006). Consequences of climatic change for water temperature and brown trout populations in Alpine rivers and streams. Global Change Biology, 12(1), 10-26.

Hauer, C., Schober, B. and Habersack, H. (2013), Impact analysis of river morphology and roughness variability on hydropeaking based on numerical modelling. Hydrol. Process., 27: 2209–2224. doi: 10.1002/hyp.9519

Heidbüchel, I., Troch, P. A., Lyon, S. W., & Weiler, M., 2012. The master transit time distribution of variable flow systems. Water Resour Res. 48(6).

Hrachowitz, M., Benettin, P., Breukelen, B. M., Fovet, O., Howden, N. J., Ruiz, L., ... & Wade, A. J., 2016. Transit times—the link between hydrology and water quality at the catchment scale. WIREs Water.

http://dx.doi.org/10.1002/wat2.1155.

Huiliang, W., Zening, W., Caihong, H., & Xinzhong, D., 2015. Water and nonpoint source pollution estimation in the watershed with limited data availability based on hydrological simulation and regression model. Environ Sci Pollut R. 22(18), 14095-14103.

Huth, R., Kyselý, J., & Pokorná, L. (2000). A GCM simulation of heat waves, dry spells, and their relationships to circulation. Climatic Change, 46(1-2), 29-60.

Ingestad, T., & Ågren, G. I. (1988). Nutrient uptake and allocation at steady-state nutrition. Physiologia Plantarum, 72(3), 450-459.

IPCC - International Panel on Climate Change (2007). Climate change 2007: Impacts, adaptation and vulnerability. Genebra, Suíça.

IPCC. (2012). Managing the risks of extreme events and disasters to advance climate change adaptation. Cambridge, UK: Cambridge University Press.

Jalabert, S. S. M., Martin, M. P., Renaud, J. P., Boulonne, L., Jolivet, C., Montanarella, L., & Arrouays, D., 2010. Estimating forest soil bulk density using boosted regression modelling. Soil Use Manage. 26(4), 516-528.

Jarvie, H. P., Withers, P. J., Hodgkinson, R., Bates, A., Neal, M., Wickham, H. D., ... & Armstrong, L. (2008). Influence of rural land use on streamwater nutrients and their ecological significance. Journal of Hydrology, 350(3), 166-186.

Jasper, K., Calanca, P., Gyalistras, D., & Fuhrer, J. (2004). Differential impacts of climate change on the hydrology of two alpine river basins. Climate Research, 26(2), 113-129.

Ji, Z. G., 2008. Hydrodynamics and water quality: modelling rivers, lakes, and estuaries. John Wiley & Sons.

Jorda, H., Bechtold, M., Jarvis, N., & Koestel, J., 2015. Using boosted regression trees to explore key factors controlling saturated and near‐saturated hydraulic conductivity. Eur. J. Soil Sci. 66(4), 744-756.

Julian, J. P., M. W. Doyle, and E. H. Stanley (2008), Empirical modelling of light availability in rivers, J. Geophys. Res., 113, G03022, doi:10.1029/2007JG000601.

Junk, W. J., Bayley, P. B., & Sparks, R. E. (1989). The flood pulse concept in river-floodplain systems. Canadian special publication of fisheries and aquatic sciences, 106(1), 110-127.

Kaltenborn, B. P., Nellemann, C., & Vistnes, I. I. (2010). High mountain glaciers and climate change: challenges to human livelihoods and adaptation. UNEP, GRID-Arendal.

Karl, T. R., & Knight, R. W. (1997). The 1995 Chicago heat wave: How likely is a recurrence? Bulletin of the American Meteorological Society, 78(6), 1107-1119.

Kelly, B., Smokorowski, K. E., & Power, M. (2016). Impact of river regulation and hydropeaking on the growth, condition and field metabolism of Brook Trout (Salvelinus fontinalis). Ecology of Freshwater Fish.

Kevin E. Wehrly, Lizhu Wang & Matthew Mitro (2007) Field-Based Estimates of Thermal Tolerance Limits for Trout: Incorporating Exposure Time and Temperature Fluctuation. Transactions of the American Fisheries Society, 136:2, 365-374, DOI: 10.1577/T06-163.1

Kronvang, B., Hezlar, J., Boers, P., Jensen, J. P., Behrendt, H., Anderson, T., ... & Nielsen, C. B., 2004. Nutrient retention handbook. Software Manual for EUROHARP-NUTRET and Scientific review on nutrient retention, EUROHARP report, 9-2004.

Kronvang, B., Hoffmann, C. C., Svendsen, L. M., Windolf, J., Jensen, J. P.,

& Dørge, J. (1999). Retention of nutrients in river basins. Aquatic Ecology, 33(1), 29-40.

Kuglitsch, F. G., Toreti, A., Xoplaki, E., Della-Marta, P. M., Luterbacher, J., & Wanner, H. (2009). Homogenization of daily maximum temperature series in the Mediterranean. Journal of Geophysical Research: Atmospheres, 114(D15).

Kusiak, A., Li, M., & Tang, F., 2010. Modelling and optimization of HVAC energy consumption. Appl. Energy. 87(10), 3092-3102.

Lamouroux, N., & Olivier, J. M. (2015). Testing predictions of changes in fish abundance and community structure after flow restoration in four reaches of a large river (French Rhône). Freshwater Biology, 60(6), 1118-1130.

Ledger M, Milner A. (2015). Extreme events in running waters. Freshwater Biol. 60, 2455–2460. (doi:10.1111/fwb.12673)

Lehner, B., Liermann, C. R., Revenga, C., Vörösmarty, C., Fekete, B., Crouzet, P., Döll, P., Endejan, M., Frenken, K., Magome, J., Nilsson, C.,

Leigh, C., Bush, A., Harrison, E. T., Ho, S. S., Luke, L., Rolls, R. J., & Ledger, M. E. (2015). Ecological effects of extreme climatic events on riverine ecosystems: insights from Australia. Freshwater Biology, 60(12), 2620-2638.

Leitner, P., Hauer, C., & Graf, W. (2017). Habitat use and tolerance levels of macroinvertebrates concerning hydraulic stress in hydropeaking rivers–A case study at the Ziller River in Austria. Science of The Total Environment, 575, 112-118.

Leopold, L.B., Wolman, M.G., and Miller, J.P., 1964. Fluvial processes in geomorphology. W.H. Freeman and Co., San Francisco, Calif.

Luce, C., Staab, B., Kramer, M., Wenger, S., Isaak, D., & mcconnell, C. (2014). Sensitivity of summer stream temperatures to climate variability in the Pacific Northwest. Water Resources Research, 50(4), 3428-3443.

Lytle DA, Poff NL. 2004. Adaptation to natural flow regimes. Trends in Ecology and Evolution 19: 94–100.

Maavara, T., Parsons, C. T., Ridenour, C., Stojanovic, S., Dürr, H. H., Powley, H. R., & Van Cappellen, P., 2015. Global phosphorus retention by river damming. Proc. Natl. Acad. Sci. U.S.A. 112(51), 15603-15608.

Maazouzi, C., Claret, C., Dole-Olivier, M. J., & Marmonier, P. (2013). Nutrient dynamics in river bed sediments: effects of hydrological disturbances using experimental flow manipulations. Journal of Soils and Sediments, 13(1), 207-219.

Martin, M. P., Lo Seen, D., Boulonne, L., Jolivet, C., Nair, K. M., Bourgeon, G., & Arrouays, D., 2009. Optimizing pedotransfer functions for estimating soil bulk density using boosted regression trees. Soil Sci Soc Am J. 73(2), 485-493.

MATLAB and Signal Processing Toolbox Release R2016a, The MathWorks, Inc., Natick, Massachusetts, United States.

Mayorga, E., Seitzinger, S. P., Harrison, J. A., Dumont, E., Beusen, A. H., Bouwman, A. F., ... & Van Drecht, G. (2010). Global nutrient export from WaterSheds 2 (NEWS 2): model development and implementation. Environmental Modelling & Software, 25(7), 837-853.

McCallum, J. L., & Shanafield, M. (2016). Residence times of stream‐groundwater exchanges due to transient stream stage fluctuations. Water Resources Research.

McDonnell, J. J., & Beven, K. (2014). Debates—The future of hydrological sciences: A (common) path forward? A call to action aimed at understanding velocities, celerities and residence time distributions of the headwater hydrograph. Water Resources Research, 50(6), 5342-5350.

Meehl, G. A., & Tebaldi, C. (2004). More intense, more frequent, and

longer lasting heat waves in the 21st century. Science, 305(5686), 994-997.

Meile, T., Boillat, J. L., & Schleiss, A. J. (2013). Propagation of surge waves in channels with large-scale bank roughness. Journal of Hydraulic Research, 51(2), 195-202.

Merz, B., Elmer, F., Kunz, M., Mühr, B., Schröter, K., & Uhlemann-Elmer, S. (2014). The extreme flood in June 2013 in Germany. La Houille Blanche, (1), 5-10.

Middelkoop, H., Daamen, K., Gellens, D., Grabs, W., Kwadijk, J. C., Lang, H., ... & Wilke, K. (2001). Impact of climate change on hydrological regimes and water resources management in the Rhine basin. Climatic change, 49(1-2), 105-128.

Milner A.M., Brown L.E. and Hannah D.M., “Hydroecological response of river systems to shrinking glaciers”, Hydrol. Process, Vol. 23, (2009), pp 62 - 77. Doi: 10.1002/hyp.7197

Moog, O. (1993). Quantification of daily peak hydropower effects on aquatic fauna and management to minimize environmental impacts. Regulated Rivers: Research & Management, 8(1-2), 5-14.

Mouthon J, Daufresne M. (2015). Resilience of mollusk communities of the River Saone (eastern France) and its two main tributaries after the 2003 heatwave. Freshwater Biol. 60, 2571–2583. (doi:10.1111/fwb.12540)

Mulholland, P. J., Tank, J. L., Webster, J. R., Bowden, W. B., Dodds, W. K., Gregory, S. V., ... & McDowell, W. H. (2002). Can uptake length in streams be determined by nutrient addition experiments? Results from an interbiome comparison study. Journal of the North American Benthological Society, 21(4), 544-560.

Naghibi, S. A., Pourghasemi, H. R., & Dixon, B., 2016. GIS-based groundwater potential mapping using boosted regression tree, classification

and regression tree, and random forest machine learning models in Iran. Environ. Monit. Assess. 188(1), 1-27.

Naiman, R. J., Alldredge, J. R., Beauchamp, D. A., Bisson, P. A., Congleton, J., Henny, C. J., ... & Pearcy, W. G. (2012). Developing a broader scientific foundation for river restoration: Columbia River food webs. Proceedings of the National Academy of Sciences, 109(52), 21201-21207.

Natho, S., & Venohr, M. (2014). Active versus potential floodplains–the effect of small flood events on nutrient retention along the river Elbe corridor (Germany). Aquatic Sciences, 76(4), 633-642.

Newbold, J. D., Elwood, J. W., O'Neill, R. V., & Winkle, W. V. (1981). Measuring nutrient spiralling in streams. Canadian Journal of Fisheries and Aquatic Sciences, 38(7), 860-863.

Newcomer Johnson, T. A., Kaushal, S. S., Mayer, P. M., Smith, R. M., & Sivirichi, G. M., 2016. Nutrient Retention in Restored Streams and Rivers: A Global Review and Synthesis. Water. 8(4), 116.

Nilsson, C., Reidy, C. A., Dynesius, M., & Revenga, C. (2005). Fragmentation and flow regulation of the world's large river systems. Science, 308(5720), 405-408.

Null, S. E., Ligare, S. T., & Viers, J. H. (2013). A method to consider whether dams mitigate climate change effects on stream temperatures. JAWRA Journal of the American Water Resources Association, 49(6), 1456-1472.

Null, S. E., Viers, J. H., & Mount, J. F. (2010). Hydrologic response and watershed sensitivity to climate warming in California's Sierra Nevada. Plos One, 5(4), e9932.

Ockenfeld, K., & Guhr, H., 2003. Groyne fields–sink and source functions of “flow-reduced zones” for water content in the River Elbe (Germany). Wat Sci

Tech. 48(7), 17-24.

Olden, J. D., & Naiman, R. J. (2010). Incorporating thermal regimes into environmental flows assessments: modifying dam operations to restore freshwater ecosystem integrity. Freshwater Biology, 55(1), 86-107.

Olden, J. D., & Neff, B. D. (2001). Cross-correlation bias in lag analysis of aquatic time series. Marine Biology, 138(5), 1063-1070.

Orlandini, S., & Rosso, R. (1998). Parameterization of stream channel geometry in the distributed modelling of catchment dynamics. Water Resources Research, 34(8), 1971-1985.

Ouedraogo, I. and Vanclooster, M., 2016. A meta-analysis and statistical modelling of nitrates in groundwater at the African scale. Hydrol. Earth Syst. Sci., 20, 2353-2381, http://dx.doi.org/10.5194/hess-20-2353-2016

Parasiewicz, P. (2008). Habitat time series analysis to define flow augmentation strategy for the Quinebaug River, Connecticut and Massachusetts, USA. River research and applications, 24(4), 439-452.

Parasiewicz, P., K. Ryan, P. Vezza, C. Comoglio, T. Ballestero, and J. N. Rogers. (2012). Use of quantitative habitat models for establishing performance metrics in river restoration planning. Ecohydrology 6:668–678.

Piccolroaz, S., Calamita, E., Majone, B., Gallice, A., Siviglia, A., & Toffolon, M. (2016). Prediction of river water temperature: a comparison between a new family of hybrid models and statistical approaches. Hydrological Processes.

Poff, N. L., & Schmidt, J. C. (2016). How dams can go with the flow. Science, 353(6304), 1099-1100.

Pottgiesser, T., & Sommerhäuser, M., 2004. Profiles of German stream types. Länder-Arbeitsgemeinschaft Wasser (LAWA). Umweltbundesamt, Dessau, Germany.[Available at: http://www. wasserblick. net/servlet/is/18727.

Powers, S. M., Stanley, E. H., & Lottig, N. R. (2009). Quantifying phosphorus uptake using pulse and steady-state approaches in streams. Limnology and Oceanography: Methods, 7(7), 498-508.

Praskievicz, S., & Chang, H. (2009). A review of hydrological modelling of basin-scale climate change and urban development impacts. Progress in Physical Geography, 33(5), 650-671.

Praskievicz, S., & Chang, H. (2009). A review of hydrological modelling of basin-scale climate change and urban development impacts. Progress in Physical Geography, 33(5), 650-671.

Preston, S. D., Alexander, R. B., Schwarz, G. E., & Crawford, C. G., 2011. Factors affecting stream nutrient loads: a synthesis of regional SPARROW model results for the continental united states1. J Am Water Resour Assoc. 47(5), 891-915.

Pringle, C. (2003). What is hydrologic connectivity and why is it ecologically important?. Hydrological Processes, 17(13), 2685-2689.

Quiel, K., Becker, A., Kirchesch, V., Schöl, A., & Fischer, H., 2011. Influence of global change on phytoplankton and nutrient cycling in the Elbe River. Reg Environ Change. 11(2), 405-421.

R Core Team, 2016. R: A language and environment for statistical computing. R Foundation for Statistical Computing, Vienna, Austria. URL https://www.R-project.org/.

Rebetez, M., Dupont, O., & Giroud, M. (2009). An analysis of the July 2006 heatwave extent in Europe compared to the record year of 2003. Theoretical and Applied Climatology, 95(1-2), 1-7.

Reid MA, Ogden RW. (2006). Trend, variability or extreme event? The importance of long-term perspectives in river ecology. River Res. Appl. 22, 167–177. (doi:10.1002/rra.903)

Richter, B., Baumgartner, J., Wigington, R., & Braun, D. (1997). How much water does a river need?. Freshwater biology, 37(1), 231-249.

Robert J. Hijmans, Steven Phillips, John Leathwick and Jane Elith, 2016. dismo: Species Distribution Modelling. R package version 1.1-1. https://CRAN.R-project.org/package=dismo

Robertson, J. C., Rödel, R., Sindorf, N. and Wisser, D. (2011), High-resolution mapping of the world's reservoirs and dams for sustainable river-flow management. Frontiers in Ecology and the Environment, 9: 494–502. doi:10.1890/100125

Rodríguez, J. P., Rodríguez-Clark, K. M., Keith, D. A., Barrow, E. G., Benson, J., Nicholson, E., & Wit, P. (2012). IUCN Red List of ecosystems. SAPI EN. S. Surveys and Perspectives Integrating Environment and Society, (5.2).

Roe, B. P., Yang, H. J., Zhu, J., Liu, Y., Stancu, I., & McGregor, G., 2005. Boosted decision trees as an alternative to artificial neural networks for particle identification. Nuclear Instruments and Methods in Physics Research Section A: Accelerators, Spectrometers, Detectors and Associated Equipment, 543(2), 577-584.

Rosenberg, D. M., mccully, P., & Pringle, C. M. (2000). Global-scale environmental effects of hydrological alterations: introduction. Bioscience, 50(9), 746-751.

Rossel, V., & de la Fuente, A. (2015). Assessing the link between environmental flow, hydropeaking operation and water quality of reservoirs. Ecological Engineering, 85, 26-38.

Rueda, F., Moreno-Ostos, E., & Armengol, J., 2006. The residence time of river water in reservoirs. Ecol. Model. 191(2), 260-274.

Runkel, R. L. (2007). Toward a transport‐based analysis of nutrient

spiraling and uptake in streams. Limnology and Oceanography: Methods, 5(1), 50-62.

Runkel, R. L., & Bencala, K. E. (1995). Transport of reacting solutes in rivers and streams. In Environmental hydrology (pp. 137-164). Springer Netherlands.

Sauterleute J, Charmasson J (2014) A computational tool for the characterisation of rapid fluctuations in flow and stage in rivers caused by hydropeaking. Environmental Modelling & Software, 55:266–278, DOI 10.1016/j. Envsoft.2014.02.004

Schär, C., Vidale, P. L., Lüthi, D., Frei, C., Häberli, C., Liniger, M. A., & Appenzeller, C. (2004). The role of increasing temperature variability in European summer heatwaves. Nature, 427(6972), 332-336.

Schirmer, M., Luster, J., Linde, N., Perona, P., Mitchell, E. A. D., Barry, D. A., ... & Durisch-Kaiser, E. (2013). River restoration: morphological, hydrological, biogeochemical and ecological changes and challenges. Hydrology & Earth System Sciences Discussions, 10(8).

Schwartz, R., 2006. Geochemical characterisation and erosion stability of fine‐grained groyne field sediments of the Middle Elbe River. Acta Hydroch. Hydrob. 34(3), 223-233.

Scruton D, Ollerhead L, Clarke K, Pennell C, Alfredsen K, Harby A, Kelley D (2003) The behavioural response of juvenile Atlantic salmon (Salmo salar) and brook trout (Salvelinus fontinalis) to experimental hydropeaking on a Newfoundland (Canada) river. River Res Appl 19(5-6): 577–587, DOI 46 10.1002/rra.733

SFOE (2014b), Rentabilität der bestehenden Wasserkraft: Bericht zuhanden der UREK-N, Swiss Federal Office of Energy, Bern.

SFOE (2015), Wochenbericht: Speicherinhalt, Swiss Federal Office of

Energy, Bern.

Shabani, F., Kumar, L., & Solhjouy-fard, S., 2016. Variances in the projections, resulting from CLIMEX, Boosted Regression Trees and Random Forests techniques. Theor. Appl. Climatol. 1-14.

Shamsaei, H., Jaafar, O., & Basri, N. E. A. (2013). Effects residence time to water quality in large water distribution systems.

Shuster WD, 47 Zhang Y, Roy AH, Daniel FB, Troyer M (2008) Characterizing storm hyrograph rise and fall dynamics with stream stage data. J Am Water Resour Assoc 44(6): 1431–1440, DOI 10.1111j. 586 1752-1688.2008.00249.x

Siebert, W. M., 1986. Circuits, signals, and systems (Vol. 2). MIT press.

Snelder, T. H., Lamouroux, N., Leathwick, J. R., Pella, H., Sauquet, E., & Shankar, U., 2009. Predictive mapping of the natural flow regimes of France. J. Hydrol. 373(1), 57-67.

Soulsby, C., Tetzlaff, D., Rodgers, P., Dunn, S., & Waldron, S., 2006. Runoff processes, stream water residence times and controlling landscape characteristics in a mesoscale catchment: an initial evaluation. J. Hydrol. 325(1), 197-221.

Stanley, E. H., & Doyle, M. W., 2002. A Geomorphic Perspective on Nutrient Retention Following Dam Removal Geomorphic models provides a means of predicting ecosystem responses to dam removal. BioScience. 52(8), 693-701.

Stewart, R. J., Wollheim, W. M., Gooseff, M. N., Briggs, M. A., Jacobs, J. M., Peterson, B. J., & Hopkinson, C. S. (2011). Separation of river network–scale nitrogen removal among the main channel and two transient storage compartments. Water Resources Research, 47(10).

Toffolon, M., & Piccolroaz, S. (2015). A hybrid model for river water

temperature as a function of air temperature and discharge. Environmental Research Letters, 10(11), 114011.

Toffolon M., Siviglia A. And Zolezzi G., “Thermal wave dynamics in rivers affected by hydropeaking”, Water Resour. Res., Vol. 46, (2010), doi:10.1029/2009WR008234.

Tong, S. T., & Chen, W. (2002). Modelling the relationship between land use and surface water quality. Journal of environmental management, 66(4), 377-393.

Tonolla D, 2012. River restoration and hydropeaking in Switzerland. International workshop on hydropeaking, the Alpine Convention. Zurich, 19 June 2012.

Toprak, Z. F., & Cigizoglu, H. K., 2008. Predicting longitudinal dispersion coefficient in natural streams by artificial intelligence methods. Hydrol. Process. 22(20), 4106-4129.

Toprak, Z. F., Hamidi, N., Kisi, O., & Gerger, R., 2014. Modelling dimensionless longitudinal dispersion coefficient in natural streams using artificial intelligence methods. KSCE J Civ Eng. 18(2), 718-730.

Truffer, B. (2010). Integrated environmental management of hydropower operation under conditions of market liberalization. In Alpine Waters (pp. 227-234). Springer Berlin Heidelberg.gical” focused analysis in the paper, and has 2 dedicated Fig.s in the Results Section

Truffer, B., Bratrich, C., Markard, J., Peter, A., Wüest, A., & Wehrli, B. (2003). Green Hydropower: The contribution of aquatic science research to the promotion of sustainable electricity. Aquatic Sciences, 65(2), 99-110.

Tuhtan J, Noack M, Wieprecht S (2012) Estimating stranding risk due to hydropeaking for juvenile European grayling considering river morphology. Ksce J Civ Eng 16(2): 197–206, DOI 10.1007/s12205-012-0002-5

Valentin, S., Lauters, F., Sabaton, C., Breil, P., & Souchon, Y. (1996). Modelling temporal variations of physical habitat for brown trout (Salmo trutta) in hydropeaking conditions. Regulated Rivers: Research & Management, 12(2-3), 317-330.

Van Nieuwenhuyse, E. E., 2005. Empirical model for predicting a catchment-scale metric of surface water transit time in streams. Can J Fish Aquat Sci. 62(3), 492-504.

Vanzo, D., Siviglia, A., Carolli, M., and Zolezzi, G. (2015) Characterization of sub-daily thermal regime in alpine rivers: quantification of alterations induced by hydropeaking. Hydrol. Process., doi: 10.1002/hyp.10682.

Venohr, M., Hirt, U., Hofmann, J., Opitz, D., Gericke, A., Wetzig, A., ... & Mahnkopf, J., 2011. Modelling of nutrient emissions in river systems–MONERIS–methods and background. Int Rev Hydrobiol. 96(5), 435-483.

Verzano, K., Bärlund, I., Flörke, M., Lehner, B., Kynast, E., Voß, F., & Alcamo, J., 2012. Modelling variable river flow velocity on continental scale: Current situation and climate change impacts in Europe. J. Hydrol. 424, 238-251.

Vörösmarty, C. J., Meybeck, M., Fekete, B., Sharma, K., Green, P., & Syvitski, J. P. (2003). Anthropogenic sediment retention: major global impact from registered river impoundments. Global and planetary change, 39(1), 169-190.

Ward, J. V. (1985). Thermal characteristics of running waters. In Perspectives in Southern Hemisphere Limnology (pp. 31-46). Springer Netherlands.

Webb, B. W. (1996). Trends in stream and river temperature. Hydrological processes, 10(2), 205-226.

Webb, B. W., & Nobilis, F. (1995). Long term water temperature trends in

Austrian rivers. Hydrological Sciences Journal, 40(1), 83-96.

Webb, B. W., & Nobilis, F. (2007). Long-term changes in river temperature and the influence of climatic and hydrological factors. Hydrological Sciences Journal, 52(1), 74-85.

Webb, B. W., Hannah, D. M., Moore, R. D., Brown, L. E., & Nobilis, F. (2008). Recent advances in stream and river temperature research. Hydrological Processes, 22(7), 902-918.

Westlake, D. F. (1966), The light climate for plants in rivers, in Light as an Ecological Factor, edited by R. Bainbridge et al., pp. 99–118, Blackwell Sci., Oxford.

WMO. Calculation of monthly and annual 30-year standard normals. (1989).

Woodward, G., Bonada, N., Brown, L. E., Death, R. G., Durance, I., Gray, C., ... & Thompson, R. M. (2016). The effects of climatic fluctuations and extreme events on running water ecosystems. Phil. Trans. R. Soc. B, 371(1694), 20150274.

Woodward, G., Gessner, M. O., Giller, P. S., Gulis, V., Hladyz, S., Lecerf, A., ... & Dobson, M. (2012). Continental-scale effects of nutrient pollution on stream ecosystem functioning. Science, 336(6087), 1438-1440.

Woodward, G., Perkins, D. M., & Brown, L. E. (2010). Climate change and freshwater ecosystems: impacts across multiple levels of organization. Philosophical Transactions of the Royal Society of London B: Biological Sciences, 365(1549), 2093-2106.

Working Group on Soil Classification of the German Soil Science Society, 1997. Soil classification of the federal republica of Germany. Mitteilungen der Deutschen Bodenkundlichen Gesellschaft. Bd. 84, p 253-275.

Worrall, F., Howden, N. J. K., & Burt, T. P., 2014. A method of estimating

in-stream residence time of water in rivers. J. Hydrol. 512, 274-284.

Yarnell, S. M., Petts, G. E., Schmidt, J. C., Whipple, A. A., Beller, E. E., Dahm, C. N., ... & Viers, J. H. (2015). Functional flows in modified riverscapes: Hydrographs, habitats and opportunities. BioScience, 65(10), 963-972.

Yates, D., Galbraith, H., Purkey, D., Huber-Lee, A., Sieber, J., West, J., ... & Joyce, B. (2008). Climate warming, water storage, and Chinook salmon in California's Sacramento Valley. Climatic Change, 91(3-4), 335-350.

Yossef, M. F., 2002. The effect of groynes on rivers: Literature review. Delft Cluster.

Young PS, Cech JJ, Thompson LC (2011) Hydropower-related pulsed-flow impacts on stream fishes: a brief review, conceptual model, knowledge gaps, and research needs. Reviews in Fish Biology and Fisheries 21(4):713–731, DOI 10.1007/s11160-011-9211-0

Zarfl, C., Lumsdon, A. E., Berlekamp, J., Tydecks, L., & Tockner, K. (2015). A global boom in hydropower dam construction. Aquatic Sciences, 77(1), 161-170.

Zimmerman J, Letcher B (2010) Determining the effects of dams on subdaily variation in river flows at a whole basin scale. River Res Appl 26:1246–1260, DOI 10.1002/rra

Zimmermann, N. E., Edwards, T. C., Graham, C. H., Pearman, P. B., & Svenning, J. C., 2010. New trends in species distribution modelling. Ecography. 33(6), 985-989.

Zolezzi, G., Bellin, A., Bruno, M. C., Maiolini, B., & Siviglia, A. (2009). Assessing hydrological alterations at multiple temporal scales: Adige River, Italy. Water Resources Research, 45(12).

Zolezzi, G., Siviglia, A., Toffolon, M., & Maiolini, B. (2011). Thermopeaking in Alpine streams: event characterization and time scales.

Ecohydrology, 4(4), 564-576.

A. Appendix: Supplementary materials

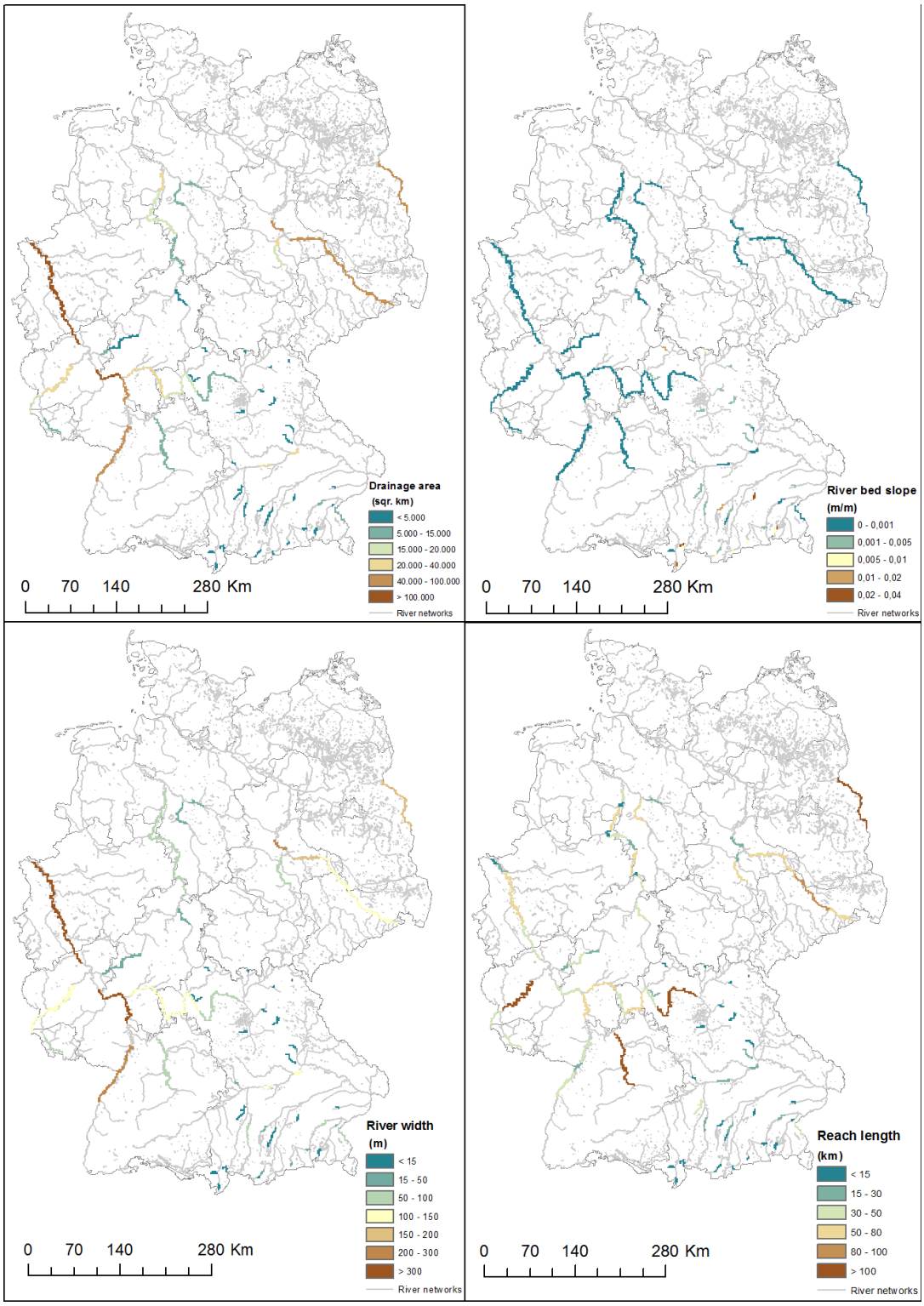

Figure A.1 Spatial distribution of geomorphology attributes of drainage area, slope, the mean river width and stream types classification for the selected river reaches.

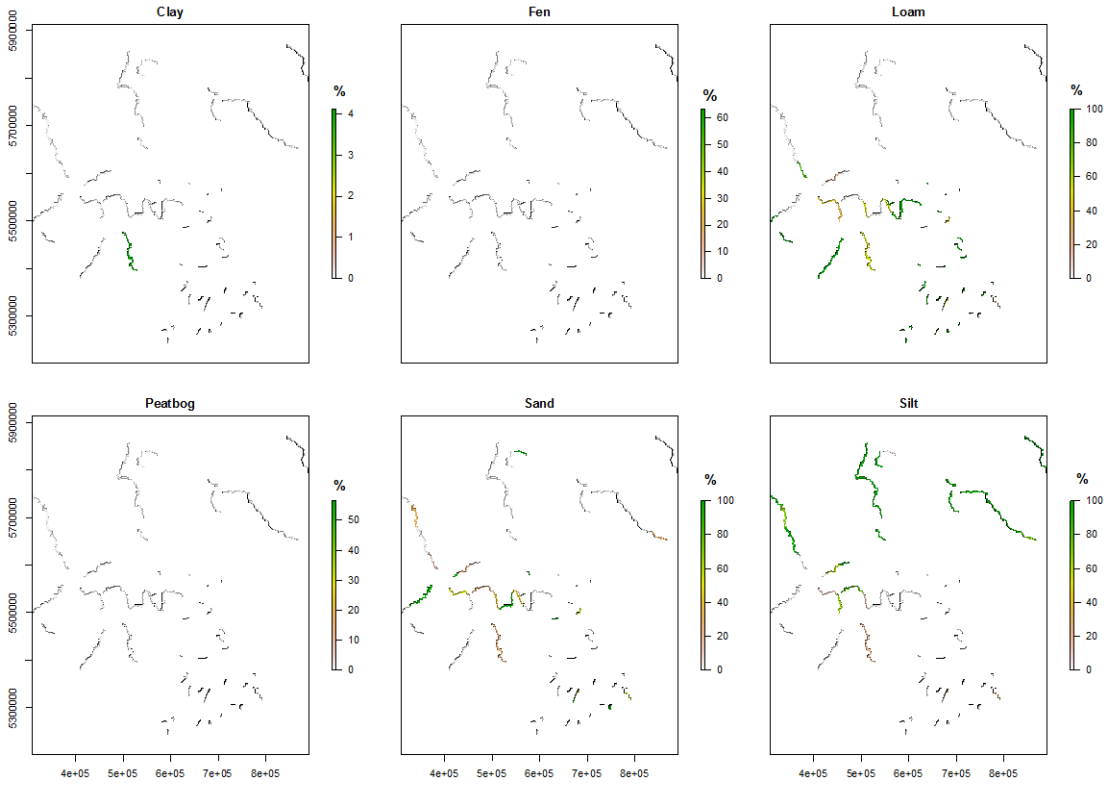

Figure A.2 Spatial distribution of substrate composition in percentage for selected river reaches.

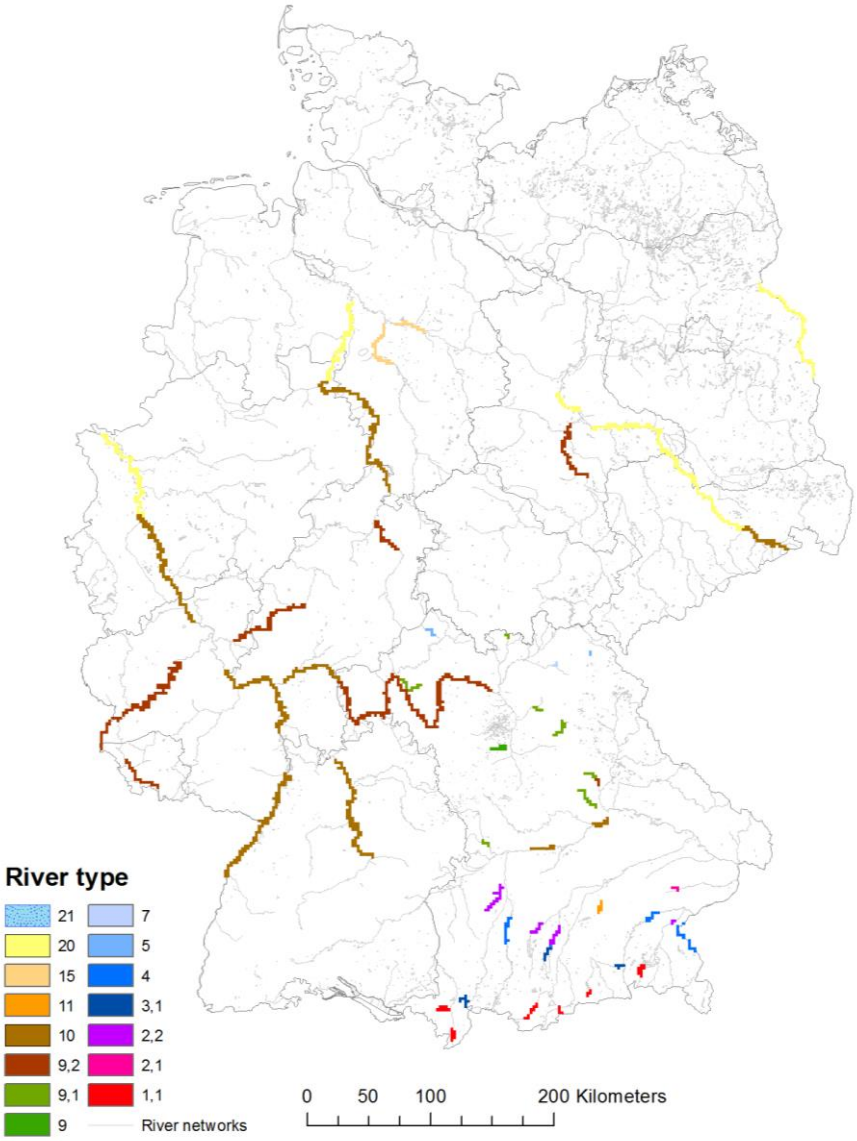

Figure A.3 Spatial distribution of stream river type classification for selected river reaches.

Table A.1 Hydro-geomorphological attributes of selected river reach with end points of upstream and downstream gauging stations in Chapter 2.

ID	Length (km)	Slope	River Type	Upstream Gauging Station					Downstream Gauging Station				
				Code	Name	Stretch Of	Elevation (m a.s.l)	Drainage Area (Sq. km)	Code	Name	Stretch Of	Elevation (m a.s.l)	Drainage Area (Sq. km)
1	2.281	0.010	3.1	12401004	Wertach	Wertach	909.69	35.1	12412000	Wertach	Wertacher Starzlach	887.44	21.1
2	3.435	0.001	21	16669009	Percha	Lüßbach	585.2	48.8	16665008	Leutstetten	Würm	582.58	3206.6
3	1.993	0.031	1.1	18463004	Prien	Prien	527.96	92.7	18465000	Dickertsmühle	Prienkanal	521.42	6.22
4	22.952	0.003	4	12003001	Landsberg	Lech	582.28	2282.6	12393201	Unterbergen	Lochbach	520.81	0.01
5	19.520	0.004	2.2	16665008	Leutstetten	Würm	582.58	326.6	16666000	Obermenzing	Würm	513.96	403.8
6	6.398	0.002	9.1	11808006	Heroldingen	Wörnitz	403.54	1108.4	11809009	Harburg	Wörnitz	400.65	1569.5
7	2.895	0.005	2.1	18835007	Kirchberg	Mertseebach	413.65	27.9	18838005	Eggenfelden	Mertseebach	400.01	32.1
8	8.007	0.001	9.2	14606008	Schmidmühlen	Vils	351.14	756.8	14608003	Dietldorf	Vils	343.36	1100.9
9	9.029	0.003	9.1	14685004	Stettkirchen	Lauterach	375.4	237.9	14606008	Schmidmühlen	Vils	351.14	756.8
10	3.101	0.008	1.1	16401006	Garmisch O, D, Partnachmündung	Loisach	711.7	248.6	16402009	Garmisch U, D, Partnachmündung	Loisach	686.5	393.6
11	3.876	0.002	3.1	18285507	Hohenofen	Kaltenbach	451.4	106.34	18209000	Rosenheim	Mangfall	443	1099.27
12	17.808	0.001	4	18004007	Kraiburg	Inn	388.6	12278.05	18004506	Mühldorf	Inn	371.23	12409.28
13	1.707	0.003	7	24116005	Untersteinach	Schorgast	312.57	244.4	24117008	Kauerndorf	Schorgast	308.07	247.2
14	1.007	0.002	3.1	16668800	Starnberg	Georgenbach	586.83	46.9	16669009	Percha	Lüßbach	585.2	48.8
15	1.260	0.013	2.2	16603000	Grafrath	Amper	530.36	1194.6	16605006	Fürstenfeldbruck	Amper	514.3	1230.3

16	24.459	0.003	9.1	13922002	Parsberg	Schwarze Laber	440.84	187	13926207	Deuerling	Schwarze Laber	371.65	423.3
17	8.255	0.002	9.1	24241710	Behringersmühle	Wiesent	320.58	423.82	24242000	Muggendorf	Wiesent	304.08	660.7
18	5.050	0.005	9.1	24220506	Michelfeld	Güntersthal	397.49	96.6	24222002	Pegnitz	Güntersthal	369.98	318.43
19	4.981	0.035	1.1	11416006	Spielmannsau	Traufbach	1026.69	8.26	11417100	Gruben	Oybach	854.08	23.9
20	12.453	0.016	1.1	11411104	Birgsau	Stillach	976.48	34	11412107	Oberstdorf	Stillach	782.5	80.5
21	12.610	0.006	1.1	18462205	Aschau	Prien	601.26	56.9	18463004	Prien	Prien	527.96	92.7
22	10.894	0.041	11	16802007	Berg	Sempt	475.84	236.7	16805005	Langengeisling	Sempt	28.7	269.1
23	4.583	0.004	2.2	18409508	Gufflham	Alz	415	0.01	18408200	Burgkirchen	Alz	396.9	2221.95
24	18.186	0.000	10	10053009	Kelheim	Donau	337.1	23031	10056302	Oberndorf	Donau	331.15	26520.7
25	11.039	0.000	3.1	16668403	Tutzing	Kalkgraben	588.53	1.2	16668800	Starnberg	Georgenbach	586.83	46.9
26	26.163	0.002	9.1	24382304	Arnstein	Wern	200	328.95	24385007	Sachsenheim	Wern	157.09	599.8
27	4.208	0.008	9.1	24165204	Neukirchen	Lauterbach	361.2	18.3	24165306	Oberlauter	Lauterbach	328.35	31.5
28	4.430	0.009	1.1	16145008	Rißbachklamm	Rißbach	828.47	182.3	16001303	Rißbachdüker	Isar	787.93	523.9
29	4.687	0.031	3.1	11443009	Gschwend	Rottach	850.47	10.7	11445004	Greifenmühle	Rottach	810.62	30.9
30	9.477	0.003	1.1	16403001	Farchant	Loisach	665.86	424.3	16404106	Eschenlohe Brücke	Loisach	634.46	467.7
31	5.681	0.008	1.1	18214000	Bad Kreuth	Sagenbach	790.65	18.7	18212004	Oberach	Weißach	742.73	96
32	35.797	0.001	4	18602009	Laufen Siegerstetter Keller	Salzach	387.05	6118.8	18606000	Burghausen	Salzach	351.62	6655.1
33	11.020	0.011	5	24431002	Unterweißenbrunn	Brend	381.06	47.1	24432504	Schweinhof	Brend	262.71	111.11

34	11.925	0.002	9	24232006	Laubendorf	Zenn	306.94	171	24232301	Kreppendorf	Zenn	288.82	248
35	30.002	0.002	2.2	11942009	Fischach	Schmutter	486.73	132.4	11944004	Achsheim	Schmutter	437.9	359.1
36	3.825	0.006	3.1	12402007	Sebastianskapelle	Wertach	884.37	60.6	12404002	Haslach Werksabfluss Ingolstadt	Wertach	862.51	83.4
37	19.283	0.001	10	10043710	Neuburg Q Förmitz	Donau	386.1	19924	10046105	Luitpoldstraße Förmitz	Donau	360.35	20252.1
38	2.485	0.013	5	56113404	Speicherzufluss	Förmitz	529.38	8.2	56114000	Speicherabfluss	Förmitz	498.3	14.1
39	10.408	0.001	1.1	11434008	Thalkirchdorf	Konstanzer Ach	731.05	23.3	11438009	Immenstadt	Konstanzer Ach	715.94	67
40	48.265	0.001	10	23300900	Kehl-Kronenhof	Rhein	133.05	39330	23500700	Plittersdorf	Rhein	106.75	48276.00
41	22.290	0.000	10	23500700	Plittersdorf	Rhein	106.75	48276	23700200	Maxau	Rhein	97.76	50196.00
42	38.652	0.000	10	23700200	Maxau	Rhein	97.76	50196	23700600	Speyer	Rhein	88.51	53131.00
43	101.780	0.001	10	23800100	Plochingen	Neckar	245.9	3995	23800690	Rockenau Ska	Neckar	119.74	12710.00
44	53.907	0.000	10	23900200	Worms	Rhein	84.16	68827	25100100	Mainz	Rhein	78.38	98206.00
45	130.727	0.000	9.2	24300202	Trunstadt	Main	223.4	11984.97	24300600	Würzburg	Main	164.55	13996.00
46	48.881	0.000	9.2	24300600	Würzburg	Main	164.55	13995.76	24500100	Steinbach	Main	146.33	17878.00
47	75.781	0.000	9.2	24500100	Steinbach	Main	146.33	17878.46	24700200	Kleinheubach	Main	119.62	21491.00
48	46.144	0.000	9.2	24700200	Kleinheubach	Main	119.62	21491.16	24700325	Mainflingen	Main	101.15	23084.00
49	64.623	0.000	10	24700325	Mainflingen	Main	101.15	23084	24900108	Raunheim	Main	82.9	27142.00
50	47.869	0.000	10	25100100	Mainz	Rhein	78.38	98206	25700100	Kaub	Rhein	67.68	103488.00
51	40.744	0.000	9.2	26400220	St Arnual	Saar	183.25	3944.7	26400550	Fremersdorf	Saar	165.5	6983.00
52	43.503	0.000	9.2	26100100	Perl	Mosel	138.5	11522	26500100	Trier Up	Mosel	121	23857.00
53	145.434	0.000	9.2	26500100	Trier Up	Mosel	121	23857	26900400	Cochem	Mosel	77	27088.00

					Giessen								
54	24.350	0.001	9.2	25800100	Klärwerk	Lahn	148.5	2352	25800200	Leun Neu	Lahn	135	3571.00
55	32.800	0.001	9.2	25800200	Leun Neu	Lahn	135	3571	25800500	Diez Hafen	Lahn	101.26	4905.70
56	21.502	0.001	9.2	25800500	Diez Hafen	Lahn	101.26	4905.7	25800600	Kalkofen Neu	Lahn	86.39	5304.00
57	40.827	0.000	10	27100400	Andernach	Rhein	51.49	139549	2710080	Bonn	Rhein	42.66	140901.00
58	34.410	0.000	10	2710080	Bonn	Rhein	42.66	140901	2730010	Köln	Rhein	34.97	144232.00
59	56.861	0.000	10	2730010	Köln	Rhein	34.97	144232	2750010	Düsseldorf	Rhein	24.48	147680.00
60	70.226	0.000	20	2750010	Düsseldorf	Rhein	24.48	147680	2770040	Wesel	Rhein	11.2	
61	23.609	0.000	20	2770040	Wesel	Rhein	11.2	157500	2790010	Rees	Rhein	8.73	159300.00
62	14.853	0.000	20	2790010	Rees	Rhein	8.73	159300	2790020	Emmerich	Rhein	8	159555.00
63	37.212	0.001	9.2	42700100	Rotenburg	Fulda	179.52	2523	42900100	Guntershausen	Fulda	140.9	6366.00
64	34.000	0.000	10	43100109	Hann.Muenden	Weser	114.95	12444	43900105	Wahmbeck	Weser	98	12996.00
65	9.317	0.000	10	43900105	Wahmbeck	Weser	98	12996	45100100	Karlshafen	Weser	94.05	12996.00
66	61.493	0.000	10	45100100	Karlshafen	Weser	94.05	14794	45300200	Bodenwerder	Weser	69.39	14794.00
67	28.886	0.000	10	45300200	Bodenwerder Hameln	Weser	69.39	15924	45700207	Wehrbergen	Weser	57.85	15924.00
68	45.684	0.000	10	45700207	Wehrbergen	Weser	57.85	17094	45900208	Vlotho	Weser	41.66	17618.00
69	14.761	0.000	10	45900208	Vlotho	Weser	41.66	17618	47100100	Porta	Weser	37.04	19162.00
70	56.329	0.000	20	47100100	Porta	Weser	37.04	19162	47500200	Liebenau	Weser	19.99	19931.00
71	11.975	0.000	20	47500200	Liebenau	Weser	19.99	19931	47900118	Nienburg	Weser	17.37	21799.00
72	41.272	0.000	20	47900118	Nienburg	Weser	17.37	21799	47900209	Dörverden	Weser	7.99	22112.00
73	79.302	0.000	15	48800108	Herrenhausen	Leine	43.81	5304	48800301	Schwarmstedt	Leine	21	6443.00

74	21.369	0.000	15	48300105	Celle	Aller	31.82	4374	48700103	Marklendorf	Aller	23.01	7209.00
75	52.105	0.000	10	501010	Schöna	Elbe	116.18	51391	501060	Dresden	Elbe	102.68	55211.00
76	94.922	0.000	20	501060	Dresden	Elbe	102.68	53096	501261	Torgau	Elbe	75.15	53096.00
77	57.924	0.000	20	501261	Torgau	Elbe	75.15	55211	501420	Wittenberg	Elbe	62.44	61879.00
78	51.925	0.000	20	501420	Wittenberg	Elbe	62.44	61879	502010	Aken	Elbe	50.2	23719.00
79	56.758	0.000	9.2	570810	Trotha-Up	Saale	69.34	17979	570910	Bernburg-Up	Saale	55.11	19639.00
80	17.039	0.000	9.2	570910	Bernburg-Up	Saale	55.11	19639	570930	Calbe-Up	Saale	48.09	23719.00
81	18.818	0.000	20	502070	Barby	Elbe	46.11	94060	502180	Magdeburg-Strombrücke	Elbe	39.88	94942.00
82	112.528	0.000	20	603000	Eisenhüttenstadt	Oder	25.16	52033	603080	Hohensaaten-Finow	Oder	0.15	109564.00